A STUDY OF ADSORPTION FROM SOLUTION BY TITANIUM DIOXIDE USING A FLOW MICROCALORIMETER

by J.A. Milne.

Submitted for the degree of Master of Science of Loughborough University of Technology.

January, 1970

SUMMARY

The flow microcalorimeter, as developed by Messrs. Groszek & Templer was the first commercially available dynamic calorimeter. It was soon recognised by the Paint Research Station, Teddington, as a potential tool to further studies in surface chemistry.

The work described in this thesis comprises an account of the manner in which the instrument was utilised. The aims were three-fold: firstly to test whether the calorimeter was an accurate and reliable instrument, secondly to establish what was being measured, and thirdly to apply it to the study of a particular system.

Results of some studies of adsorption on titanium dioxide are reported. The conclusions reached are that this instrument is insufficiently precise to be considered anything other than semi-quantitative, since it does not have a high order of reproducibility. Much additional information is necessary in order to make the fullest use of results in interpretational theory.

ACKNOWLEDGEMENT

Grateful acknowledgement is made to the Paint Research Station for providing me with the opportunity to submit this thesis, and to Dr. V.T. Crowl in particular for continued guidance.

I am also indebted to Dr. M.J. Jaycock of the University of Technology, Loughborough, for patient helpful supervision, and to Dr. G.D. Parfitt, British Titan Products, for his constructive criticism throughout.

CONTENTS

Chapter 1

Introduction

Adsorption from Solution

CHAPTER 1

INTRODUCTION

1.1. General Introduction

1.1.1. Dispersions

Much of the work described in this dissertation has been an integral part of a research programme within the Paint Research Station, concerned with the stability of pigment dispersions.

Such dispersions are generally in organic (hydrocarbon) media, although it is recognised that the presence of only trace amounts of water will radically alter the properties of the system. This suggests that electrical properties of solute and solvent are of importance; when the effect of water as solvent has been compared with some organic solvents results have often been similar with materials such as acetone and low molecular weight alcohols.

The theory of the electrical double layer around the solid particles is generally accepted for classical colloidal solutions such as silver iodide or colloidal gold; detailed quantitative theories regarding double layer interactions have been developed independently by Verwey and Overbeek[1] and Derjaguin and Landau[2] and

these may be used to describe the stability of a colloid in hydrocarbon media where only a charge mechanism is involved.

However, pigment dispersions cannot truly be described as colloidal since the particle size is usually too large. Yet several authors[3,4] have applied the theory to systems resembling the pigment system and with only minor reservations have found it still holds valid. Provided the particles have a significant surface charge, (this is often prevented by the low dielectric constant of non-polar media) an electric double layer is formed which can stabilise relatively large particles, $\geq 1\mu$ diameter.

The other factor in non-aqueous systems or involving certain non-ionic or polymeric surface-active agents appears to be the existence of adsorbed layers of the solute at the pigment surface.[5,6] Such a coating, resembling a peel on an orange, can prevent particles from coming together - flocculating - by interaction of the adsorbed layers, during which the entropy per adsorbed molecule decreases, and hence a stable suspension is achieved. If there is no surface charge, or as is more common, the adsorbed layer is comparable in thickness to the particle diameter (say, 0.01 - 0.5μ) then so called 'steric hindrance' will be the major

stabilising factor.

1.1.2. Adsorption

The adsorption process is the loss of at least one degree of freedom by a molecule on its removal as solute, from the bulk liquid to the surface of a solid immersed in that liquid. The interface between the liquid and the solid may comprise solute molecules only, or a mixture of both solute and solvent.

When non-polar solute molecules are adsorbed, 'London - van der Waals' attractive forces are responsible. With polar molecules, however, ionic bonding is generally observed between adsorbate and adsorbent, and the forces involved are usually often considerably greater. Hydrogen bonding, dipole-dipole, dipole-non polar, induced dipole and ion-dipole interactions may also be observed and are of lower energy.

The ease of wetting of a powder is dependant on the changes in surface free energy. This is the work in ergs, required to increase the area of the liquid surface by one cm^2, and is numerically equal to the interfacial tension. The greater its reduction, the easier the powder is wetted. Adsorption taking place on an already-dispersed powder will usually stabilise the dispersion.

Adsorption from solution is employed in several industrial processes including detergency, lubrication, dyeing, ink and paint manufacture. In the latter case pigment is ground of milled in oil or a solution of a resin, its aggregates broken up, to result in the formation of a paint dispersion. The importance of adsorption in this process has become apparent: oils contain mixtures of glycerides of fatty acids, and the adsorption of these components, unchanged saturated or unsaturated acids, or unchanged glycerol, either individually or together, on to a pigment surface inhibits flocculation of the particles in the dispersion.

1.1.3. Aims of the Programme

The advent of the Flow Microcalorimeter afforded a method of examining such adsorption processes by monitoring accompanying heat changes. Although results will be quoted not only for the adsorption of stearic, lauric and oleic acids for example, but also for resin solutions, a large portion of time has been allotted purely to evaluating the instrument critically, as a "viable" and realistic tool in this field. Initially problems of temperature and environment control had to be eliminated, then the importance of flow rate, sensi-

tivity, control setting, weight of pigment samples used, and calibration precision investigated. Reproducibility was examined and optimum working conditions established.

Existing values in the literature for quantities such as heats of immersion, adsorption and solution have been measured by static calorimetry almost without exception. See for example, accounts by Harkins[7] and Zettlemoyer et. al.[8] describing calorimeters they have built. It was necessary to establish first that the flow microcalorimeter gave results of a similar order of magnitude to those by other methods. Further, there was the need to determine exactly what process was being measured, and to check any such theory by comparison of quantities such as the heat of adsorption. (It was immediately apparent that the results given directly by this instrument were not actual heats of adsorption but rather net heats of "preferential" or "exchange" adsorption).

1.2. Choice of Systems

In order to be able to combine experimentally - derived figures with literature values, well-characterised systems must be used. However, some difficulty has been encountered in selecting 'raw materials' for use, because

of the requirement of the Paint Research Station that actual paint materials be used. To take the case of titanium dioxide pigment in particular: this is widely used as a white pigment because of its high refractive index and "superior whiteness". Pure titanium dioxide is satisfactorily prepared in the laboratory in the rutile form by hydrolysis of titanium tetrachloride, but it was required that manufacturers' grades of rutile be studied. To obtain a pure form (say, not less than 99.5% pure TiO_2) is difficult, as almost all commercially available grades have been treated further to produce surface coatings which improve the spreading, covering and ageing properties of the paint. Hence rutile R1 and anatase 10b (see section 3.1.1.3.) are the purest forms of pigmentary titanium dioxide here examined and it is unlikely that adsorption data even for these samples is identical to that for pure samples.[9]

A further difficulty, from the point of view of comparison of results arises from the fact that the best way to standardise the pigment's condition prior to adsorption was not to dry it but to equilibrate with a standard atmosphere of 60% relative humidity, this condition relating more closely to the likely condition of the pigment at the time of paint manufacture. The vast majority of work on rutile and anatase quoted in

the literature is for rigorously-dried, laboratory-prepared samples.

Various straight-chain fatty acids have been used as adsorbate, particularly lauric acid, $C_{11}H_{23}COOH$, stearic acid, $C_{17}H_{35}COOH$, and oleic acid, $C_{17}H_{33}COOH$ in addition to isolated sections dealing with the adsorption of stearylamine, butanol or alkyd resin. The reason for use of these acids is that although resins contain the requisite head groups for adsorption by ionic or hydrogen bonding, the exact chemical constitution of such resins is often uncertain. Hence those acids were chosen as "type compounds"[9] enabling resin components to by studied individually and to represent various functions present in the resin such as carboxyl, and chain-unsaturation (other type-compounds could be selected to demonstrate say, hydroxyl or ester functionality).

The results of these studies were anticipated to facilitate a fuller understanding of mechanisms of alkyd adsorption, and also supply some information of characteristic behaviour and site/energy heterogeneity of pigments.

1.3. Thermodynamics of Adsorption

There are two chief methods of studying interactions of the liquid/solid interface: one is dependent on contact angle measurements, the other on calorimetric

techniques. Some principles governing the latter will be discussed in the following pages.

1.3.1. Heats of Emersion

The surface tension, γ_S, of a crystal corresponds to the lateral force or tension in the surface plane. It is related to the surface energy, E_S, or enthalpy H_S, of a clean, dry, non-porous solid by the expression:

$$H_S = \sum_S \left[\gamma_S - T\left(\frac{\partial \gamma_S}{\partial T}\right)_P \right] \qquad \text{(where } \textstyle\sum_S = \text{surface area)} \qquad 1.1.$$

If the solid is now immersed in a liquid the solid surface is replaced by a solid-liquid interface with an enthalpy:

$$H_{SL} = \sum_{SL} \left[\gamma_{SL} - T\left(\frac{\partial \gamma_{SL}}{\partial T}\right)_P \right] \qquad 1.2.$$

The areas of the solid surface and the interface are assumed to be equal:

$$H_S - H_{SL} = \sum \left[\gamma_S - \gamma_{SL} - T\left(\frac{\partial \gamma_S}{\partial T} - \frac{\partial \gamma_{SL}}{\partial T}\right)_P \right] \qquad 1.3.$$

$= H_{E(SL)}$, the enthalpy of emersion, i.e: the heat absorbed when a solid is emersed from a liquid into a vacuum and the liquid-solid interface removed.

At a constant pressure, the relationship between changes in enthalpy and internal energy is:

$$dH = dU + PdV$$

$$(dU \equiv dE)$$

as dV is negligible in the emersional process:

$$dH \simeq dU$$

i.e: $h_{e(sL)} \simeq e_{i(sL)}$

The heat of emersion, $h_{E(sfL)}$, of a solid containing an adsorbed film in equilibrium with its saturated vapour is thus found:

$$h_{E(sfL)} = \gamma_{(sf)} - \gamma_{(sL)} - T\left(\frac{\partial \gamma_{(sf)}}{\partial T} - \frac{\partial \gamma_{(sL)}}{\partial T}\right)_{P,\Sigma} \qquad 1.4.$$

(where $\gamma_{(sL)}$ is interfacial tension at solid-liquid interface.

$\gamma_{(sf)}$ is surface tension of a solid containing adsorbed film in equilibrium with its saturated vapour.

$h_{E(sfL)}$ is the emersional heat per unit area)

Using the relation:

$$\gamma_{(sf)} = \gamma_{(sL)} + \gamma_L \cos\theta$$

$$h_{E(sfL)} = \left[\gamma_L - T\left(\frac{\partial \gamma_L}{\partial T}\right)\right]\cos\theta + T\,\gamma_L \sin\theta \frac{\partial\theta}{\partial T} \qquad 1.5.$$

(where θ is the contact angle of liquid on solid)

Assuming $\theta = 0$

That is, the heat of emersion of each square centimeter of the film-covered powder is equal to the total surface energy or enthalpy of the surface of the liquid used.

Similarly, equation (1.3) - equation (1.4) gives:

$h_{E(SL)} - h_{E(SFL)}$ = reduction in total surface energy.

Hence, at least two heats of emersion must be measured.

The heat of emersion so defined and used by Harkins[7] has been introduced so that heat values quoted for adsorption and wetting processes are positive; he and Jura[10] further apply it to absolute surface area determinations. It is numerically-identical to the heat of immersion, but opposite in sign.

1.3.2. Heats of Adsorption

The same author relates the heat of emersion to the heat of adsorption as follows[7]:-

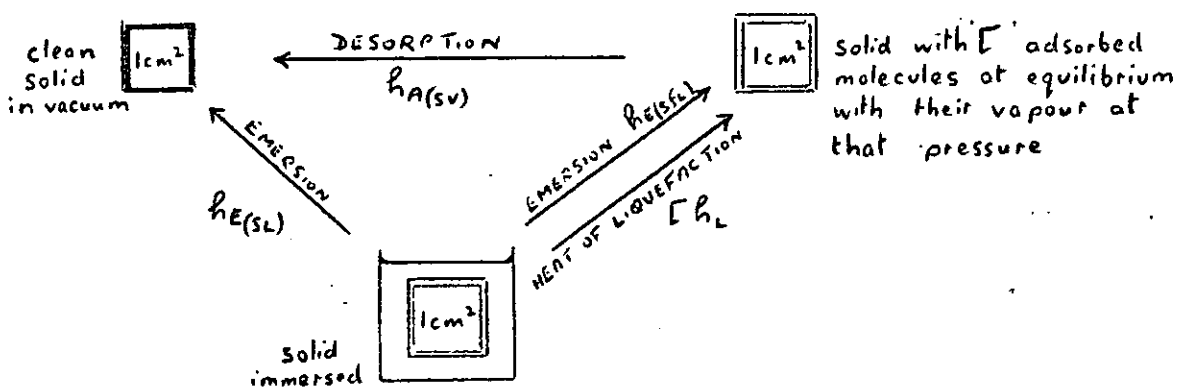

The heat changes involved in returning from $1cm^2$ immersed solid to $1cm^2$ in vacuum without the surface film are independent of the path taken:-

(clockwise) $\Delta H_1 = h_{E(sL)}$

(anti-clockwise) $\Delta H_2 = h_{E(sfL)} + \Gamma h_L + h_{A(sv)}$

$$\therefore \quad h_{A(sv)} = h_{E(sL)} - h_{E(sfL)} - \Gamma h_L \qquad \text{---- 1.7}$$

(where h_L = molar heat of liquifaction.

Γ = a surface excess function, the number of molecules of adsorbate in the surface film. It is determined from the adsorption isotherm for the same system).

Knowledge of the emersional heats of both the clean and film-covered solid thus leads to a value for the heat of adsorption. This in turn enables a value to be assigned to the average electrostatic field of the surface, as heats of adsorption of various functional end-groups plotted against the dipole moment of each group in the wetting liquids form a linear plot.[11, 12, 13].

The energy involved in taking a molecule from bulk liquid to the surface = $E_A - E_L$. The net enthalpy of adsorption of the first layer of molecules (equating

E and H) $\simeq H_{i(SL)} - H_{i(sfL)}$. In the first layer there are Γ molecules, so for $1cm^2$:

$$h_{i(SL)} - h_{i(sfL)} \simeq \Gamma(E_A - E_L) \qquad 1.8.$$

($E_A - E_L$) can be evaluated from equations (1.6) and (1.8).

This interaction involves a number of terms: for polar molecules on a polar surface:

$$E_A - E_L = E_D + E_\mu + E_\alpha + E_{int.} \qquad 1.9.$$

E_D: London Dispersion Energy (Non-Polar)

E_μ: Energy associated with permanent dipole and electrostatic field of surface

E_α: Polarisation of liquid molecules by surface

$E_{int.}$: Lateral interaction of liquid molecules in adsorbed phase; assumed same as in liquid, so ignored.

$$\therefore \quad h_{i(SL)} - h_{i(sfL)} = \Gamma(E_D + E_\alpha) + \Gamma E_\mu \qquad 1.10$$

But,

$$E_\mu = -F.\mu.\cos\theta \qquad 1.11.$$

(where F is the field strength

μ is the dipole moment

θ is the contact angle between axis of dipole and direction of magnetic field.

$= -F.\mu.$

i.e:- One can plot some heat term (equivalent to E_μ) against dipole moment to get a straight line, the gradient of which is related to F, which suggests that $(E_D + E_\alpha)$ is constant.

1.3.2.1. Integral Heat of Adsorption

The previously-mentioned heat of adsorption is an integral heat: it is the heat evolved directly when the specified amount of adsorbate is adsorbed on to the clean dry surface. It is identical to the heat of immersion in pure liquid adsorbate at $P \cdot P_0$, and also the theoretically-derived isosteric heat of adsorption: the Claussius-Clapeyron Equation states:

$$\frac{d \ln P}{dT} = \frac{\Delta H}{RT^2} \qquad 1.12$$

for a gaseous system. If one assumes that the number of moles adsorbed is constant, equation (1.12) can be re-written:

$$\left(\frac{\partial \ln P}{\partial T}\right)_\Gamma = \frac{q_{st}}{RT^2}$$

(where q_{st} is the isosteric heat of adsorption) or for the liquid phase:

$$\left(\frac{\partial \ln a}{\partial T}\right)_{\Gamma} = \frac{q_{st}}{RT^2}$$

(where a = activity of solute in equilbrium with an adsorbed layer of given surface excess).

In fact, several authors[14, 15] have found the theoretical and experimental values to agree quite well. One used experimental results of adsorption isotherm determination at different temperatures in conjunction with the Claussius-Clapeyron Equation to measure the isosteric heat of adsorption; this method lends itself more especially to vapour phase measurements. However, it is difficult in practice as it requires precision of results since the isotherms at temperature differences of say, 20°C are not very large, and one must also have proof of reversibility.

1.3.2.2. Differential Heat of Adsorption

Having determined q_i as a function of Γ, i.e: results are plotted as integral heat of adsorption against the number of moles adsorbed, the gradient is the differential heat of adsorption.

$$q_d = \left(\frac{\partial Q}{\partial n_s}\right)_{\Sigma,T}$$

for constant surface and temperature.

The integral heat is measured in such a way that no 'PV work' is done, and it can be shown[16] that:

$$q_{st} = q_d + RT \qquad \text{1.13.}$$

The differential heats of adsorption generally decrease steadily with increasing amount adsorbed; provided only physical adsorption is taking place, it tends to approach the heat of liquefaction of the adsorbate as the pressure approaches saturation value.

1.3.3. Relationship of Enthalpy with Free Energy of Adsorption

If the free energy of adsorption is available as a function of temperature, the enthalpy may be deduced directly:[17]

$dq = dU + pdV + Vdp$ from the First law of Thermodynamics

and

$$dG = dH - TdS - SdT$$
$$= dU - pdV - Vdp - TdS - SdT$$

For a reversible process:

$$dU = TdS$$

and at constant volume and pressure:

$$dG = -SdT$$

$$S = -\left(\frac{\partial G}{\partial T}\right)_{p,V}$$

$$\Delta G = \Delta H - T\left(\frac{\partial \Delta G}{\partial T}\right)_{p,V} \qquad 1.14.$$

This may be rearranged to the form:

$$\frac{\Delta H}{T^2} = \left(\frac{\partial \Delta G}{T} \Big/ \partial T\right)_{p,V} \qquad \text{when} \quad \Delta G = 0.$$

$$\Delta H = -\left[\frac{\partial(\Delta G/T)}{\partial(1/T)}\right]_{p,V} \qquad 1.15.$$

ΔG is measured experimentally from the equation

$$\Delta G = -RT \ln K$$

K having been deduced from adsorption data plotted as specified by Langmuir, for example, see reference 18.

1.3.4. <u>The Entropy Relationship</u>

Analogous to the expression:

$S = -\frac{\partial \gamma}{\partial T}$ (where S= entropy, the temperature differential of surface tension).

is

$S = -\left(\frac{\partial \Delta G}{\partial T}\right)_{p,n,s}$ (at constant pressure and surface coverage).

= temperature differential of free energy change on adsorption.

1.4. Adsorption Isotherms - Interpretational Theory

1.4.1. Early Theories

Early theories were largely developed for the gas-solid interface as it involved a single adsorbed component only. Solution adsorption was realised to be generally a two-component system, that is both solute and solvent molecules may comprise the adsorbed layer. A measure of the difference in the amounts of solute and solvent taken up is described by the means of an "adsorption isotherm" (necessarily a "composite isotherm" if describing a binary system).

This is the variation of the quantity of one component adsorbed as its concentration in the solution changes; a constant temperature is observed. Such adsorption is almost always physical; no chemical change occurs either to the substrate or the adsorbate in any systems described here, and the adsorption has always been found to be reversible to varying extents.

The replacement of solvent by solute at the solid surface is governed by their relative size and "affinity" for that surface. The adsorption energy of the solute must exceed the desorption energy of the solvent in order to displace it. The overall net energy change accompanying an adsorption process in a multi-component system will be the sum of the individual adsorption and desorption energy changes.

Under such conditions and if the solutions remain dilute, many theories originally enunciated for gaseous adsorption apply also to liquid systems.

1.4.1.1. The Freundlich Isotherm

Details were first published[19] in 1907 (and translated later[20]) of isotherms measured empirically and based on the equation:

$$\frac{x}{m} = \alpha c^{\frac{1}{n}} \qquad \text{1.16.}$$

(where x = weight adsorbate taken up by weight m of solid.

c = concentration of solution at equilibrium

α and n are constants ($n > 1$).)

This isotherm rises steeply from the origin to a shoulder, but then levels off to a plateau which is not horizontal. He interpreted the adsorption as a condensation upon a boundary surface, governed by attraction forces similar to those relating to condensation by capillary-active substances at the liquid-gas interface.

1.4.1.2. The Langmuir Isotherm

The Freundlich isotherm had no theoretical basis and some nine years later was superceded by an equation put forward by Langmuir[21], based on the kinetic theory of gases.

$$\frac{\rho}{x/m} = \frac{N}{N_s b} + \frac{N\rho}{N_s} \qquad 117.$$

(where x = number of moles adsorbed on Mg. solid.
N_s = number of elementary spaces per g. solid.
ρ = pressure of gas.
b = a constant.
N = Avogadro's Number).

This was adaptable as an approximation for adsorption from dilute solutions by replacing p by c, provided the solvent was readily displaced from the surface by

the solute, and the maximum adsorption plateau was reached while still at low concentration. Experimental data should be plotted as $\frac{c}{x/m}$ v. c ; the plot is then linear according to the model.

Neither isotherm describes adsorption from the liquid mixtures well since they neglect the presence of the second component. Even applying the several extensions Langmuir made to allow for:-

1) more than one type of elementary space.

2) more than one type of adsorbed molecule per space.

3) adsorbed layer greater than one molecule's thickness.

it is still severely limited.

1.4.1.3. The Composite Isotherm

This is now drawn by combining the individual isotherm for adsorption of each component into a "composite isotherm". Its application is especially necessary if a wide range of mole fractions is to be studied. The fundamental assumption made in this treatment[22] of data is that there is negligible change in the volume of the bulk solution on adsorption.

An easily comprehensible derivation of the equation:

$$\frac{n^{\circ}\Delta x_1}{m} = n_1^{s}(1 - x_1^{L}) - n_2^{s} x_1^{L}$$

1.12.

(where $n^o = n_1^o + n_2^o$ = total initial number of moles of two components.

Superscript S refers to surface phase.

" L " " liquid " .

x_1 and x_2 are mole fractions of two components in bulk liquid phase.

m = weight of solid used).

is made in Kipling's book[23].

If $n^S = n_1^S + n_2^S$, equation (1.18) can be re-written as:

$$\frac{n^o \Delta x_1}{m} = n^S x_1^S - n^S x_1^L \quad (x_1^S + x_2^S)$$

$$= n^S (x_1^S - x_1^L) \qquad 1.19$$

When this quantity is positive it infers that component 1 is preferentially adsorbed, and if negative, component 2 is. If zero, the composition of each phase is the same.

There are several approximations which may be made to this expression: in very dilute solution, x_1 becomes negligible and x_2 approaches unity.

$$\therefore \frac{n^o \Delta x_1}{m} \simeq n_1^S \qquad 1.20.$$

However, this is not widely applicable: x_1 must be less than about 0.01 so even in the concentration range

described for the radio-tracer adsorption systems (section 3.2) the above expression (1.20) may only be applied to around 3.5 mM equilibrium concentration or less.

1.4.1.4. Analysis of the Composite Isotherm

The existence of multi-layer adsorption is uncertain in many cases. Proof is supplied, however, when $x_2 = 0$ in equation (1.18)

$$\text{i.e: } \frac{n^o \Delta x_1}{m} = n_1^S (1 - x) \qquad 1.21.$$

This means that the surface is completely covered by component 1. Should, for any value of x:

$$\frac{n^o \Delta x_1}{m} > n_1^S (1 - x)$$

the monolayer condition is exceeded.

Further support for this is supplied by Schay and Nagy's analysis[24, 25] of the linear section of many composite isotherms. Over that section, equation (1.18) will define a straight line, and constant composition of the adsorbed phase is inferred; this can be calculat-

ed if the linear section is extrapolated to $x_1^L = 0$ and $x_1^L = 1$. The intercepts are $(n_1^S)_c$ and $-(n_2^S)_c$ respectively (subscript c denotes constant composition).

If molecular areas of the components are known, a specific surface area of the solid can be deduced; should this be already-known, multi-layer adsorption may be detected.

U-shaped isotherms with a linear section often fall off to zero at $x_1^L = 1$ i.e: $-(n_2^S)_c = 0$. This means that the adsorbed layer consists of only one component and the individual isotherm is then of the Langmuir type. An extreme example of this shape is shown by the adsorption by molecular seive of one component of a binary liquid system.

1.4.2. Everett's Treatment.

1.4.2.1. Ideal Systems

In part 1,[26] dealing with perfect systems of his article entitled "The Thermodynamics of Adsorption from Solution", Everett stresses that to define activity coefficients or surface excess functions, which are common measures of the extent of deviation from ideality of a system one must have a simple physical model of the system, as a reference state. This hitherto lacking,

he suggests a Langmuir-type adsorbing surface covered by liquid which is considered to be subdivided into lattice planes, stacked parallel to the surface. The average mole fractions of the solution components are the same in all planes bar the first one, adjacent to the surface. Here, owing to preferential adsorption of one component (giving: "a perfect adsorbed monolayer") it is a different case, defining the adsorbed phase, σ.

He developes the argument to derive an equation closely analogous to that of the Langmuir Isotherm. Extensions discuss chemical potentials, determination of surface areas and correlation of equations for solid-vapour, solid-solution and solution-vapour interfaces.

Directly pertinent to the question of heats of adsorption and immersion, however, is the derivation of surface excess. Assuming a Gibbs dividing surface at the solid surface: if there were no adsorbed layer and the bulk liquid were of constant mole fraction right up to the dividing surface, the number of molecules of component 1 present would be:

$$N_1^{L} = x_1^{L} (N^{L} + N^{\sigma})$$

However there are:

$$N_1^{L} + N_1^{\sigma} = x_1^{L} N^{L} + x_1^{\sigma} N^{\sigma}$$

moles of component 1 in the system. The surface excess is hence $(x_1^{\sigma} - x_1^{L}) N^{\sigma}$, or in terms of concentration;

$$\Gamma_1 = \frac{n^{\sigma}}{A} (x_1^{\sigma} - x_1^{L}) \text{ moles per unit area} \qquad 1.22.$$

If one now considers the changes in concentration on establishing adsorption equilibrium, one gets initially :- $+n^{o}$ moles solution, x_1^{o} composition, ($n_1^{o} = x_1^{o} n^{o}$, $n_2^{o} = x_2^{o} n^{o}$) moles of components 1 and 2, and finally :- $+n^{\sigma}$ moles in adsorbed phase, n^{L} moles in liquid phase, liquid composition is x_1^{L} . The observed change in solution composition is:

$$\Delta x_1^{L} = x_1^{o} - x_1^{L} = \frac{n^{\sigma}}{n^{L}} (x_1^{\sigma} - x_1^{o}) \qquad 1.23.$$

and $$\Delta x_1^{L} = \frac{n^{\sigma}}{n^{o}} (x_1^{\sigma} - x_1^{L}) = \frac{A}{n^{o}} \Gamma \qquad 1.24$$

from equation (1.22).

The heat of immersion is similarly derived. In the initial state there are (n^{o} moles solution, n^{S} moles solid).

$$H^i = n_1^o h_1^L + n_2^o h_2^L + n^S h^S$$

$$= n^o (x_1^o h_1^L + x_2^o h_2^L) + n^S h^S$$

After immersion and the attainment of equilibrium;

$$H^f = n_1^L h_1^L + n_2^L h_2^L + n_1^\sigma h_1^\sigma + n_2^\sigma h_2^\sigma + n^S h^S$$

$$= n^L (x_1^L h_1^L + x_2^L h_2^L) + n^\sigma (x_1^\sigma h_1^\sigma + x_2^\sigma h_2^\sigma) + n^S h^S$$

Hence the enthalpy change is:

$$\Delta H = n^o \left[(x_1^L - x_1^o) h_1^L + (x_2^L - x_2^o) h_2^L \right] + n^\sigma \left[x_1^\sigma h_1^\sigma - x_1^L h_1^L + x_2^\sigma h_2^\sigma - x_2^L h_2^L \right] \quad 1.25.$$

since $n^o = n^L + n^\sigma$.

As: $\Delta x_1^L = x_1^o - x_1^L$ (equation 1.23).

$$\Delta H = x_1^\sigma \Delta H_1^o + x_2^\sigma \Delta H_2^o \quad 1.26.$$

(where: $\Delta H_1^o = n^\sigma \Delta ah_1$

$\Delta H_2^o = n^\sigma \Delta ah_2$, the heats of immersion per g. of the solid in 2 pure liquids).

Hence the heat change for the adsorption process can be calculated in an ideal system exhibiting approximately monomolecular coverage, if the heats of wetting of the solid in the pure components are known.

1.4.2.2. Non-Ideal Systems

To allow for non-ideal behaviour, e.g: if a large range of mole fractions is considered, Everett[27] assigned 'heat of mixing' terms to the equation (1.25) (one each for the bulk and surface phases).

$$\Delta H = n^o \Delta x_1^L (\Delta ah_1^o - \Delta ah_2^o) + n^\sigma (x_1^L \Delta ah_1^o + x_2^L \Delta ah_2^o) + n^L \left[h^{E,L}(x_1^L)\right] + n^\sigma \left[h^{E,\sigma}(x_1^\sigma)\right] - n^o \left[h^{E,o}(x_1^o)\right] \quad 1.27.$$

(where: Δah_1^o = enthalpy change on adsorption of 1 mole of component 1

$h^{E,L}(x_1^L)$ etc.= excess enthalpies in bulk and surface phases).

1.4.2.3. Application to Experimental Systems

Such an equation can be simplified and adapted as follows[28] to a system as envisaged in the flow microcalorimeter:

$$\Delta H_A = \Delta H - \Delta H_I - (\text{mixing term})$$

(where: ΔH_A = heat of adsorption

ΔH = net heat (evolved)

ΔH_I = heat of formation of interfacial film

cf: Harkin's treatment, section (1.3.2).

For flow of pure solvent:

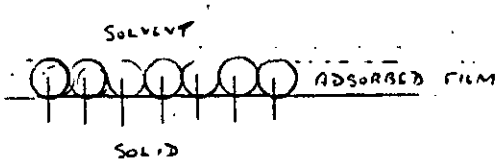

$$\Delta H = H_A^{\sigma} - H_A^{o} + n^{\sigma} H_I \qquad (1.28)$$

omitting the mixing term.

However, for the adsorption of both components from a binary mixture on to a surface previous coated with component 1, the equation (1.28) is expanded:

$$\Delta H = n_1^{\sigma} \bar{H}_{A_1}^{\sigma} + n_2^{\sigma} \bar{H}_{A_2}^{\sigma} + H_{I_{(1+2)}} + n_1^{L} \bar{H}_1^{L}$$

$$+ n_2^{L} \bar{H}_2^{L} - n_1{}^{o}H_{A_1}^{\sigma} - H_{I_{(1)}} - n_1{}^{o}\bar{H}_1^{L} \qquad 1.29.$$

If one assumes component 2 is preferentially adsorbed and completely displaces all of component 1 present:

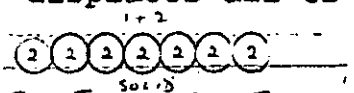

$$\Delta H = (n_2^{\sigma} \bar{H}_{A_2}^{\sigma} - n_1^{\sigma} \bar{H}_{A_1}^{\sigma}) + (H_{I_{(2)}} - H_{I_{(1)}})$$

$$+ (n_1^{L} \bar{H}_1^{L} + n_2^{L} \bar{H}_2^{L} - n_1{}^{o}H_1{}^{L}) \qquad 1.30.$$

= Heat evolved from solid/liquid interface
+ Heat of film formation + mixing terms, i.e. the bulk solution changes.

This is the probable process for most of the flow microcalorimeter data. Quantities such as $H_{I_{(1)}}$, $H_{I_{(2)}}$, $H_{I_{(1+2)}}$ are calculable from surface tension data (equation (1.1)); n_2 (solute) can be derived from the adsorption isotherm of this system, and hence deduce n_1 from a knowledge of molecular sizes and adsorbent surface area.

Provided the solutions used are always dilute, the mixing term should be negligible. Similarly, the variation of surface tension between 100% n-heptane, say, and 0.02 molar acid solution in n-heptane is also minimal and so the film formation or interface term can also be neglected.

This means that ΔH is best expressed as a "heat of exchange adsorption" (equation 1.30). Where a carboxylic acid is in an organic solvent it is partially in an associated (dimeric) state, however, it has not been known to adsorb in dimeric form[29] so there must be included a heat term for the dissociation process. The same fraction of the acid adsorbed must be first dissociated as that which exists as dimer in the original solution. Minor changes in concentration may cause a shift in the monomer $\rightleftharpoons$ dimer equilibrium, but this will be very small, and be accounted for anyway, in any allowance made for the heat of dilution.

1.4.3. Method of Young, Chessick and Healey[30]

A similar conclusion may be arrived at employing the discussion by Young, Chessick and Healey[30] regarding adsorption behaviour of n-butanol from aqueous solution on Graphon. This paper showed excellent agreement

between experimentally-derived heats of wetting, and those deduced from an equation postulated for the system. In spite of the marked difference between their systems and these, their model seems to be modifiable to, for example, heterogeneous surfaces.

Assuming the inter-molecular reactions in the bulk liquid remain the same in the adsorbed phase, the only enthalpy changes will be for surface and interfacial changes. If θ is the fraction of the surface covered, the enthalpy change for the process of adsorption is:

$$\Delta h_{11} = \theta (h_S - h_{S_1})$$

(where: h_S = surface enthalpy of adsorbent

h_{S_1} = " " " " + film);

Similarly, the enthalpy change for the formation of the interface between adsorbed layer and solution is:

$$\Delta h_{21} = \theta (h_{S_1} - h_{1\sigma})$$

(where: $h_{1\sigma}$ is the enthalpy of that layer)

Equivalent expressions for the solvent molecules are:

$$\Delta h_{12} = (1 - \theta)\,(h_S - h_{S_2})$$

$$\Delta h_{22} = (1 - \theta)\,(h_{S_2} - h_{2\sigma})$$

Hence the total enthalpy change for the wetting process is:

$$\Delta H_W = \Delta h_{11} + \Delta h_{12} + \Delta h_{21} + \Delta h_{22}$$

$$= \theta\,(h_S - h_{S_1}) + (1 - \theta)\,(h_S - h_{S_2}) + \theta\,(h_{S_1} - h_{1\sigma}) + (1 - \theta)\,(h_{S_2} - h_{2\sigma})$$

Inclusion of a heat term for dilution effects, leads to an expression for the total heat effect measured, ΔH_I, on immersion of the solid:

$$\Delta H_I = \Delta H_W + \Delta H_D \qquad (1.31.)$$

$$\Delta H_W = \Delta H_I - \Delta H_D$$

$$= \theta \Delta h_{S_1} + (1 - \theta)\,\Delta h_{S_2} + \theta \Delta h_{1\sigma} + (1 - \theta)\,\Delta h_{2\sigma} \qquad (1.32.)$$

Δh_{S_1} and Δh_{S_2} are the net integral energies of

adsorption: all the terms in equation (1.32.) can be evaluated from adsorption isotherms, or heats of immersion or solution; heats of wetting obtained from both equations (1.31.) and (1.32.) compare very favourably.

An equation which is analogous to equation (1.31) and which is applicable to the Flow Microcalorimeter process may be written:-

$$\Delta H_A = \Delta H_{EA} - \Delta H_{W_{Solvent}} \pm \text{effects of}$$

dimerisation, intermolecular reaction, hydration and water displacement, where applicable. ——— (1.33)

(where: ΔH_A = heat of adsorption of solute

$\Delta H_{W_{Solvent}}$ = heat of wetting of solvent, enthalpy change due to expulsion of solvent mols. from adsorbed layer

ΔH_{EA} = heat of exchange adsorption of acid observed).

This expression has been found to be the most useful in interpreting many of the flow microcalorimeter results. By assigning estimates for these values of the system under examination, one can convert with

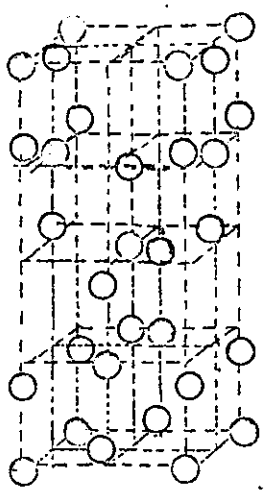

Fig. 1.1.a. The Anatase Structure.

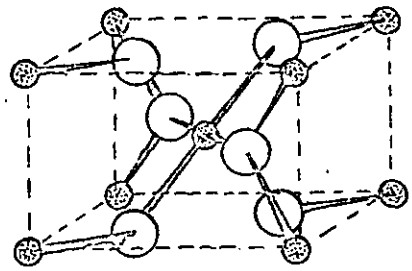

Fig. 1.1.b. The Rutile Structure.

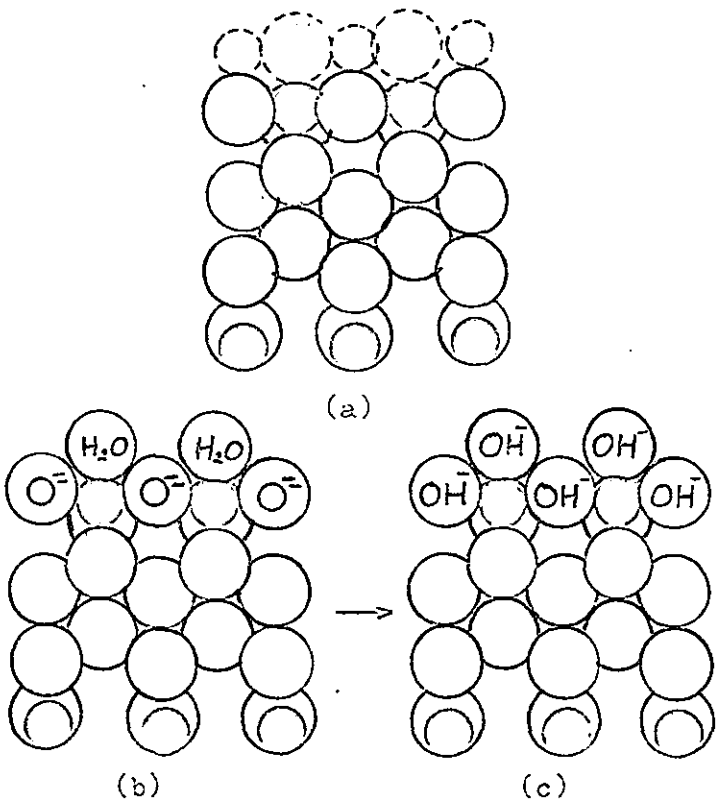

Fig. 1.1.c. Structures of (001) crystal faces of Anatase

(a) clean (b) hydrated (c) hydroxylated

The broken circles show how the lattice would continue

reasonable accuracy and assurance from the "heats of exchange adsorption" measured directly by the Microscal instrument, to "heats of adsorption".

1.5. Surface Characteristics of Titanium Dioxide

The vast majority of systems examined here are concerned with various titanium dioxides. There are two crystalline modifications of importance only, anatase and rutile, of which the latter is a distorted octahedral crystal form of the former.[31] (see figures 11a and 11b). The features which distinguish the various types are a function of their respective surface treatments, modifications made to improve dispersion in various vehicles, and eliminate photochemical activity.

Various amounts of compounds of aluminium, zinc and silicon are frequently used, being incorporated with the pigment either during the wet or dry milling or by mechanical mixing. The resulting layer rarely completely covers the pigment surface but totally changes its chemistry and behaviour. Surface active agents are also popular, as improvements in wetting dispersibility and the resulting gloss of paint arises. Precipitation on the pigment surface of the hydrophosphate of titanium, titanium phthalate, zirconium

phosphate, basic phosphates of aluminium and titanium and hydrated oxides of aluminium, silicon, titanium and zinc, have been reported in many patent specifications as well as surfactants such as, ethylenic oxides, sodium stearate, aluminium palmitate and cyclohexamine salts of phosphoric or boric acids.[32]

Titanium dioxide in pure pigmentary form is completely hydroxylated; (see figure 1.1.c)[33] this is proved by infra red spectroscopy[34] and from the fact that surface esters were formed on reaction with ethanol for example, in an autoclave. The extent of surface hydration is dependent on the temperature of pre-treatment:[32,35,36]

1. If removed at up to 100°C, molecular water bound by physical adsorption or capillary condensation
2. If removed at 100°C - 150°C, molecular water by hydrogen bonding
3. I f removed at 250°C - 400°C, as hydroxyl groups

Investigations of the nature and quantity of hydroxyl groups present continue as new techniques and instrumental precision are evolved. The properties of the electrical double layer particularly, and the behaviour of the surface adsorbed layer also, each appear to be a complex function of the chemical and thermal history of a given sample in a given solvent.

Care must be taken, however, when drying the sample: heating in a vacuum usually causes reduction of surface Ti^{++++} ions to Ti^{+++}, perceptible by a darkening of the powder. This is a reversible change - if later exposed to rigorously-dried air, it will re-oxidise. In addition at temperatures in excess of about 130°C sintering of the surface coating could take place.

It has been shown that alcohols are adsorbed by a mechanism of hydrogen bonding between the hydroxyl groups[37]; carboxylic acids are adsorbed either by hydrogen bonding of the carboxyl group or by proton transfer to the surface, the so-called "acidic" or "ionic" mechanisms.[38] Amines adsorb probably by ionic mechanism on surfaces which are relatively more acidic (for example, a silica-rich surface treatment).

1.6. Results on Analogous Systems

Colloidal dispersion stability determinations based on adsorption measurements have been carried out for some thirty years. Carbon black and various metallic oxides have been a popular choice of substrate to study, chiefly on account of their fine particle size. Studies widened to include pigmentary grades of oxides ($\geqslant 0.1$ diameter) during the 'fifties. Clashes of opinion

occured over mechanisms of stabilisation: charge stabilisation on the one hand and adsorbed layer steric hindrance on the other.

Koelmans and Overbeek[3] suggested that van der Waals' attractive forces can only be overcome if the stabiliser chain length is comparable with the particle size, in non-polar solvent. A considerable volume of work carried out by Dintenfass[39, 40] involving selective polar adsorption on pigments also established that the titanium dioxide surface is heterogeneous. The adsorption of various functional head groups on rutile from toluene is reported as well as various acids from a range of solvents. This heterogeneity accounts for the catalytic and adsorptive properties and the variation of thermionic and photoelectric work functions on the same crystal. Harkins[7] has indicated that no account has been taken for the possible effects of different crystal faces, edges and corners, the observed adsorption and energy relations being a statistical summation of all these.

Subsequent work[37, 38] dividing polar adsorption into "acidic" and "ionic" types tends to discount some of the postulates of Dintenfass, viz: no preferential adsorption of longer chain compounds with identical head group, and no "discrimination" of

adsorbate groups by various active sites.

Kajanne[41] has shown that more unsaturated fatty acids were preferentially adsorbed at low concentrations on haematite during a froth flotation process when linseed oil fatty acid adsorption was examined. The adsorbed layer was multimolecular. Petit et.al.[42] examined the adsorption of lauric acid on titanium dioxide from a mixture of saturated aliphatic hydrocarbons and found good agreement with previous results up to 5% acid concentration.

Later work, for example by Kipling and Wright,[29] Ottewill and Tiffany[17, 18] has dwelt on theories of orientation of adsorbed species, particularly acids in organic solvent, on titanium dioxide. By assuming values for the areas of cross section of the vertically - and the horizontally - oriented molecule, and knowledge of the limiting value of adsorption either from a plateau, or an isotherm extrapolated to the limit of solubility of the system, orientations are easily deduced.

A series of papers[37, 43, 44] by Sherwood, Rybicka and Kelman tends to highlight adsorption mechanisms and effects of water as an impurity at the surface. Doorgeest[45] has also studied the influence of water on the adsorption on rutile of resins, stearic acid and

stearyl alcohol in an article which concluded, like Sherwood and Rybicka[9] that chemisorption of the acid but not the alcohol, is evident on moist, zinc-bearing rutile and that the different adsorbate molecules are adsorbed on the same surface sites.

Chapter 2

The Flow Microcalorimeter

2.1. Principles of Calorimetry

Calorimeters are used in the study of a wide range of systems. They are designed to fulfil such a number of needs for the individual operator that they necessarily vary considerably in design features and operational techniques.

Static calorimeters are used at constant or nearly constant temperature between well defined, stable initial and final states which are generally in equilibrium. Dynamic calorimeters have a continuously changing temperature and true equilibrium states can only be achieved when using the so-called "saturation technique" in which a substrate, already equilibrated with a flow of solvent is allowed to re-equilibrate with a solution.

The major problem in practical calorimetry is generally the control of undesirable heat losses. Early calorimeters were contained within large jackets of air or a fluid so that the temperature rise of the jacket was negligible when the calorimeter's temperature rose, and the actual heat exchange between the two could be deduced from Newton's Law of Cooling.

Around the turn of this century adiabatic jackets came into popular use; these reduced considerably, but

not entirely eliminated, uncontrolled heat losses or gains of the calorimeter by maintaining the jacket temperature the same as that of the calorimeter. This infers the necessity to be able to supply or remove heat to the jacket continuously, independently of the calorimeter, which is very difficult in practice to do accurately.

The alternative approach was to evaluate heat exchanges between the jacket and calorimeter, were they large or small, from a knowledge of the specific heats, masses and densities of the system. The jacket temperature was kept constant, as a consequence of heavy lagging of the calorimeter.

Evaluation of heat exchanges was recognised to be avoidable by use of twin or differential calorimeters in which two matched calorimeters were placed in the same or identical jackets, one containing a standard system, the other an experimental one, and evaluating the latter by difference from the standard. This method requires the change in temperature of the experimental system to be of a higher order than the difference between the initial temperature and that of the surroundings. Alternatively electrical calibration involving heat changes of the same order as these anticipated in use immediately compensated heat losses incurred.

2.2. The Commercial Instrument

The flow microcalorimeter was developed by A.J. Groszek in the research laboratories of the British Petroleum Co., at Sunbury, and later manufactured and marketed by 'Microscal Ltd', 20 Mattock Lane, Ealing, W.5. Early systems studied involved metals and metal oxides in powdered form, which adsorbed detergents from lubricating oils[46] and works involving the adsorption of hydrocarbons on to cast iron[47] and also on to molybdenum disulphide, boron nitride[48] and tungsten sulphide, graphite[49] soon followed. With some adaptation the instrument proved useful in the photographic field, especially with regard to the adsorption of gelatine[50,51] and stabilisers[52] on silver and silver compounds. It is known to be proving of considerable interest in the research fields of pigments, dentistry, metal corrosion, and catalysis, as well as research generally in surface chemistry and solution thermodynamics.

2.2.1. Design

The purpose of the instrument when originally conceived was to enable a study of surface reactions by monitoring the accompanying heat changes. If the

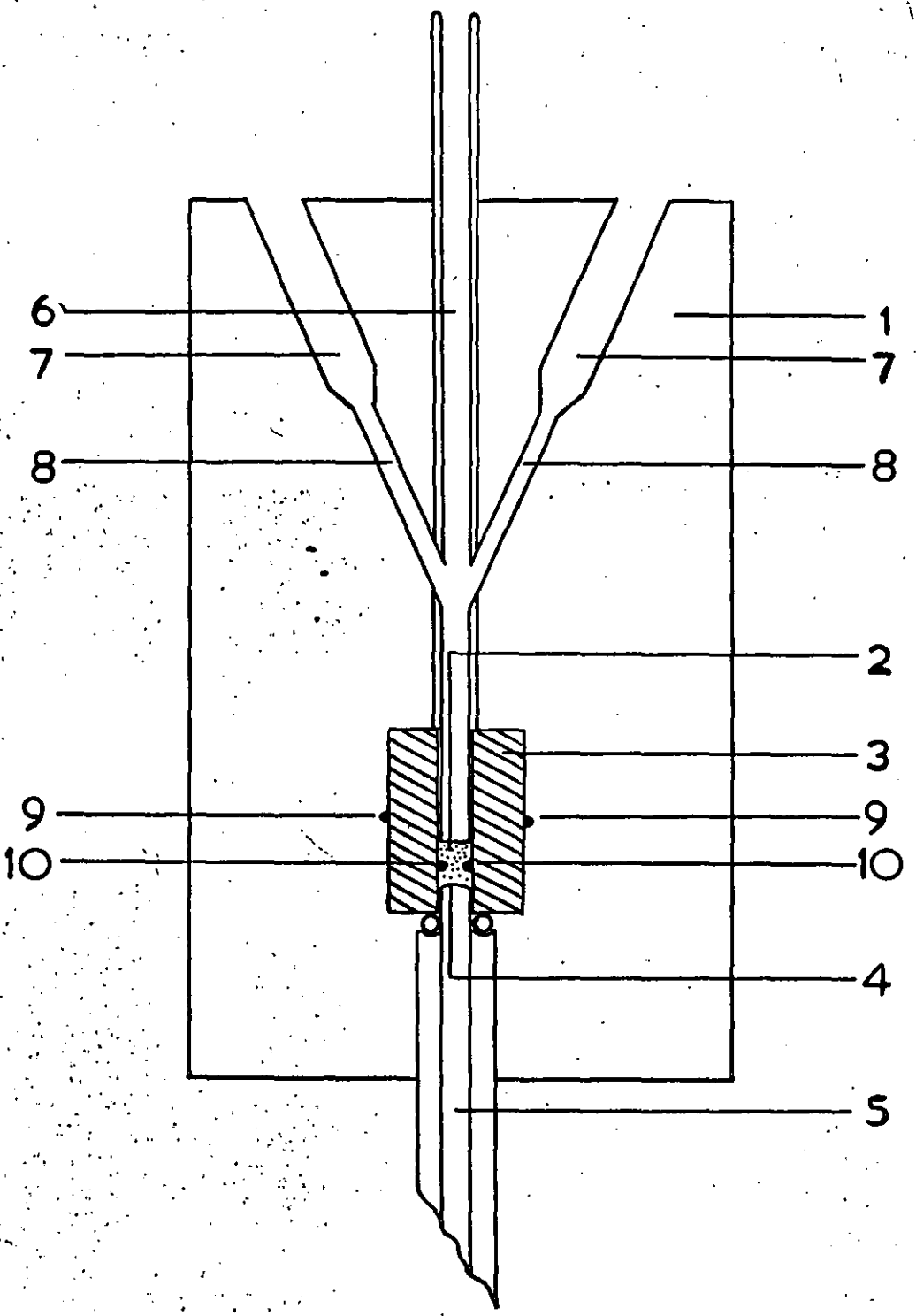

Fig. 2.1: THE FLOW MICROCALORIMETER.

adsorbent could be in powder form, the adsorbate which may be gaseous or in liquid phase would be allowed to enter the surface phase when permeated through the powder bed in the calorimeter. Thermistors were realised to be the most compact and sensitive detectors of temperature change.

2.2.2. Construction

A schematic diagram of the flow calorimeter is shown in figure 2.1. It consists of a cylindrical aluminium block (1) 16.5 cms in height and 15.5 cms in diameter. A hole drilled through its axis houses a Teflon cell (3) 6mms internal diameter and about 3cms in length. The base of the cell is closed by clamping against it, a spring-loaded outlet tube (5) having a stainless steel 500-mesh gauze (4) surrounded by a rubber O-ring for a liquid-tight joint. This supports the powder (2) under examination, an outlet tube (6) is secured by screws; its base fits snugly against the top of the cell.

Temperature changes are detected by two thermistors (10) which protrude from the cell walls and are covered by the powder. They are connected in a Wheatstone Bridge circuit (figure 2.2.a) and are.

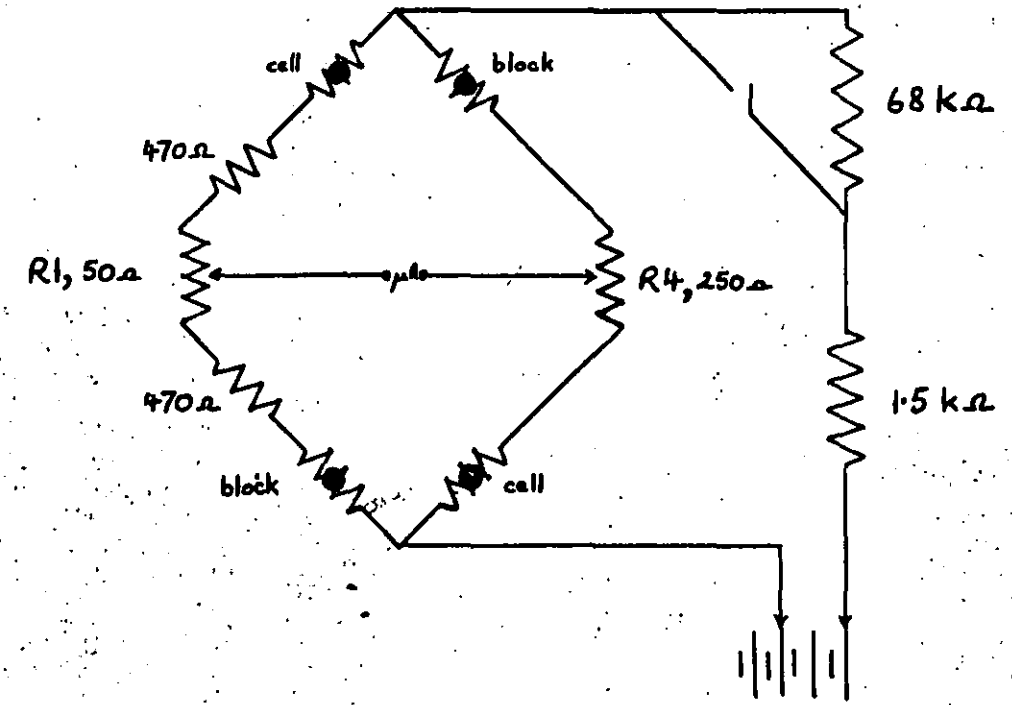

Fig. 2.2.a: THERMISTOR BRIDGE CIRCUIT.

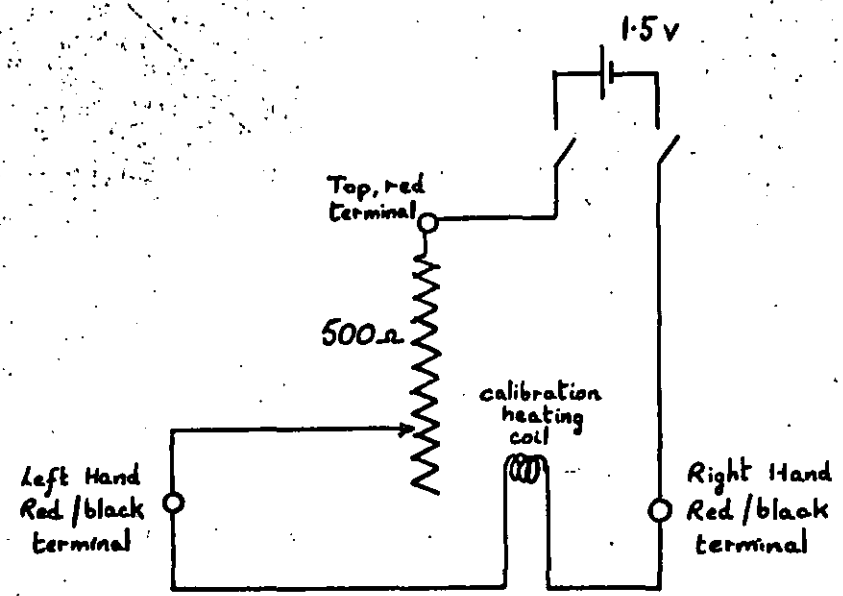

Fig. 2.2.b: CALIBRATION CIRCUIT.

opposed by two reference thermistors (9) embedded in the metal block. The output (imbalance is caused by temperature change) is fed via an amplifier unit to a potentiometric recorder.

There is provision for experimentation above ambient temperature: the metal block may be heated up to 150°C by means of a thermocouple embedded in the block which is fed by a stabilised power supply via a variac control unit. It will give an output of approximately 40 μ volts/°C above room temperature. There are two further cylindrical cavities (7) to accommodate containers of solvent and solution and allow their temperatures to reach that of the calorimeter, prior to reaction. The liquid then percolates through the narrow channels (8) into the cell.

The powder bed formed in the cell occupies approximately 0.15 ccs when its level is 2 mms above the level of the thermistors.

The block is heavily lagged and mounted with electrical components and batteries inside a cabinet which stands on three legs, allowing ready access to the base of the cell. (figure 2.3)

A bank of four 1.5 volt batteries feeds the bridge circuit (figure 2.2.a) and the sensitivity switch connects in one, two, three or all of these; a supple-

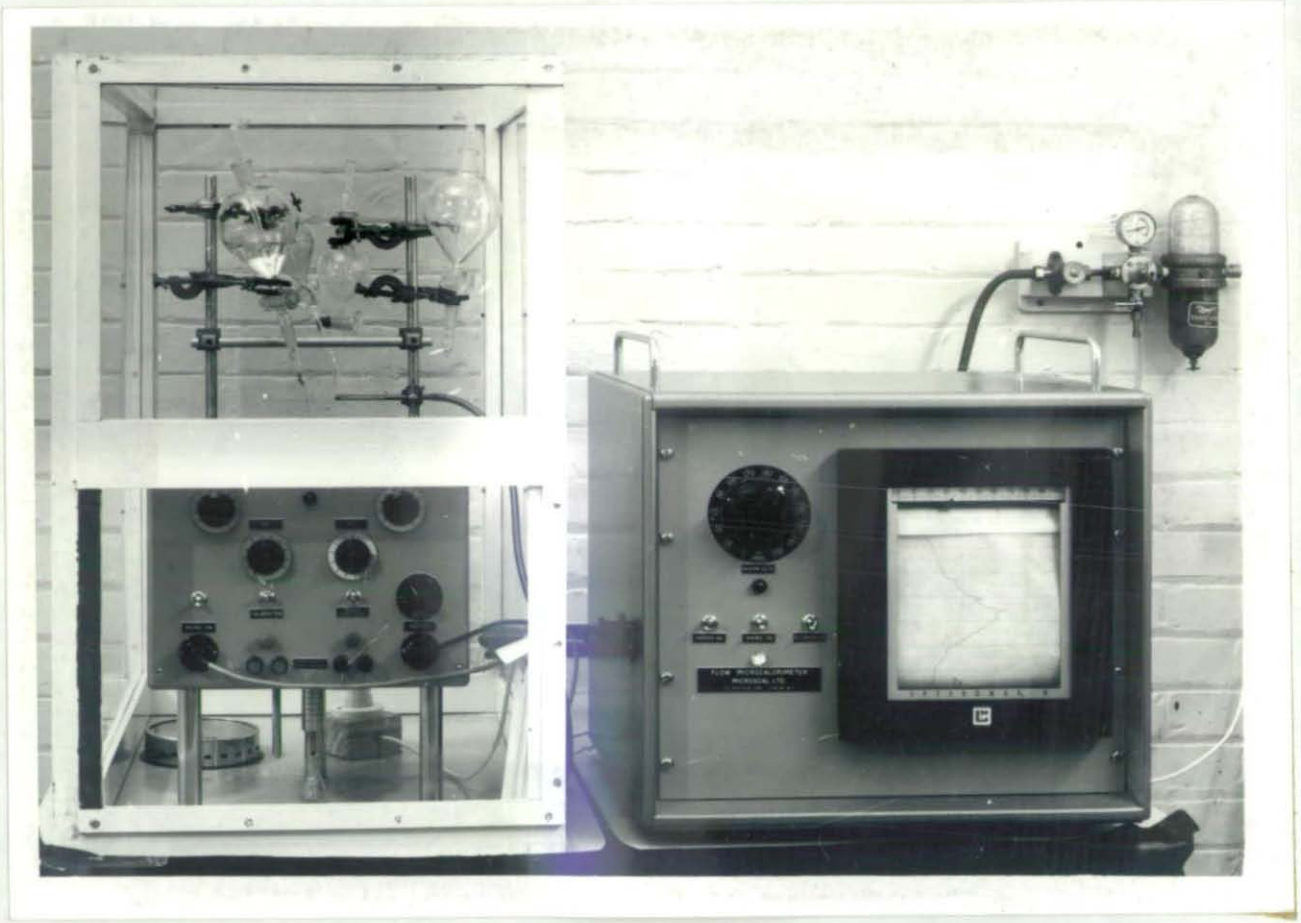

Fig. 2.3: THE FLOW MICROCALORIMETER

mentary toggle switch connects into the circuit an additional resistor to reduce sensitivity. R1 and R4 are adjustable resistances which are required to adjust the output voltage (i.e: the position of the pen on the potentiometer slide wire and hence on the chart). The thermistors are matched pairs of the 'bead at the end of a glass probe' type having resistance of approximately 4.15 K_Ω at 25°C and a temperature coefficient of - 3.7% per degree centigrade at 20°C. The current they pass is considered to be directly proportional to the voltage applied when operating in the calorimeter.

2.2.3. Calibration

A third adjustable resistor, R2, is used in the calibration circuit, figure 2.2.b, together with a single 1.5 volts battery, bipolar switch and an adapted outlet tube containing a small heating coil soldered into the stainless steel gauze. By applying a voltage across this coil for varying periods of time, heating effects are produced and a series of peaks of different shapes and sizes are observed on the recorder chart.

Each peak comprises two curves, one heating and

one cooling.

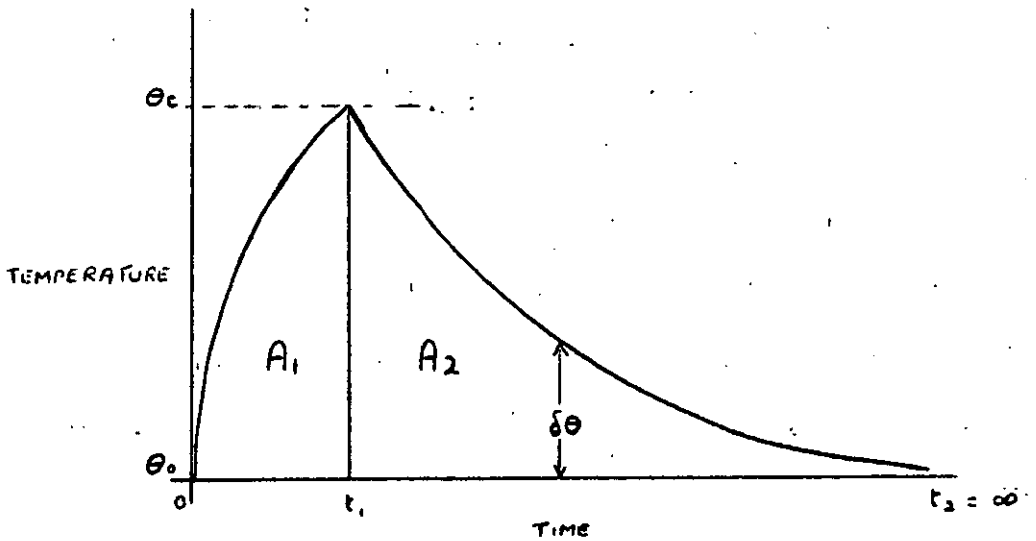

Over the heating portion of the curve the energy input is proportional to time of flow of current; over both portions the heat lost is proportional to the excess of the higher temperature over that of ambient, provided Newton's Law of Cooling is obeyed:

$$\text{i.e:} \quad -Q = \text{heat lost} = K \times \int_{t_1}^{\infty} \delta\Theta \, dt$$

$$= K.A2$$

(where: K = some constant

A2 = area under curve as shown)

Similarly, heat lost during heating:

$$= K.A1$$

Since the original and final temperatures are the same, the total heat loss must equal the total heat input.

i.e: $K (A_1 + A_2)$ = total energy input.

Hence the energy input is proportional to the peak areas; this is found to be so up to about 60 millicalories' output from solid/liquid systems.

2.2.4. Sensitivity

Extremely small temperature changes are generally observed for surface reactions. As so little adsorbent is examined, involving perhaps less than $1m^2$ surface, the instrument is necessarily sufficiently sensitive to detect a change of temperature as little as $10^{-4}{}^{o}C$. With reference to figure 2.2.a, assuming the output is measured from the midpoints of each of R1 and R4, and considering each side of the bridge to be a potential divider, its output voltage can be shown to be 94.85mV for $1^{o}C$ temperature change at the thermistors in the cell.

Using a similar potential divider method (comprising kilo-ohm 1% tolerance resistors and a 1.8ohm 5% tolerance wound resistor), a full scale

deflection (f.s.d.) of the recorder is obtained from an input voltage of 1 millivolt i.e: each scale division (.01 x f.s.d.) represents a temperature change of 1.05×10^{-4} °C at maximum sensitivity which would occur from heat effects close to 25 μcalories. The variation of temperature changes which give rise to a f.s.d. with sensitivity is shown in table 2.1.

Table 2.1. Variation of Sensitivity of Calorimeter.

Sensitivity Setting	Bridge Voltage (volts)	Bridge Output (mV/°C)	Temperature Change/f.s.d.
4N(maximum)	5.42	94.85	.0105
3N	4.10	71.75	.0139
2N	2.70	47.25	.0212
1N	1.33	23.275	.0430
4R(reduced)	0.68	11.90	.0840
3R	0.505	8.838	.1132
2R	0.33	5.775	.1732
1R(minimum)	0.155	2.713	.3687

Such sensitivity is made possible as a result of its high thermal stability; it is amply lagged and the thermal capacity of the cell is very low; most heat which is developed is absorbed by the solvent flow. The effect of solvent flow rate on the effective

thermal capacity is estimated using the calibration coil; current is passed until a new position of equilibrium is attained on the chart. It will vary slightly according to the flow rate and as both the rise in temperature and the heat supplied are known, the effective thermal capacity can be deduced to be approximately constant over this range of flow rates:-

Table 2.2. Variation of Effective Thermal Capacity with Flow Rate

Flow Rate (n heptane)		Displacement of Base Line		Time to Attain Equilibrium (secs)	Effective Thermal Capacity (mcals/^{o}C)
needle	mls/min	Divisions	^{o}C		
28G	.096	74	.0157	430	2.00
30G	.057	72.8	.0154	485	2.29
32G	.035	72.8	.0154	500	2.37
34G	.003	70.6	.0150	460	2.24

Subsequently - marketed models have incorporated a D.C. Amplifier between the calorimeter and the potentiometer amplifier, to increase the sensitivity.

In practice there is also a limit on the permissible time duration of a heat change process, particularly if this is relatively small: this limit is governed by the base-line stability. If the recorder deviates from

its base-line for more than about 60 minutes as a result of a heat change, an extremely steady and non-drifting base-line is demanded in order to interpolate with confidence between start and finish of peak. In fact a base-line whose drift is not greater than 1 f.s.d. in 18 hours (i.e: 1 scale division, say 2×10^{-4} °C, in 10 minutes) is sufficiently stable. The chart moves at 1 foot per hour.

The flow rates from the two flasks must be identical, otherwise the base-line will be unstable at the point of changeover. The thermistors, passing current, have a power dissipation: "maximum mean power dissipation in liquid at 20°C averaged over any 20 millisecond period does not exceed 100 mW" ≡ .024 calories per sec . Such dissipation will be reduced by the increased cooling effect of an increased flow rate through the cell. The thermistors will detect this as an apparent endothermic process, and the bridge balance will be shifted.

2.2.5. Operating Technique

Reactional heat changes are assumed to take place at constant temperature, and no correction is made for heat losses.

The calorimeter is constructed on the micro scale to reduce overall temperature changes and ensure they remain uniform throughout the cell: the weight of titanium dioxide pigment used is generally 250 mgs and extremely low but accurately-controlled flow rates (in the region of 0.05 mls/minute) are employed.

Having ensured the cell is cleaned and free of dust (inspection is facilitated by use of a small 'pen' torch) the outlet tube is clamped in position, and it is plugged with a rubber bung. About 2 mls of the solvent to be used are pipetted into the cell to fill it and the weighed quantity of pigment (about 250 mgs) poured into the cell via a funnel. It is allowed to settle and form a bed on the gauze: to try to ensure uniform and constant packing of this bed, an arbitrary period of three minutes is devoted to the settling process, following which the solvent is drained away, the inlet tube clamped in position and the flow of solvent established, from a 250 ml. tap funnel clamped in position as shown in figure 2.3.

Having adjusted the sensitivity to the desired level, (the maximum level possible without the expected peak going off chart) altered R1 and R4 to move the pen into position on the chart, prepared a solution from which adsorption will be studied and obtained a stable base-line on the chart, the adsorption process may be

commenced. Adsorbate is introduced into the cell in one of two ways.

The method, generally employed so-called the "saturation technique" involved use of a second identically set-up flask containing the solution and the flow of solvent is immediately replaced by flow of solution. Ideally, one adsorption peak is now observed: the desorption process is followed by reverting to solvent as before without disturbing the flow. After any surface reaction, provided the flow rate is the same as initially, the base-line should be in exactly the same position on the chart as before the reaction.

Alternatively, the solution is injected from a microsyringe into the undisturbed solvent flow, the so-called "pulse technique" when, if a reversible adsorption process occurs, a peak, followed by a desorption trough is observed, as the solvent immediately washes off the surface most or all adsorbate which had just adsorbed.

In conclusion, the inlet and outlet tubes are removed and pigment removed by washing with low boiling point petroleum spirit in conjunction with ultrasonic irradiation to clean them. A wash-bottle containing the same petroleum spirit and pipe cleaners are used

to remove with care, residual pigment in the cell, around the thermistors.

The most suitable way of measuring the peak area, is to trace each one on to fine quality unruled foolscap paper, cut out the tracing, and weight it. This, perhaps surprisingly, has been found to be more accurate than use of a planimeter (which is ideally used only for areas in excess of 50 cms^2 or so, while some calibration peaks are only 2-3 cms^2 in area) or the counting of squares of chart paper within the peak.

In studying organic pigments it was found to be necessary to pretreat them in order to improve the permeability of the bed they formed. They were mixed into a slurry with water, dried overnight in an oven at 120°C, crushed in a mortar and sieved dry between 100 and 200 mesh sieves. This ensured that no clusters $>150\mu$ in diameter, and no primary particles were used in the calorimeter; most were $\geq 75\mu$.

2.2.6. Modifications

The operation of so sensitive a calorimeter demanded close regulation of temperature control. Initially it appeared to be remarkably unaffected by draughts, but the slightest changes of temperature, even of the

order of 0.5°C, in the room caused a prolonged drift of the pen owing to the delay in the heating or cooling of the block to that of the surrounding air.

The room was therefore thermostatted accurately; the thermostat unit mounted on the wall behind the calorimeter was connected to a small 3 KW fan heater fixed to the wall at the opposite side of the room. An old balance cabinet was fitted with perspex sides and two sliding doors at the front to provide access, and placed over the calorimeter. Its edges were crudely sealed with Sellotape and air from a compressed air line was fed into the cabinet, at the room temperature via a tube of diameter 4.5 cms and 25 cms in length, which was packed with silica gel. This ensured a continuous change of air in the cabinet and allowed control of humidity down to around 10% if necessary.

During winter time when the heat losses from the room (which is situated directly beneath a flat roof) are considerable, the fan heater was switched on with increased frequency and could cope quite adequately with control of temperature. However, as the heating required is reduced in summer, the heat output tended to become erratic and it was necessary to by-pass this system with an auxilliary one involving a 'Transtat' non-indicating temperature controller which is fully

transistorised and uses a platinum resistance bulb as a sensing element.

Figure 2.3 also shows two smaller flasks to which capillary outlet tubes were fused. Flow rates were timed from each flask and compared; equalisation was achieved by snapping off short lengths of the capillary of the slower flow-rate flask until equal to the other. This procedure was tedious and the capillaries were exceedingly accident-prone, so two tap funnels had ground glass Quer-type nozzles fused to their outlet tube. This allowed ready interchange of 2" long stainless steel hypodermic needles between the flasks. In this way an exactly reproducible and equal flow was obtained from different flasks at any time. However, if standard needles were used it reduced the flow rates possible to three of four distinct values (depending on the internal gauge of the needle) instead of a whole range of capillary sizes. It also precluded the use of two liquids whose viscosities varied widely, but as only dilute solutions were ever used this was of no disadvantage.

In order to safeguard against individual failure of the cells which feed the bridge, and hence irregular variation of the sensitivity settings, it is proposed to replace the switch with five hundred-ohm resistors

connected in series with all four batteries and several tappings to connect in one or more of these into the bridge circuit and so vary its voltage.

The flow system is considered to be adequate; some users have led liquid from each flask in turn down a single inlet tube via a three-way tap, often using the tap to adjust the rate of flow. While this prevents any heat changes within the calorimeter cell arising out of mixing there, it is difficult to reproduce a flow rate precisely by adjustment of this tap, and the flow rate has been shown to cause variation in the peak area for a given heat input, particularly when the former is increased above 0.075 mls/min[53] which is still a relatively slow flow rate. The change-over of flasks described previously means a doubled flow rate for about three seconds which cannot be observed on the chart. (The opening and closing of flask taps while 'in situ' is avoided as they are not greased and can stick or fall out, or the needle can be damaged, when being hurriedly manipulated).

CHAPTER 3

EXPERIMENTAL

3.1. Materials

3.1.1. Pigments

All experimental work has been carried out using titanium dioxide of various forms, with the exception of the investigations made in connection with surface area measurement; in this case a range of metals, metal oxides and organic pigments were used. The titanium dioxide samples were always commercial grades, except for a series of treated rutile samples, kindly supplied by Dr. H. Rechmann of Titangesellschaft A.G.

3.1.1.1. Storage and Drying

All pigments were used exactly as supplied except in one isolated case where dialysis was carried out to remove water-soluble surface material. The conditions of storage varied, however, and the pigment was defined according to these:

.i. Weighed quantities of the 'dried' pigment had been placed overnight in an oven at a temperature between 120° and 130° . This temperature was considered not to be high enough as to cause dehydration of the surface treatments, but sufficient to remove all but the first or part of the first, mono-

layer of water on the surface, (that is, the loosely held, physically-adsorbed water molecules). It was then rapidly transferred to the calorimeter via a desiccator.

.ii. The "normal" pigment was stored for at least a week in a desiccator containing a saturated solution of sodium bromide whose S.V.P. was 60% relative humidity @ 25°C. In this state it was considered to contain several layers of loosely held water on the surface, and corresponded most closely to the batch pigments actually used at the time of paint manufacture.

.iii. The "wetted" pigment was stored over water, for a week or more prior to use.

3.1.1.2. Surface Area Determination

The surface-treated rutile samples were supplied with surface area data, but other pigments required a determination to be made. This was done by the method of Brunauer, Emmett and Teller[54] using nitrogen as the adsorbate, at 77.5°K. A monolayer volume, Vm, deduced using the equation:

$$\frac{p}{V\,(po - p)} = \frac{1}{Vm\ C} + \frac{(C-1)}{Vm\ C}\,\frac{p}{po} \qquad (3.1.)$$

(where p = pressure of nitrogen

po = S.V.P. Of "

V = volume adsorbed

C = a constant, related to the energy of the gas adsorption).

The left hand side of equation 3.1. is plotted against the partial nitrogen pressure $^{p}/_{po}$ to obtain a straight line over an approximate $^{p}/_{po}$ range 0.05 - 0.35. Its gradient is (C - 1)/Vm C and its intercept 1/Vm C. It can be deduced that Vm = 1/(gradient + intercept) and this is converted to a value of the specific area if it is assumed that the area occupied by a nitrogen molecule in the monolayer is 16.2 A_o^2. mol^{-1}.

$$S.A. = \frac{Vm.No.\ 16.2}{22.4 \times 10^3 \times 10^{20}}\ m^2\ g^{-1} \qquad (3.2.)$$

(where Vm is measured in ccs. at S.T.P

No is Avogadro's Number).

3.1.1.3. Surface Area Results and Analysis Data

Surface Area results quoted below have been

TABLE 3.1. ANALYSIS DATA

	$\%TiO_2$	%ZnO	$\%Al_2O_3$	$\%SiO_2$	$\%P_2O_5$	%Loss @ 105°C	% Soluble Salts	Surface Area $m^2 g^{-1}$
Rutile R_1	99.5	nil	nil	nil	-	-	-	7.22
Rutile 5	93.5	1.0	2.0	1.5	0.2	0.7	0.1	14.72
Anatase 10b	98.5	<0.002	<0.10	0.05	0.4	0.4	0.3	9.30
Treated Rutiles T_1	-	nil	0.5	1.8	-	-	-	8.42
T_2	-	nil	1.0	1.8	-	-	-	8.50
T_3	-	nil	1.5	1.8	-	-	-	10.40
T_4	-	nil	2.1	1.8	-	-	-	11.74
T_5	-	nil	2.1	0.9	-	-	-	10.90
T_6	-	nil	2.1	0.35	-	-	-	9.33
T_7	-	nil	2.1	nil	-	-	-	9.19

measured at the Paint Research Station. The analysis figures of R1, R5 and 10b are not to be regarded as specifications, but merely as typical analysis results, from the manufacturer.

3.1.2. Solvents

3.1.2.1. n-heptane

Early work was completed using n-heptane as a solvent; it is easily characterised, relatively free of homologues, and other difficult - to - remove impurities.

The n-heptane was supplied by May and Baker Ltd (laboratory chemicals). Each winchester quart was opened upon receipt and some dried Molecular Seive type 4A added to allow some drying to take place over the initial period of storage. It was then slowly distilled, and only the fraction boiling between 98°C and 98.5°C was collected, then to be stored in a litre flask containing fresh sodium wire and supplied with a glass stopper covered with a teflon sleeve.

The refractive index was occasionally measured, of the fractions so prepared, by Abbé Refractometer and checked against a literature value of n_D^{20} =

1.38765,[56]. Arbitrary experimental limits of n_D^{20}: 1.389 - 1.387 were chosen.

The water content of the n-heptane was not measured as it was below the limit of detection of the Karl Fischer apparatus.

3.1.2.2. Benzene

This solvent also was supplied by May and Baker Ltd (as "Sulphur-free, crystallisable") and stored over calcium hydride as a desiccant, but prior to distillation, it was refluxed over a soxhlet containing fresh calcium hydride for about 24 hours ensuring that all azeotropes had disappeared. Distillation was then carried out, at 80°C and then storage was over Molecular Sieve type 4A, in a similar flask as before, for never more than three days. Karl Fischer Analyses showed the water content to rise appreciably after this period. The Refractive index was occasionally checked to be $n_D^{20} = 1.501 \pm 0.001$ [56]

3.1.2.3. Measurement of Water content of benzene

The Karl Fischer[57] method is used, in which a technique of back titration[58] may be employed;

excess of Fischer reagent is added to a known volume of benzene and then titrated with a standard solution of water in methanol, to determine the excess.

Fischer reagent is a mixture of methanol, pyridine, iodine and sulphur dioxide and is believed to react with water and consume iodine according to the following mechanism[59]:

$$2C_5H_5N + H_2O + I_2 + SO_2 \longrightarrow$$

$$2C_5H_5N\langle^{H}_{I} + C_5H_5N\langle^{SO_2}_{O}$$

$$C_5H_5N\langle^{SO_2}_{O} + CH_3OH \longrightarrow C_5H_5N\langle^{H}_{SO_4CH_3}$$

The end point is the change of dark brown to pale yellow, but as this is not easy to detect visually, it is generally done electrometrically by connecting two small platinum electrodes immersed in the reaction vessel in series with a spot galvanometer (see figure 3.1.). A small potential (~ 2mV) is applied across them and current flows while excess reagent remains, as iodine compounds in solution depolarise the electrodes. When no

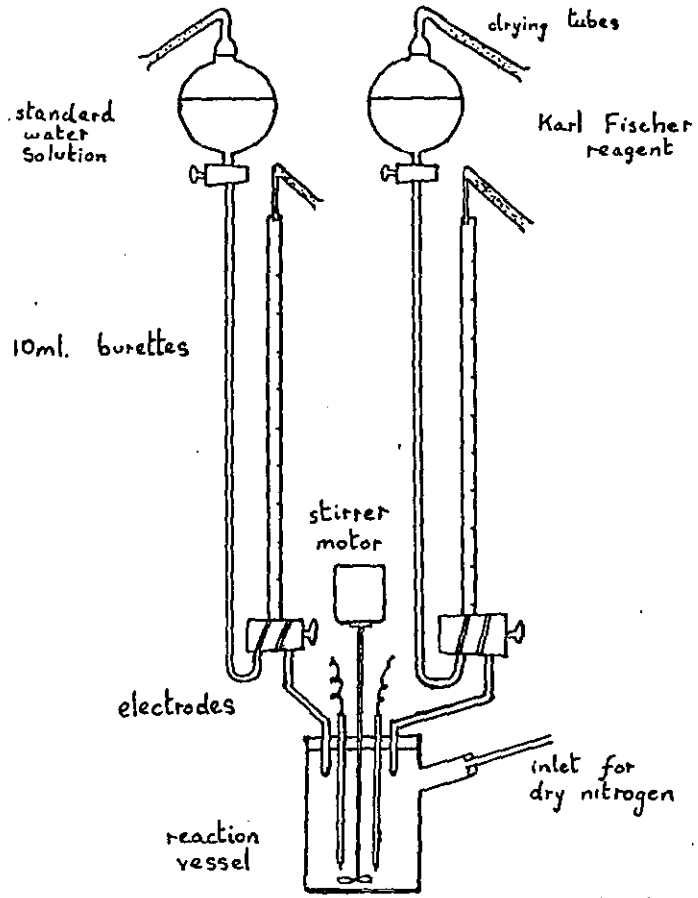

A: TITRATION APPARATUS

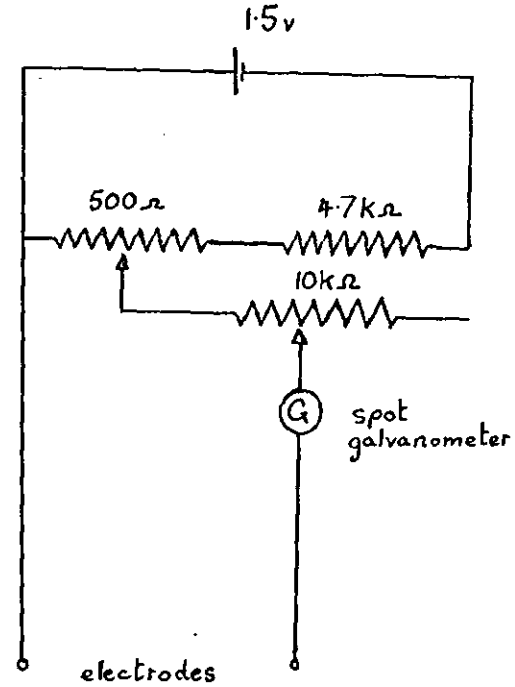

B: ELECTRICAL CIRCUIT FOR DETECTION OF TITRATION ENDPOINT

Fig. 3.1. Apparatus for Determination of Water Content of Benzene

iodine remains, one electrode becomes polarised and the galvanometer deflection falls sharply to zero.

The contents of the reaction vessel are continuously stirred and dry nitrogen flushed through to displace any moist air. About 15 mls. standard solution of water in methanol are run in from the right hand burette, an approximate end point observed on running in Fischer reagent from the other burette, a few mls. excess added, then a more accurate end point attained with water solution back titration. Each titration carried out systematically takes three minutes.

The lowest reliable limit of detection of water with this instrument is 0.020 mg. $ml.^{-1}$ (Table 3.2.).

3.1.3. Adsorbates

These were generally Fluka (grade, puriss) with the exception of several samples supplied either by Kodak Ltd. or by Koch - Light Laboratories. All were used as supplied without any further purification process.

The alkyd resins were commercial grades. In the pulse injection work, Paralac 10 (a long oil linseed penta glycerol resin) was used from solution

TABLE 3.2. WATER CONTENT OF BENZENE

TREATMENT	WATER: $mg.ml^{-1}$	WATER p.p.m. by weight
As supplied	0.275 ± 0.020	313.9 ± 22.8
Stored 1 week over CaH_2	0.124 ± 0.009	141.6 ± 10.3
Immediately after reflux and distillation	0.020	22.8
Distilled + 1 day's storage	0.020	22.8
Distilled + 2 day's storage	0.020	22.8
Distilled + 3 day's storage	0.051 ± 0.004	58.2 ± 4.6
Distilled + 4 day's storage	0.063 ± 0.005	71.9 ± 5.7
Distilled + 5 day's storage	0.118 ± 0.009	134.7 ±10.3

in benzene.

3.2. Measurement of Adsorption Isotherms

3.2.1. Apparatus

Adsorption isotherms of lauric and stearic acid were determined by a liquid scintillation counting method using a Panax SCLP2-counter which contained an EH 60975 photomultiplier (water cooled for constant temperature and background noise reduction). The scaler and timer were Panax 6 decade indicating types P7100, P7200. Small flat bottomed glass vials (D.J. jars) were used to contain samples to be counted; to these had been added a liquid scintillator, Nuclear Enterprises' (Edinburgh) N.E. 214 which is a xylene-based scintillator containing naphthalene to shift the wavelength at which maximum emission occurs to 4200 A^{o}, the region of maximum sensitivity of the photomultiplier tube.

The oleic acid system was suspected to be quenched when counting commenced (see section 3.2.2.) so a Panax windowless counter was employed to count, via a plastic phosphor and similar photomultiplier, very small evaporated samples on aluminium

plancettes. The efficiency of this method is inferior, however, to liquid scintillation counting, although problems of quenching or self absorption are eliminated.

3.2.2. Principles of Operation

The solution containing radioactively-labelled molecules of acid is mixed with an excess volume of scintillator (volume ratio solution: scintillator= 1 ml: 5 mls.) in the D.J. jar. Carbon-14 is a low energy β - emitter; when the scintillator is struck by an ionising particle it is excited, and on returning to its original ground state it emits a photon; each of these is detected by the photomultiplier and converted into a voltage pulse. Such pulses are proportional to the energy lost by the β - particle. They are amplified and fed via a pulse height analyser to the decade counter, i.e: it acts as a spectrometer.

This method of counting ensures geometrical reproducibility, as with all fluid counting methods, the counting is extremely rapid (up to 10^4 c.p.s may be achieved before coincidence losses break down the accuracy and 10^5 counts are sufficient

for statistical purposes) and the accuracy can approach ± 0.5%. The disadvantages of the method are that one must avoid the analysis of supersaturated solutions, (as radioactive material may be deposited on the walls of the container) the necessary cooling of the assembly (either by fridge or with water, to reduce the background noise level) and the necessity to used very pure solvents to avoid 'quenching'. This is the prevention of light flashes from being registered by the photomultiplier tube either owing to the colour of the solution or to compounds present which absorb the energy, giving rise to scintillations prior to the actual light emission.

The use of planchettes requires either an infinitely thick or an infinitely thin solid film be counted to ensure the geometry for a reproducible number of β - particles to reach the phosphor. Although this method eliminates concern over quenching or self absorption losses, it introduces considerable pipetting errors as small pipettes are used, and most important, reduces the overall efficiency of counting from around 80% for liquid scintillation counting to around 15%.

3.2.3. Optimum Settings of the Counter

The overall response is largely a function of the settings of the high voltage from the scaler unit to the photomultiplier (E.H.T.), the pulse height analyser threshold or discriminator bias voltage, and the counter amplifier gain.

Sealed ampoules of both a standard and a background were counted at differing settings of the E.H.T. voltage with two discriminator bias values, (e.g. figure 3.2.). A plot was then made (e.g. figure 3.3.) of the (source count rate)^2 divided by the background count rate, again at two values of the discriminator bias: maximum efficiency was achieved when (source count rate)^2/ (background count rate) was a maximum. From this two approximate E.H.T. settings were chosen and at these values, count rate against discriminator bias voltage were plotted, to determine the optimum bias voltage, where the curve deviated from linearity. (e.g. figure 3.4.).

The final settings chosen thus gave a high source count rate with relatively low background count rate, a source count rate which didn't change significantly with E.H.T. variation and which produced only small change of count rate with discriminator bias. These were found to be 1200 volts E.H.T. and 12 volts bias for stearic acid (figures 3.2.,3.3.,3.4.)

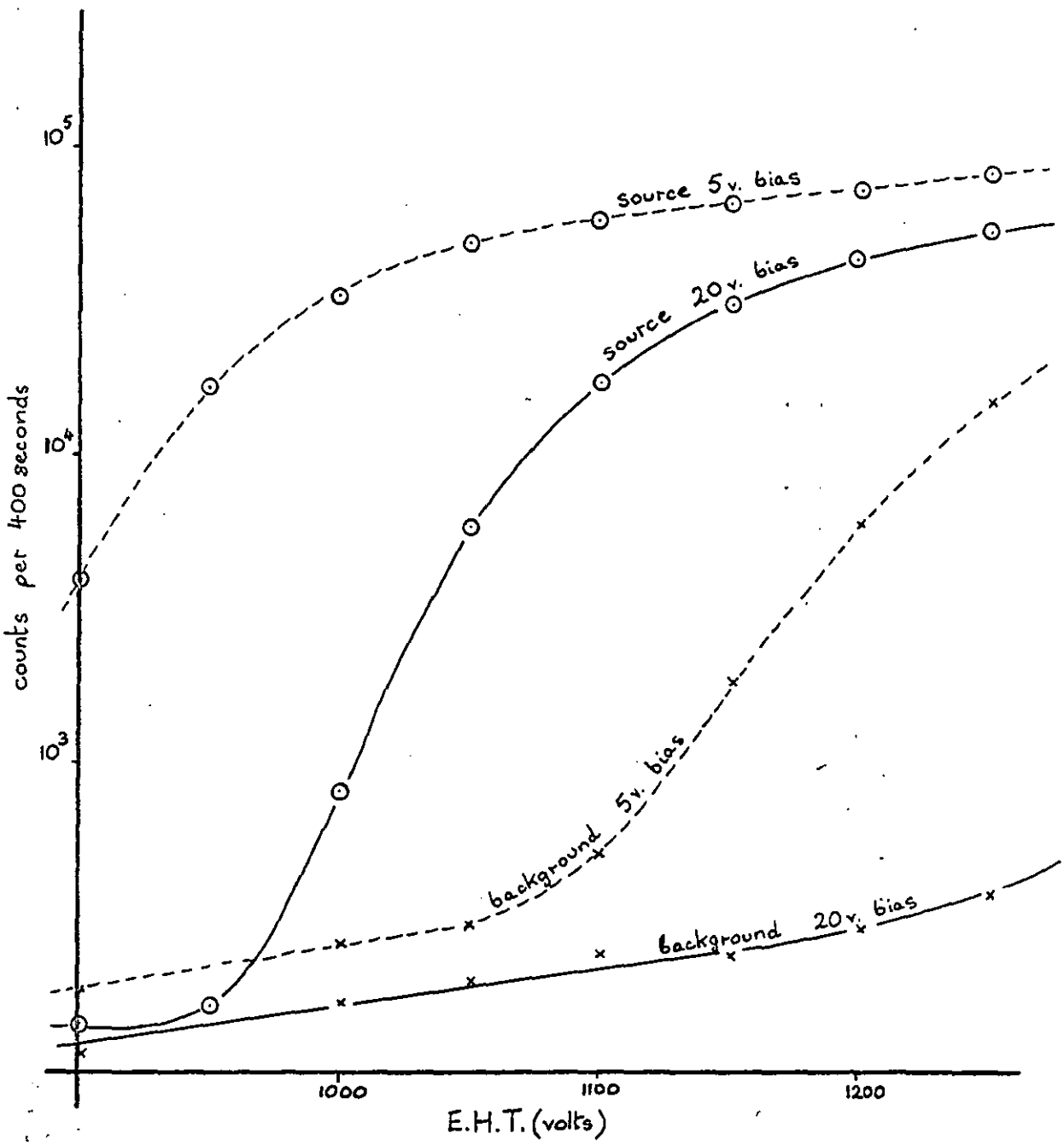

Fig. 3.2. Typical curves of Count Rate Against E.H.T. Voltage

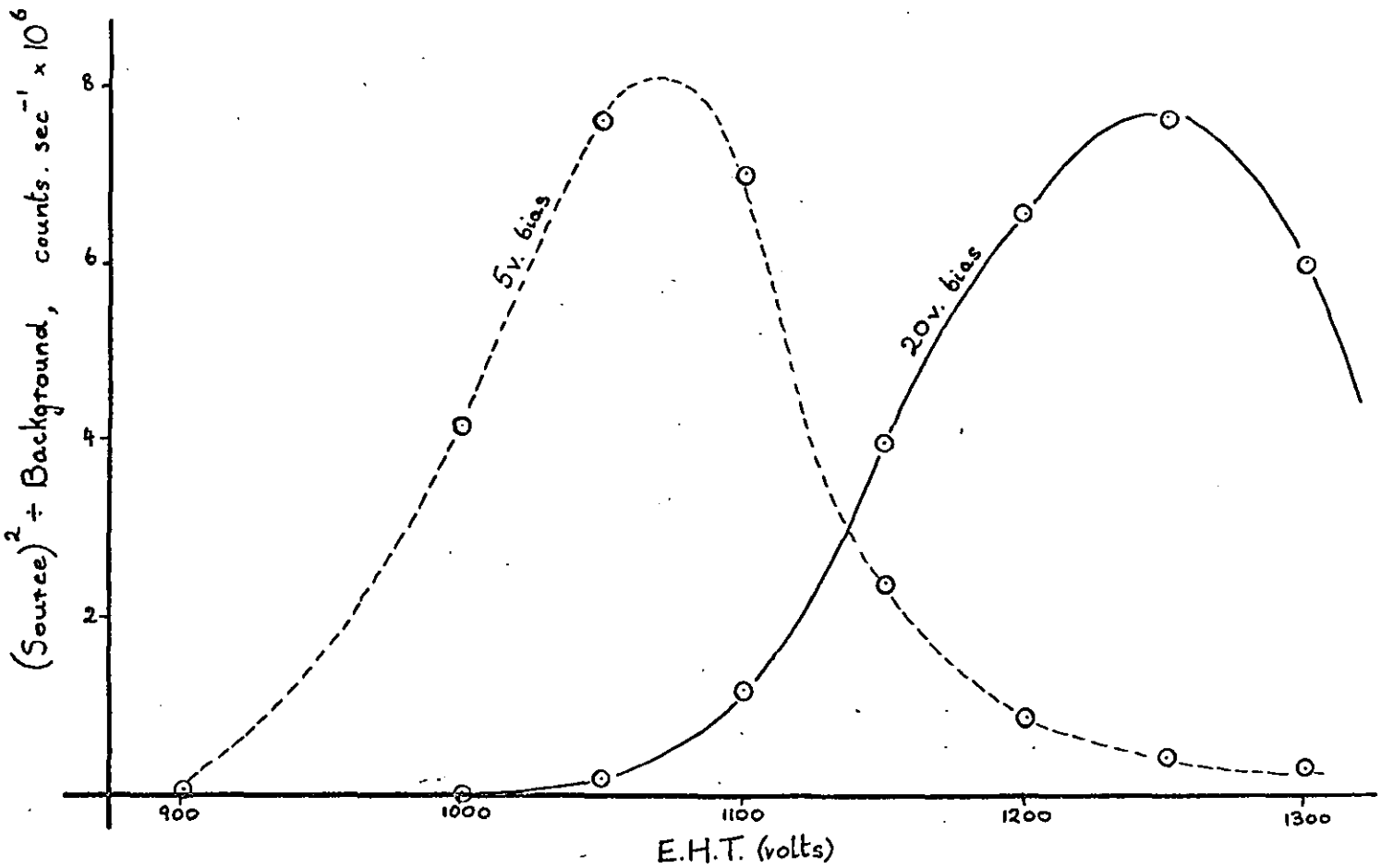

Fig. 3.3. Typical Determination of Optimum Discriminator Voltage Setting for Greatest Efficiency of Counter

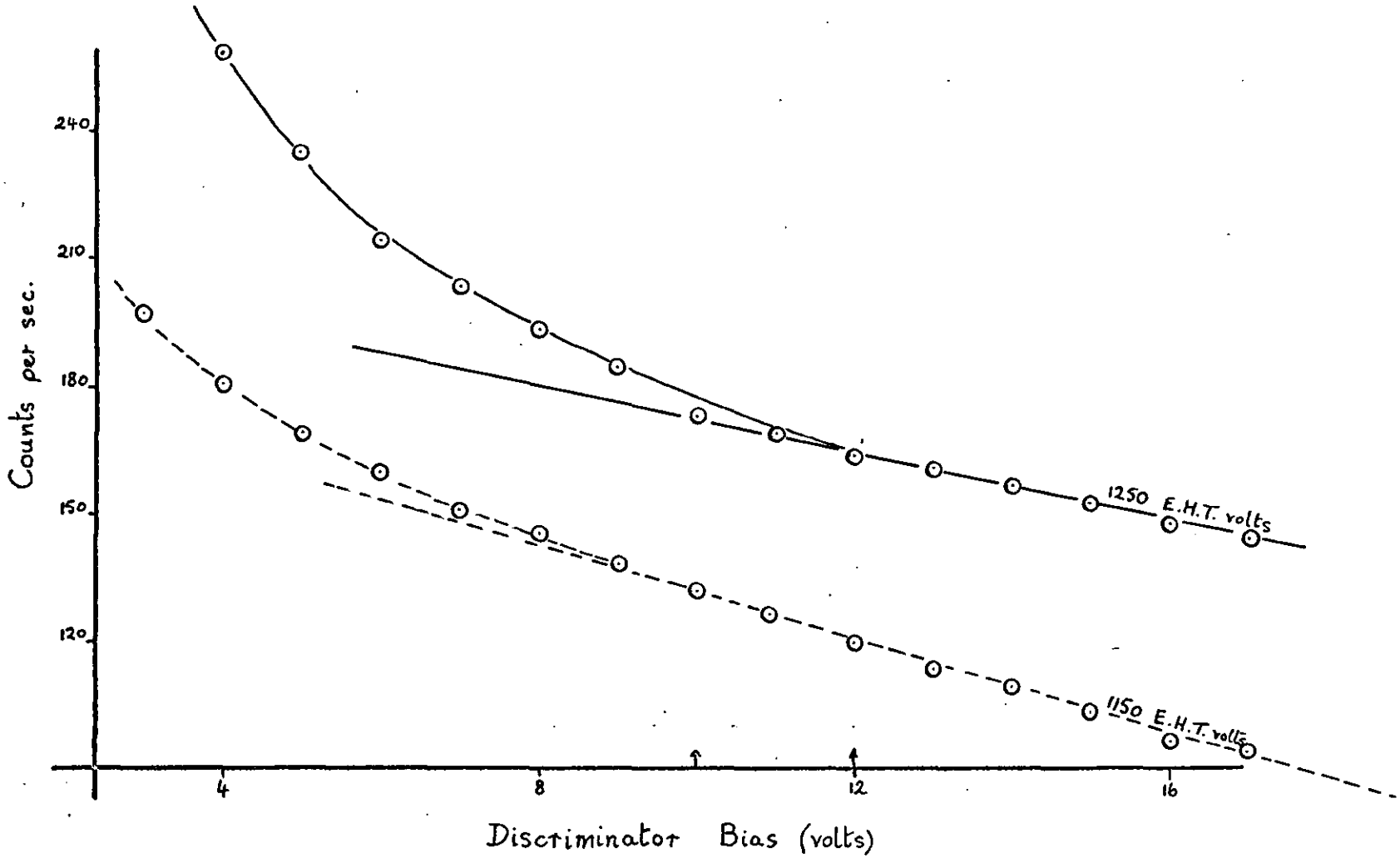

Fig. 3.4. Typical Curves of Count Rate Against Discriminator Voltage Setting

Slight differences were observed at the time of the lauric and oleic acid counts.

3.2.4. Preliminary Experiments

3.2.4.1. Preparation of Solutions

It was found, when examining the oleic acid isotherm, to be unsatisfactory to prepare samples of acid solution, add to the pigment, then include a small quantity of labelled acid for counting purposes. The used of 0.1 ml., 1 ml. and 2 ml. pipettes and even a microsyringe was to be avoided wherever possible owing to large errors associated with their use. Hence "stock solutions" containing labelled acid were prepared and diluted as required for the other isotherms.

As supplied from the Radiochemical Centre, Amersham, the carbon 14 labelled acids, lauric, stearic and oleic were in solution in benzene. This was removed by freeze drying and the residual acid re-dissolved in n-heptane: ordinary acid was added to prepare a concentrated stock solution which could be diluted as required.

Making the premise that 1 μc of activity gives

a count rate of 2.2×10^6 counts per minute, the level of activity (in $\mu c.ml.^{-1}$) of the stock solution could be adjusted to give suitable count rates even at the lowest expected level of concentration (e.g: 100 c.p.s) as the initial total activity of the acid was known.

No problems of solubility were encountered preparing oleic and lauric acid solutions and 40 - 60mM concentration was considered to be adequate to indicate the plateau region of the Langmuir type isotherm which was expected. However, even 20mM stearic acid in heptane was unattainable, and a rough dilution was necessary (by heating the flask and removing 100mls of the litre of solution at the elevated temperature. This later necessitated a titration to check the concentration).

3.2.4.2. Titrations

Methanolic potassium hydroxide was used to standardise the acid. This was first standardised with a prepared solution of benzoic acid in methanol at about 60°C using phenolphthalein as indicator. Samples of the adsorbate acid were then shaken with methanol and also titrated hot with potassium hydrox-

ide with the same indicator.

Careful titration was made of stearic acid to establish its 'stock' concentration. Rough titration only was carried out on oleic and lauric acids already equilibrated under experimental conditions with pigment to check that the plateau region of the isotherm had been arrived at: there was some doubt with oleic acid titrations!

3.2.4.3. Calibration of Pipettes

All pipettes except a graduated pipette were re-calibrated with n-heptane as originally they were designed for use with water. As the surface tension of n-heptane is considerably less than that of water, less was retained in the pipette when drained, so it actually delivered more than its stated volume.

Repeated checks were made of the weight of heptane delivered per pipette and the volume checked assuming a density of 0.684 g/cc.[60] However, a small systematic error had been introduced by the fact that the heptane solutions were made up at 20°C and those of lauric and stearic acids used at 25°C. Hence all actual concentrations are fractionally lower than those quoted.

3.2.4.4. Calibration of Sealed Ampoules

A standard and background count on the liquid counter were taken daily to check:

a) the instrumental stability of the counting unit
b) the general level of background in the laboratory, in case of spillage or contamination elsewhere.
c) contamination of the photomultiplier or lead castle itself, from any previous jars which may have leaked.

These were most satisfactorily carried out using sealed ampoules of standard, active material and background, non active material. Hence their count rates had to be expressed in terms of a prepared (i.e: unsealed) standard (stock solution) and background (n-heptane) in D.J. jars, necessitating an initial calibration.

3.2.4.5. Quenching

A check for quenching in systems subsequent to the oleic acid isotherm was effectively made when examining the linearity of response of the counter to

solutions of varying activity. Deviation from linearity would certainly be observed were quenching occuring. Figure 3.5. shows an exactly linear response for a series of active lauric acid solutions. This graph also became useful as an apparently more-reliable means of estimating concentration than deduction from a proportion of the standard count rate as the latter figure tended to vary significantly from day to day. This was probably explained by poor optical contact between jar and tube; each is immersed in low-viscosity silicone fluid to reduce stray reflections at the point of contact. Occasionally a bubble may have lodged beneath the jar.

3.2.5. Experimental Procedure

A number of 1 oz. glass vials were carefully selected free of blemishes and having well-fitting screw caps. The rubber gasket was replaced by a polythene then an aluminium foil one. Each bottle was washed out in chromic acid and distilled water, dried, and then approximately 1 g. of titanium dioxide pigment weighed accurately into all bar two of the bottles. These had their pigment omitted to enable an estimation to be made of the adsorption taking

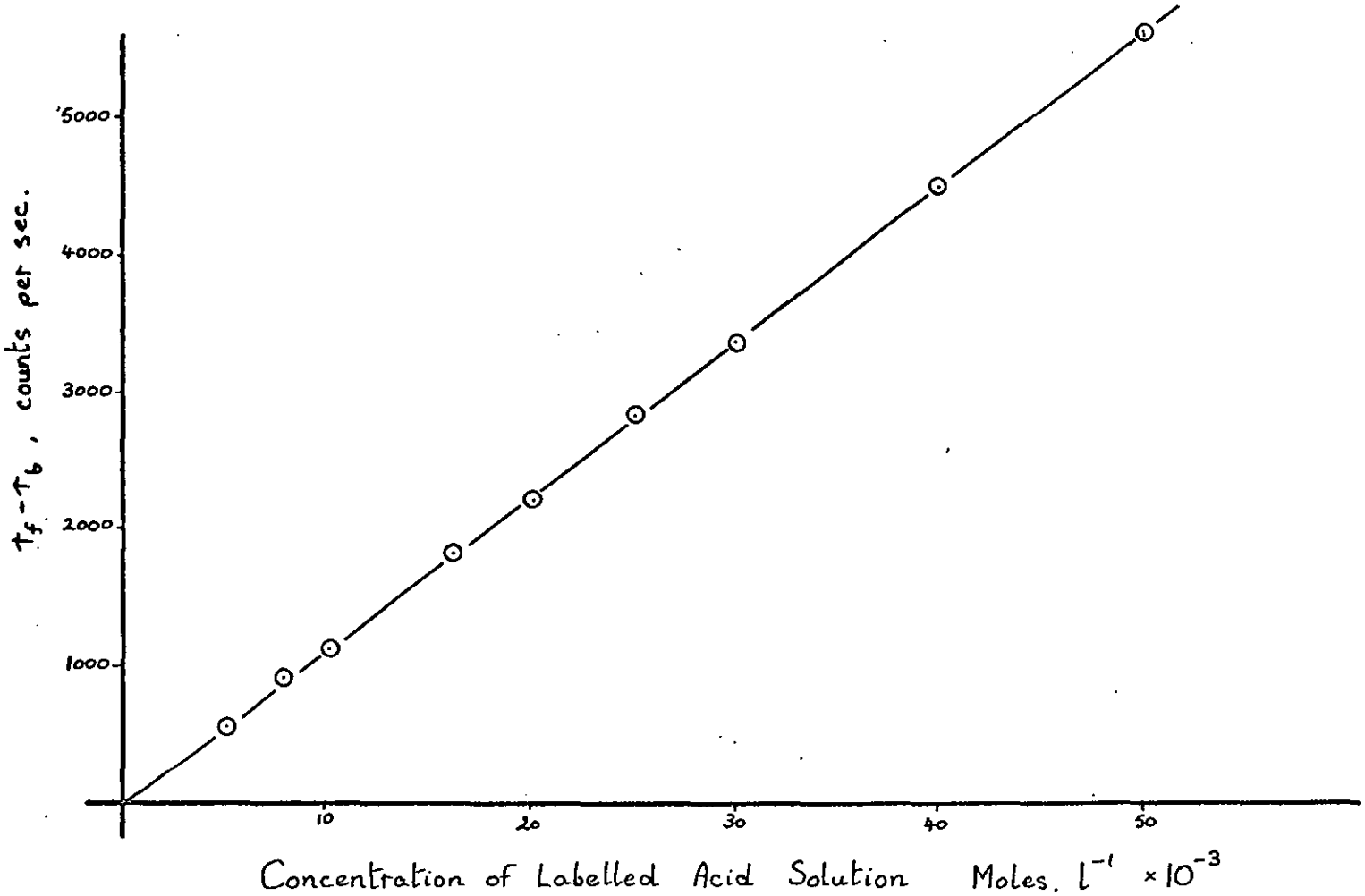

Fig. 3.5. Linearity of Response of Scintillation Counter for Stearic Acid of Varying Levels of Activity

place on the walls of the vials during the course of the experiment. The pigment was preconditioned in an atmosphere of 60% relative humidity. In the case of the oleic acid isotherm, the vials were blackened on their outer surface to reduce oxidation at the double bond by stray light.

The subsequent procedure for this system also varied from that of the other two: 250 mls. each of 10^{-2} $\bar{M}$, 10^{-3} $\bar{M}$ and 10^{-4} $\bar{M}$ oleic acid solutions were prepared and the freeze-dried labelled acid made up to 50 ml. of solution in heptane also. To eliminate use of a microsyringe to transfer the active acid to the vials, 40 mls. of the labelled solution were diluted to 100 mls. giving an approximate level of activity of 0.8 μc. ml.$^{-1}$.

1 ml. of this labelled solution was added to each flask, then, working in duplicate, varying proportions of stock solutions and solvent added via a 2 ml. graduated pipette to the bottles to give a range of initial concentrations. Those without pigment received the same total volume, 11 mls. of the most concentrated solution.

Five small glass balls were added to each vial to promote dispersion, the caps screwed tightly, and sealed with paraffin-wax tape to ensure water-tight

seal and then they were attached to a perspex disc rotating in a vertical plane in a 20°C thermostatted water tank and allowed to equilibrate for 3 days or so.

The vials were allowed to stand on a tray in the tank to allow their contents to settle, then a 0.1 ml. capillary pipette was used to remove samples of the solution from each vial on to an already-heated narrow-rimmed plancette, thus allowing the heptane to evaporate rapidly and collect a thin evenly-distributed film of oleic acid for counting in the windowless counter.

The difference between the initial and final count rates for a sample from the 'un-pigmented' vial gave an indication of the extent of adsorption on the foil gasket and the glass; allowance was made for this in computing the results.

The main differences in procedure adopted for the following systems were that the temperature of equilibration was 25°C and that the labelled acid was incorporated into the stock solutions. No pipette smaller than 5 mls. was used in sample preparation so the errors were restricted; pipettes of 5,10,15 and 20 mls. were used to transfer 20 mls. of varying solutions to the vials, again in duplicate. Equilibration was attained with the vials on a revolv-

ing spit in a constant temperature room.

After equilibration and settling, 1 ml. aliquots were removed from each vial to a D.J. jar, 5 mls. phosphor, N.E.214, added, and these shaken briefly and counted in the liquid scintillation counter as soon as possible afterwards, storing them meanwhile away from light.

Three corrections were applied for each count:

1) Dead time losses e.g: 20 μsec. per count, during which time other scintillations will not be counted.
2) Background count rate (sealed ampoule) is lower than the true background rate (D.J.jar containing n-heptane)
3) Initial count rates are obtained from the quenching curve; this figure must first be corrected to allow for adsorption on the walls of the vial.

3.2.6. Calculation of Adsorption

Let the initial count rate of a particular sample be R_i c.p.s and that of the equilibrium sample be R_f c.p.s, as the background count rate for these is the same, R_b c.p.s:

$$\frac{R_i - R_b}{R_f - R_b} = \frac{C_i}{C_f}$$

(where C_i = initial concentration of acid, moles.l^{-1}
C_f = equilibrium concentration of acid, moles.l^{-1}).

R_f includes allowance for adsorption on the glass walls of the vial and the D.J. jar. Such an allowance is deduced from the 'blank vial' solution before and after equilibration only, and to apply this correction as a proportion of the count over the whole range of concentration studied, infers that the adsorption isotherm of fatty acid on glass is identical to that on titanium dioxide. This is not true, but since adsorption on glass is to such a small extent, it is considered reasonable to make the same deduction numerically, from every count.

If now the amount of acid adsorbed in moles.g^{-1} of pigment is written as 'x' it can be seen that:

$$x = \frac{C_i - C_f}{w} \cdot \frac{v}{1000} \quad \text{moles.g}^{-1}$$

(where w = weight of pigment in vial, g
v = volume of solution in vial, mls).

$$= \frac{C_1 v}{10^3 w} \left[1 - \left(\frac{R_f - R_b}{R_1 - R_b} \right) \right]$$

3.2.7. Errors in Measurement

Under the conditions of radioactive counting as described the number of counts, n , observed will fillow a Poisson distribution about its mean value. The statistical spread of measurements is expressed as the 'variance', V , which is defined as the mean square deviation: its mean square root is the 'standard deviation', σ . There is a 68.3% chance that any single value will lie within $\pm \sigma$ of the true count, and hence that the true mean count is within $\pm \sigma$ of the total count, n, assumed to be the true count. The standard deviation may further be assumed to be $\sqrt{n}$, i.e: the fractional standard deviation is $\sqrt{n}/n = n^{-\frac{1}{2}}$.

The 68.3% level of confidence is not very high, however; if this is increased to 95.5% and the random error allowed is the same ($\sqrt{n}/n \times 100\%$ i.e: 1% for 10^4 counts) one must now measure 4×10^4 counts. Generally, active solutions gave count rates of between 5×10^3 and 100 c.p.s and a substantial number

of counts are soon amassed. However, the background count rates (and the planchette sample count rates) were as low as 1 c.p.s, so the target number of 4×10^4 counts was never achieved, hence these were an additional source of error. At this 95.5% confidence level, the random error varies exponentially between $\pm$ 4.47% on 2×10^3 counts and about 0.75% on 10^6 counts or more.

Each count rate recorded is the mean of three or more determinations and the % random error is that associated with the sum of these counts (e.g: 4×10^5 counts measured four times = 0.75%) and of their corresponding background counts (e.g: 1000 counts measured three times = 3.65%). These % errors are then converted into a number of counts, added together and a new % random error evaluated. For "$R_i - R_b$" values read from the quenching curve, an additional allowance is made for a possible error of $\pm$ 15 c.p.s in reading-off values.

Pipettes were the main source of error when preparing or transferring solutions; apart from the error from use with n-heptane instead of water, for which the calibration was carried out, the following random errors were ascribed to the various pipettes used:

0.1 ml.	±	5.0%
1 ml.	±	2.0%
2 mls.	±	1.5%
5 mls.	±	1.0%
10 mls.	±	0.5%
15 mls.	±	0.4%
20 mls.	±	0.3%
25 mls.	±	0.2%

Hence for example, the 50 mM lauric acid stock solution was prepared with negligible weighing error, but the 40 mM and 10 mM solutions prepared by dilution of the former involved use of two 25 ml. pipettes, i.e: ± 0.4% random error.

The graduated pipettes were considered to deliver only within 0.02 mls. of the required measure. (i.e: 1.1% random error for 1.8 mls. delivered, 2% for 1 ml). This pipette was never allowed to drain completely.

All weighings of pigment samples were either 0.5g ± 0.0004g not greater than 0.2% or 1.0g ± 0.0004g, not greater than 0.1%.

3.3. Calorimetric Measurements

The design and operational features of the

calorimeter have been described already in Chapter 2, together with an account of the general experimental procedure involving either the pulse injection technique - comparatively rarely used - or the saturation adsorption technique. Measurements made may now be classified further into their respective sections according to the aim of the research programme.

3.3.1. Determination of Surface Area

It had been suggested[61] that the flow microcalorimeter could be used to determine the surface area of powders by recording heat changes accompanying adsorption from solution. Provided a mechanism of hydrogen bonding is accepted as the force binding alcohol molecules to the surface, the surface area, S, is said to be "directly proportional to the integral heat of adsorption per g. of solid, $\overline{\Delta H}$,

i.e: $S = K\,\overline{\Delta H}$

(where K is a proportionality constant in $m^2\ cal^{-1}$,

$\overline{\Delta H}$ is the total heat effect produced in cals.)

when n-butanol forms a close-packed monolayer on the surface".

This was examined with a variety of pigments and using a butanol solution in n-heptane at the fixed arbitrary concentration of $2g.l^{-1}$ (27 mM). The pigments were dried overnight in an oven at 120°C to remove most of the free water at the surface. A single peak was obtained at the most favourable maximum sensitivity for each sample and a range of heat effects measured.

One sample was now taken as having an accurately known surface area, as determined by nitrogen adsorption by the B.E.T. method (see 3.1.1.2. and [54]) and a figure deduced for the other pigments, from proportions of their heats of displacement.

3.3.2. Pulse Injections

The pulse injection technique was similarly examined briefly to see what information it might yield. For this, the adsorption of an alkyd resin was carried out i) on two titanium dioxides at a single concentration of 5%w/v. Successive injections of 20 µls. were made on the same bed of sample.

ii) on three titanium dioxides each

in the "dried","normal" and "wetted" state. Caprylic acid and capryl alcohol (short chain compounds chosen merely so as to ensure a desired level of concentration) in 2% w/v solution in dried benzene were injected both before and after a similar injection of resin on different samples in the bed. The aim was to determine whether any repression of the acid or alcohol was observed owing to resin or moisture or both, present on the surface.

In each series the measurements were made rapidly but reproducibility was poor and results were only semiquantitative.

3.3.3. The Silica-Alumina Surface-Treated Rutiles

The aim of this study was to establish a relationship between the surface groups on the pigment and the quantity of material adsorbed. Stearic acid adsorption was examined from benzene solution, primarily to conjunct with adsorption studies on the same system being carried out elsewhere at the Paint Research Station.

One calibration served for all samples; an arbitrary concentration of $3 g.l^{-1}$ (10.5 mM solution) acid was used. Several peaks were obtained and

evaluated for each pigment, and a mean value recorded. This procedure was followed for both the "dried" and the "normal" pigment (see 3.1.1.1.). A $10g.l^{-1}$ (37.1 mM solution) solution of stearylamine was also thus studied: if the alumina content controlled the acid adsorption which proved to be the case, might not the silica, being more acidic in nature control the amine adsorption? Millipore filtration of the freshly-prepared amine solution was found to be necessary as it was hazy in appearance; this was probably due to carbonation of the solid (Fluka grade "purum") stearylamine. The solutions could not be stored owing to the formation of a solid film on the liquid surface. This was prevented in the drip flask by attaching a soda lime tube to the air bleed.

All adsorption peaks observed in this section were accompanied by a "trough": (as indeed is any peak obtained for adsorption from aromatic solvent) considerable speculation has been made over the nature of cause of this trough (see 4.3.3.). It suffices here to say that no allowance has been made for its presence in the results quoted, so the latter are purely arbitrary values useful only as a direct comparison amongst themselves, and cannot be called 'heats of adsorption' merely 'heats of exchange adsorption'.

All results furthermore are quoted as a heat of exchange adsorption at various percentages of alumina content by weight of the overall surface treatment.

3.3.4. Adsorption of Acids on Titanium Dioxide at a Fixed Concentration

The relative affinities of various acids for a particular titanium dioxide surface were next examined. The solvent used was n-heptane, the concentration chosen was $3g.l^{-1}$, believed sufficiently high as to produce an adsorbed weight corresponding to the plateau region of the expected Langmuir-type adsorption behaviour for each acid, but also low enough to permit solutions of straight chain acids as long as stearic acid (longer chain acids are less soluble in n-heptane). This procedure was inadvisable: constant molar concentrations rather than weight concentrations ought to have been used. Allowance may be necessary in interpreting results, section 4.4.1.

The only unsaturated acids examined were oleic and elaidic acids (cis , trans isomers). No dibasic or aromatic acids (except benzoic acid) showed sufficiently high solubility in n-heptane to be

included. Results were quoted as heats of exchange adsorption as a function of acid chain length, and for longer chains there was a relationship.

3.3.5. Adsorption of Acids on Anatase at varying Concentrations

The difference in the levels of adsorption of lauric and stearic acid, determined in the previous section was considered worthy of more detailed examination. Solutions of these acids at varying concentrations in n-heptane were examined at 25°C together with oleic acid solutions at 20°C, to combine with adsorption isotherm results.

A standard procedure was adopted as much as possible of preparing 100 mls. of a particular solution, and while using a portion of this, pipette 50 mls. to another clean (chromic acid for 24 hours plus rinses in distilled water) dry 100 ml. flask. Making up to 100 mls. with further solvent effected a dilution by two.

An erroneous choice of preparing solutions at 20°C, (the temperature of calibration of the flask) and use at 25°C was made. As n-heptane has such a large coefficient of thermal expansion it would

have been more satisfactory to make both preparation and use of solutions at 25°C.

One peak per pigment sample was recorded, and a mean value deduced from several recordings at each concentration. The ranges of concentrations were up to 60 mM for lauric and oleic acids and up to 20 mM for stearic acid. Dilute solutions of 2 mM or less generally gave heat effects spread over an hour or so and could not be measured accurately.

Occassionally anomolous results occurred for which no explanation was apparent. Critical checks were made of the time for which the solvent in the drip flask was exposed to the cabinet atmosphere, the time of settling of the pigment when forming the bed, and variations in day-to-day temperatures, humidities and sample weights, but no pattern was revealed: the only way to detect these results was to make multiple determinations and when five or more heat values contradicted the original value, it could be legitimately discarded.

Up to four peaks per day were easily measureble; each heat effect was recorded on a graph of heat of exchange adsorption against equilibrium concentration; (it was necessary to assume the final, equilibrium concentration of effluent from the calorimeter, after

the peak was completed, was the same as that flowing in), the maximum limits of random error were included for all points and the best-fitting curve drawn through these points.

This heat curve was then combined with the adsorption isotherm to produce a third curve of 'differential heats of exchange adsorption', the heat evolved per mole acid adsorbed which in turn led to an estimation of the total proportion of active sites on the surface. The systematic errors caused by the temperature discrepancy mentioned were the same for each curve and so cancelled each other out.

3.3.6. Errors in Measurement

3.3.6.1. Calibration Errors

Some reproducibility measurements made on several orders of size of peak showed the random error to be:

± 5.0% for a 10 mg peak
± 2.3% for a 50 mg peak
± 1.6% for a 480 mg peak

All times were correct to the nearest 0.5 second.

Cell voltages measured by A VO meter and were ± 0.01 volts. The coil resistance, deduced from a Wheatstone circuit comprising two 0.1% grade variable resistances, a standard resistance of low tolerance and microammeter, had an error of ± 0.05 ohms. The internal series resistance, R2, measured similarly was to the nearest 2.0ohms.

A typical calibration curve is illustrated in figure 3.6. The broken lines represent the limits of error in constructing this curve. The second line is obtained by plotting the heat evolved for a particular period of current flow against the corresponding peak weight for that time period, read from the first line.

The heat evolved is calculated from the expression

$$H = \frac{I^2RT}{J} \quad \text{calories}$$

(where I = current flow, amps
R = resistance of coil, ohms
T = period of current flow, seconds
J = 4.184 joules.cal^{-1})

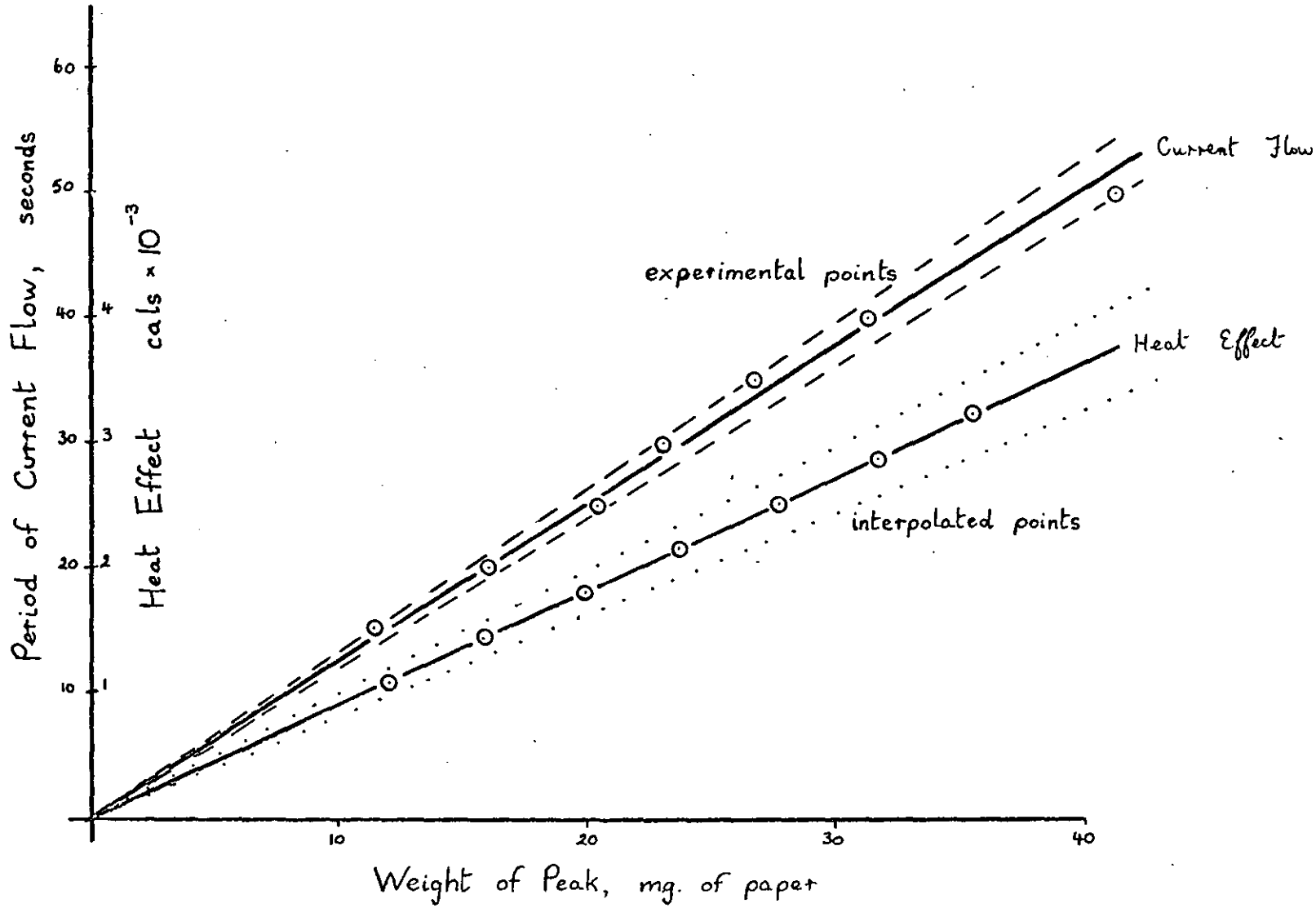

Fig. 3.6. Typical Calibration Curves from Calorimeter

I is rewritten as $\frac{V}{(R+r)}$

(where V = voltage across coil, volts

r = external series resistance, ohms)

The dotted lines show the limits of the error accumulated from the uncertainity of peak weight deduced from the first curve plus the calibration errors mentioned above.

3.3.6.2. Errors in Preparation of Solutions

The 25 ml. pipette used has a random error of $\pm$ 0.2%. Weighings of solid adsorbate varied between 0.04 g and 1.2g. As the random error associated with the balance used is not greater than $\pm$ 0.4 mg. the errors in weighing adsorbate vary between 1% and 0.03%.

In plotting the heat curve, these errors, cummulative in determining equilibrium concentrations were found to be insignificant compared with those associated with the heats of exchange adsorption, and so were ignored.

CHAPTER 4

RESULTS AND DISCUSSION

4.1. Surface Areas

One of the preliminary exercises with the flow microcalorimeter was that of a feasibility study of surface area measurement. This incorporated a familiarisation of procedure, and an examination both of the calorimeter's reproducibility and of an extension of the systems, used by Groszek[61] to include a range of pigments as adsorbents. The same conditions were employed as in his paper, viz: 0.2% butanol in n-heptane was adsorbed at room temperature.

4.1.1. Surface Area Measurement - Results

Table 4.1. shows the results of exchange adsorption measurements. Pigment 10b, anatase having been the subject of a reproducibility examination of the B.E.T. apparatus was considered to have a precisely - known surface area, and was taken as the standard. The final two columns in this table show a deduced surface area from the solution adsorption results, and the B.E.T. surface area by gas adsorption for comparison.

4.1.2. Surface Area Measurements - Discussion

TABLE 4.1. SURFACE AREA MEASUREMENT

PIGMENT	HEAT OF EXCHANGE ADSORPTION (m cals.g^{-1})	APPARENT SURFACE AREA $m^2.g^{-1}$	B.E.T. NITROGEN ADSORPTION SURFACE AREA $m^2.g^{-1}$
Anatase 10b	329.6	-	9.3
Zinc Dust	15.0	0.42	0.7
Iron Oxide D	203.9	5.85	5.9
Iron Oxide E	174.5	4.92	5.1
Rutile 5a	400	11.39	14.7
Rutile 5b	315.3	8.90	12.0
Rutile R1	283.9	8.0	7.2
Tungstic Acid	872.4	24.62	23.4
Phthalocyanine Blue A	13.2	0.4	63.7
" " C	16.8	0.5	67.1
" " D	5.6	0.2	59.7
" Green	430.0	12.1	51.8
Toluidine Red	103.6	2.9	10.4

The adsorption from solution in heptane of butanol is dependant on its ability to form hydrogen bonds with the surface of the substrate. Hydroxyl fundamental infra-red absorption bands are invariably broadened, intensified and displaced to lower frequency due to hydrogen bonding with adsorbed alcohol molecules. Evaluation of the heat of adsorption of butanol on say, titanium dioxide might have been made, to check that a value in the region of 9-13 K cals.mole^{-1} was obtained, corresponding to the hydrogen bonding energy. The inorganic materials in table 4.1. all have deduced surface areas remarkably close to the B.E.T. value. Although this is somewhat surprising, it is explicable on the basis that such surfaces are completely hydroxylated, the area of cross section of the butanol molecule(20.7 $\mathring{A}^2$ limiting area[7]) is close to that of the nitrogen molecule (16.2 $\mathring{A}^2$) at - 195°C so it will occupy the equivalent area in pores and capillaries and the butanol adsorption is considered to be from ideal solution. Nitrogen adsorption should give a slightly higher surface area if pores whose cross-sectional areas at the surface are between 16.2 $\mathring{A}^2$ and 20.7 $\mathring{A}^2$ are present.

Hydrogen bonds cannot, however, be formed at the

organic pigments surface, as the hydrogen atom of the hydroxyl group requires a centre of high electron density such as an oxygen atom with completed octet, for bonding to take place. The adsorbed material is held very loosely, by Van der Waal's forces, and little heat is evolved. The proportionality between heat evolved and surface area clearly breaks down: it is interesting to note, however, that for phthalocyanine green (a halogenated tetrabenzoporphyrazine structure) and toluidine red (a monoazo pigment containing both nitro - and hydroxyl-groups, see figure 4.1.) deduced surface areas lie considerably closer to the B.E.T. area. Presumably, some degree of dipole - non - polar interaction occurs between the polar alcohol and these centres of relatively high electron density.

4.1.3. Surface Area Measurements - Reproducibility

At this stage, the adsorption reproducibility of butanol from heptane on two pigments was examined. Table 4.2. lists the results on rutile 5b, and on toluidine red.

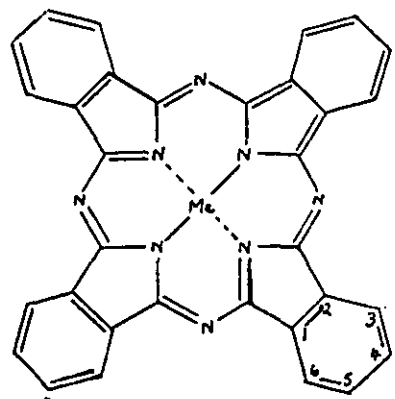

Fig. 4.1.a Phthalocyanine Blue

(Phthalocyanine Green is formed by complete halogenation (14 - 16 halogen atoms per molecule) of this molecule, substitution taking place at positions marked 3 - 6 of the benzene nuclei)

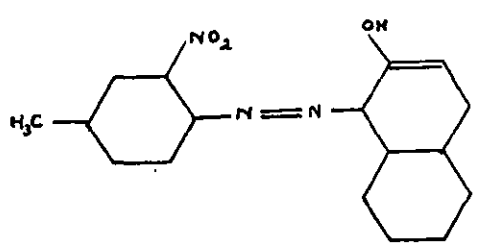

Fig. 4.1.b Toluidine Red

TABLE 4.2. REPRODUCIBILITY TESTS: HEATS OF EXCHANGE ADSORPTION OF n-BUTANOL FROM n-HEPTANE ON (i) RUTILE (ii) TOLUIDINE RED

RUTILE 5b			TOLUIDINE RED		
Mean Heat of Exchange Adsorption (m cals.g)	No. of determinations	Spread	Mean Heat of Exchange Adsorption (m cals.g)	No. of determinations	Spread
315.3	8	± 12%	103.6	7	± 100%

The spread of results of ± 12% for rutile is taken as a guide line to the general reproducibility of the instrument for titanium dioxide systems.

The reproducibility of peak size measurement was also tested: three arbitrarily - chosen peak sizes were taken, and multiple tracings of these made and then weighed. These results suggested that for subsequent weighings, the error be taken as ± 5% for a 10 mg peak, ± 2.3% for a 50 mg peak and ± 1.6% for a 480 mg peak.

4.2. Pulse Injections

The technique of pulse injection was examined using two systems. The first was inconclusive; this involved the injection of a dilute solution of short chain acid or alcohol on to titanium dioxide whose water and prior coating of resin varied. The peak sizes were not reproducible, and it was realised that as the injection is made into an otherwise-undisturbed solvent flow, this will start the desorption process simultaneously with the adsorption process. A true equilibrium is never achieved as with the saturation technique.

The second system was selected to try to attain a

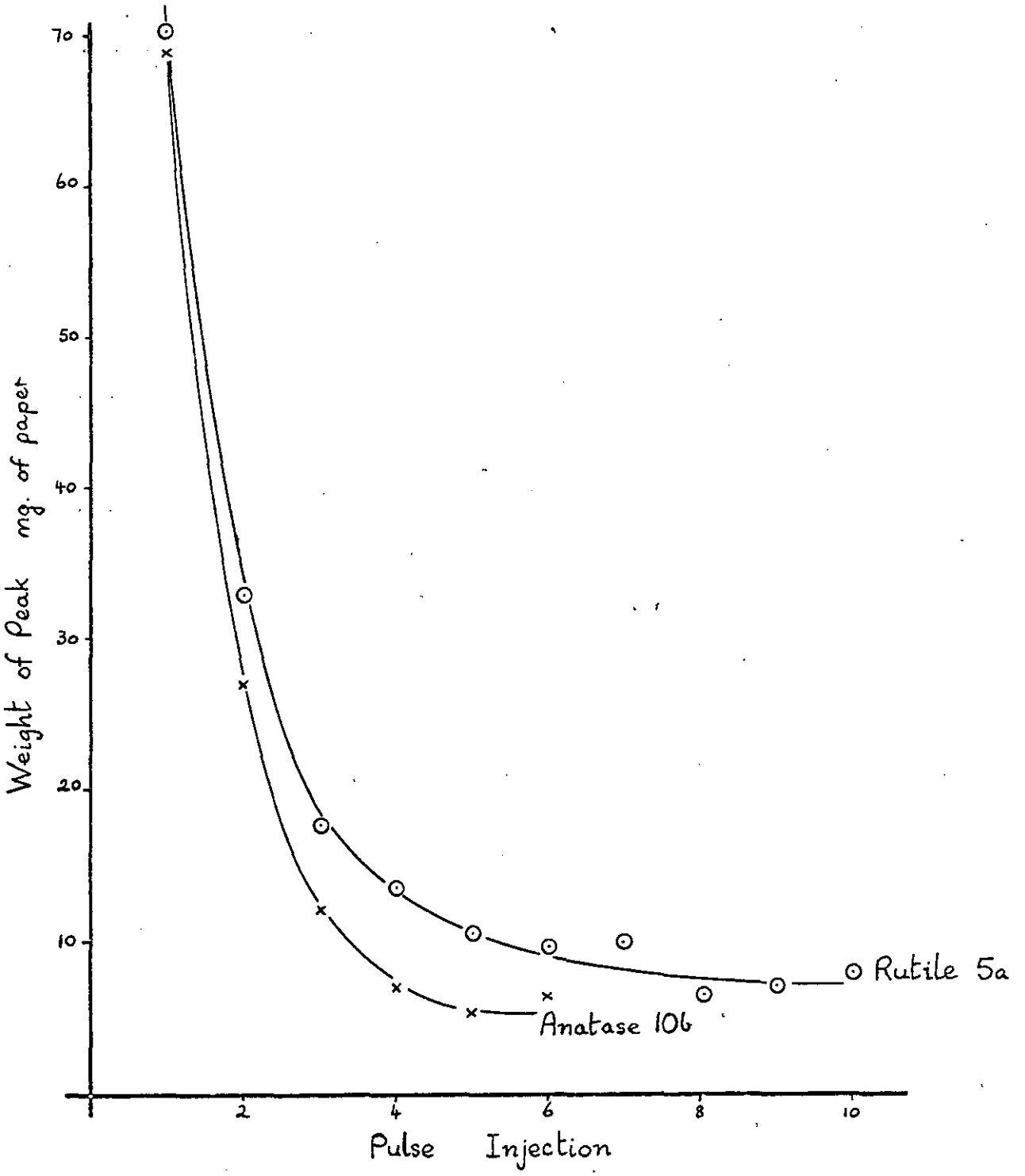

Fig. 4.2. The Adsorption of Alkyd Resin from Solution in Benzene on Titanium Dioxide Variation of Peak Size with Succession of Pulse Injections

semi-quantitative measure of the reversibility of alkyd resin adsorption on titanium dioxide from benzene solution. The pigments were rutile 5a and anatase 10b, the injection volume 20 μl, and the resin concentration 5% w/v. Figure 4.2. shows the variation of peak weight (conversion to heat units was unnecessary) with successive injections on the same sample bed, for each pigment. It appears to be an exponential curve. Peak 2: Peak 1 = Peak 3: Peak 2 = Peak 4: Peak 3, etc., is 0.39 = 0.39 = 0.41 = 0.55. For the run on rutile, the curve is asymptotic to a peak weight value of 8 mg, and for anatase, 5mg. This weight can be considered to represent the heat evolved by reversible adsorption of alkyd resin since injections subsequent to the sixth give rise to a small constant heat evolution when the surface is virtually covered by irreversibly adsorbed resin: the difference between this figure and the net peak size is due to irreversible adsorption.

4.3. The Silica-Alumina Surface-Treated Rutiles

4.3.1. Results

The results of the investigations made into the variation of stearic acid and stearylamine adsorption,

with nature of the pigment surface are expressed in Table 4.3. and figure 4.3. Between two and five determinations of the acid exchange adsorption heat were made on each pigment sample.

Within the limits of experimental error of the calorimeter, the heat of exchange adsorption, expressed as heat evolved per unit area when stearic acid was adsorbed, was proportional to the percentage content of alumina in the surface treatment, reaching a maximum value at 100% alumina. A similar but inverse proportionality was observed for the adsorption of stearylamine only as far as 45-50% alumina content in the surface; beyond this level, the heat of exchange adsorption remained approximately constant. The adsorption of amine was generally much stronger than that of acid (in terms of heat units) while the presence of additional moisture on the pigment surface enhanced the adsorption of acid.

4.3.2. Discussion

Earlier work[43] has shown the zinc oxide modification of a titanium dioxide pigment to dominate the adsorption of carboxylic acid from organic solution. These pigments, however, were known to be zinc-free.

TABLE 4.3. ADSORPTION OF STEARIC ACID AND STEARYLAMINE FROM SOLUTION IN BENZENE ON SURFACE-TREATED TITANIUM DIOXIDES.

PIGMENT SAMPLE SURFACE TREATMENT:-	T1	T2	T3	T4	T5	T6	T7
Alumina % by wt. of total pigment.	0.5	1.0	1.5	2.1	2.1	2.1	2.1
Alumina % by wt. of total treatment.	21.7	35.8	45.5	53.9	70.0	85.7	100.0
Silica % by wt. of total pigment.	1.8	1.8	1.8	1.8	0.9	0.35	0.0
Silica % by wt. of total treatment	78.3	64.2	54.5	46.1	30.0	14.3	0.0
HEAT OF EXCHANGE ADSORPTION: m cals.m^{-2}							
i Acid on Dried Pigment	3.4;3.8;2.85;3.0	4.9;5.5;6.5;5.9	6.4;6.1;5.95	7.6;7.3	6.6;8.4;7.8;6.1	9.8 7.1;8.8;7.6	11.15;11.05
" " " Mean Value	3.3	5.7	6.15	7.45	7.85	7.85	11.1
ii Acid on 'Normal' pigment	5.9;5.4	8.0;4.6;11.0;7.6	13.8;7.7;11.3;10.3	11.8;14.0	12.5;13.5	23.5;16.25;17.2;10.8	24;14.7;22.5;13
" " " Mean Value	5.7	7.8	10.8	12.9	13.0	17.0	18.55
iii Amine On Dried Pigment	35.3	30.5	24.3	24.6	23.8	23.9	25.7

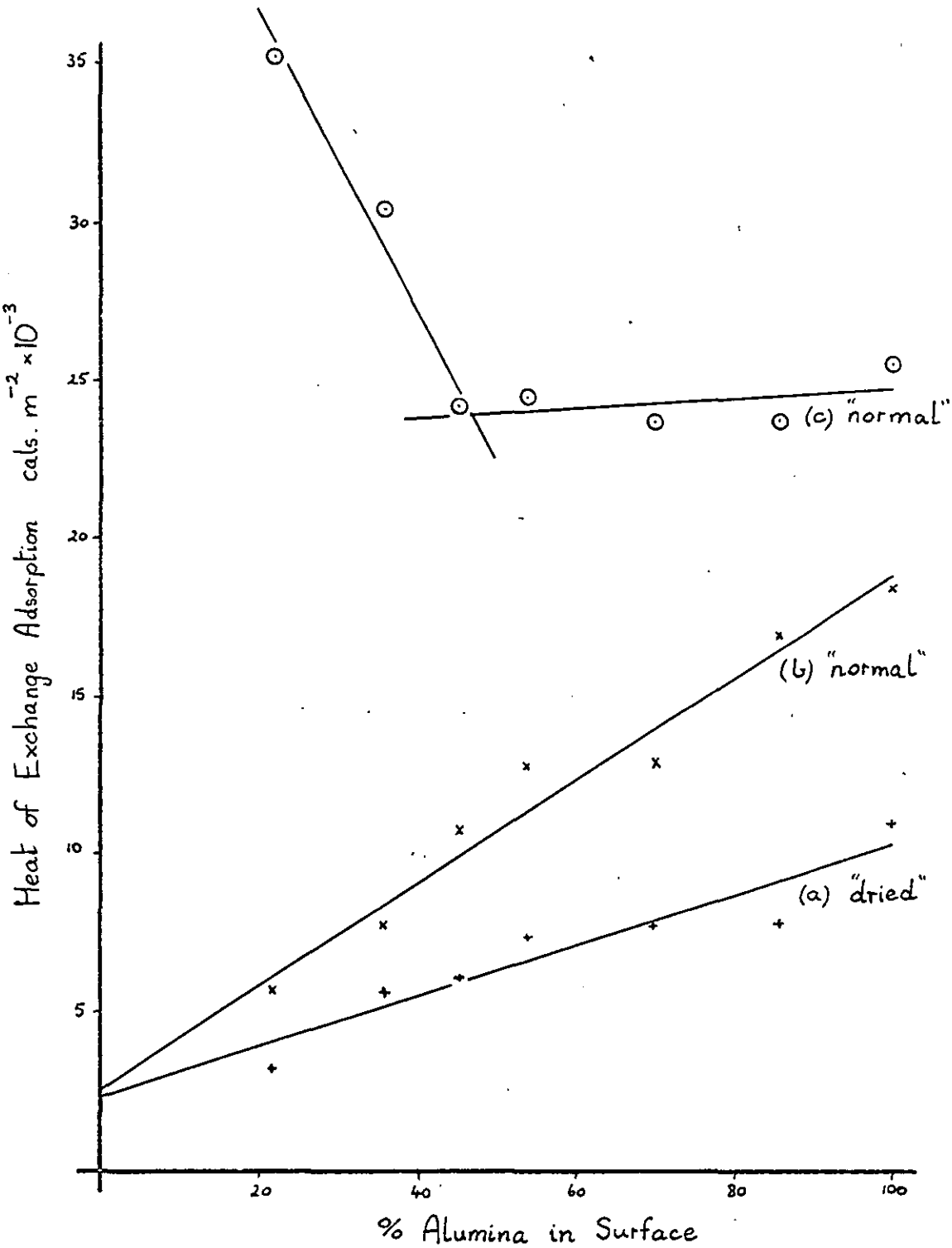

Fig. 4.3. The Heat of Exchange Adsorption of Stearic Acid, curves (a) & (b) and Stearylamine, curve (c), on Surface-Treated Rutiles

Infra red spectra showed an ionic adsorption mechanism to be operative, with the acid associated with the alumina (band frequency 1580 cm^{-1}). The relative intensity of this band appeared to increase with the alumina content of the surface. There was no evidence of hydrogen bonding which would be expected if silica were involved in the adsorption process.

Adsorption isotherms determined elsewhere for these systems were of the familiar Langmuir-shape and the maximum specific adsorption - the plateau level - was also found to be directly proportional to the alumina content[62]. When the exchange adsorption heat values were expressed as "heat evolved per mole adsorbed" (from a combination of these results) they were found to be approximately constant: 2.0 K.cals. $mole^{-1}$, the mean of five determinations whose standard deviation was 0.124 K.cals. $mole^{-1}$.

For the amine systems the adsorption isotherms had appreciably-sloping 'plateaux'. The maximum specific adsorption was indeterminate, but when measured at a fixed arbitrary concentration level was found to fall steeply with increasing alumina content of the pigment surface until around 45% alumina, then rose again though only slightly. Such a curve of specific adsorption v. equilibrium concentration al-

most exactly corresponded to the calorimeter heat curve. The heat of exchange adsorption could be re-expressed as 5.4 K.cals. $mole^{-1}$ with a standard deviation (on five determinations) of 0.49 K.cals. $mole^{-1}$.

Infra-red spectra of the adsorbed species on the pigment showed there to be the expected ionic bonding band for high alumina content material. A similar band structure was observed for stearylamine equilibrated with pure alumina. However, for the coated pigment rich in silica, evidence was seen of co-ordination compounds present; the amine and the silica had formed a complex, probably based on hydrogen bonding. It was not possible to interpret the spectra quantitatively.

4.3.3. Nature of the Trough

Adsorption reactions studied from aromatic solution invariably exhibited an exothermic effect, a peak, followed by an endothermic effect, a trough.

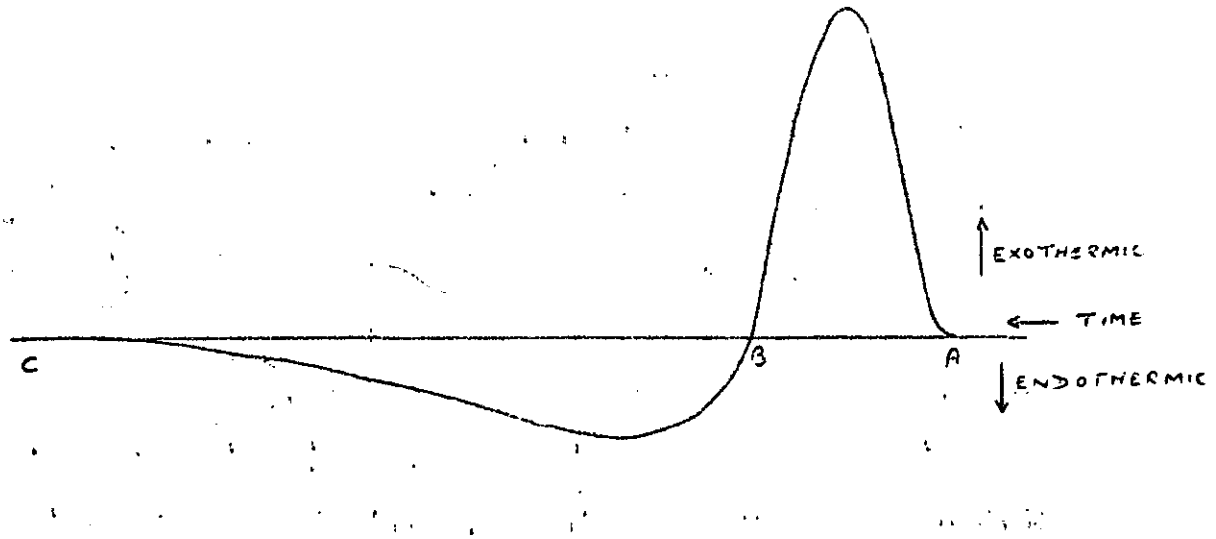

It was first observed in a synthetic iron oxide/benzene/stearic acid system in which the pigment was dried overnight in the oven at 120°C. However, soluble iron (probably iron stearate) was confirmed to be present in the effluent, so the trough was ascribed to a heat of solution effect. The same effect was soon observed in titanium dioxide systems, however, where no soluble salts could be detected; a dialysed, non-surface coated rutile, R1, readily gave rise to a trough. In addition if dissolution of the pigment bed were taking place, one should observe a constant drifting base line which might never return to its original position.

Consideration was made of the possibility of the adsorbate causing some de-flocculation within the pigment bed in turn resulting in an altered flow rate.

This was discounted as a cause of the trough as it did not occur in aliphatic solvent and the likely effect of deflocculation is to reduce the flow rate which would be observed on the recorder chart as an exothermic effect.

Water vapour both adsorbed on the pigment surface and in the solvent seems the probable cause. The size of these troughs was related to the time of storage of the benzene after the drying operation (see section 3.1.2.3.). Subsequent work not reported here has been concerned with the adsorption of fractionated alkyd resins on titanium dioxide from toluene. When one fraction was adsorbed immediately following another, its accompanying heat effect never included a trough, while the first one always did: this suggests all re placeable surface water is replaced at the first adsorption.

It is suggested that from aliphatic solvent, the adsorbate is believed to be adsorbed on to a water layer at the pigment surface, though there must remain some interaction between it and the substrate since different acids have characteristic peaks. When adsorption takes place from aromatic solvent, the adsorbate finds it possible to displace the water layer to varying extents, and this passes into

solution; energetically this is not feasible in aliphatic solvent and it would have to be removed as an immiscible phase.

Such replacement of water is highly endothermic, water competing strongly with adsorbate for surface sites. Its effect does not commence at B, but at A, so the peak is actually considerably reduced in size while exothermic and endothermic effects oppose each other. This is seen to be so in practice when comparison is made of the peak size of a particular acid adsorbed from each solvent.

Unfortunately it has not been possible to prove unequivocally that water is the sole cause of the trough, as it has been impossible to carry out an adsorption in a totally dry system. An attempt was made to dry a weighed pigment sample in a glass bulb at elevated temperature under vacuum. It was then sealed, broken under rigorously dried solvent, and the slurry transferred to the calorimeter. This transfer was the critical stage: a glove box was not available so it was carried out in the normally-used cabinet in which the relative humidity was 15%. The transfer had to be done slowly as already wetted pigment tended to be washed out through the outlet tube gauze unless settling had started to take place. Recovery of the

pigment for re-weighing was necessitated nevertheless. Even were all this procedure completed satisfactorily, the resulting pigment bed was "irregular", irreproducible, and each adsorption peak observed contained "secondary" peaks, due to movement within the bed. The trough was still observed!

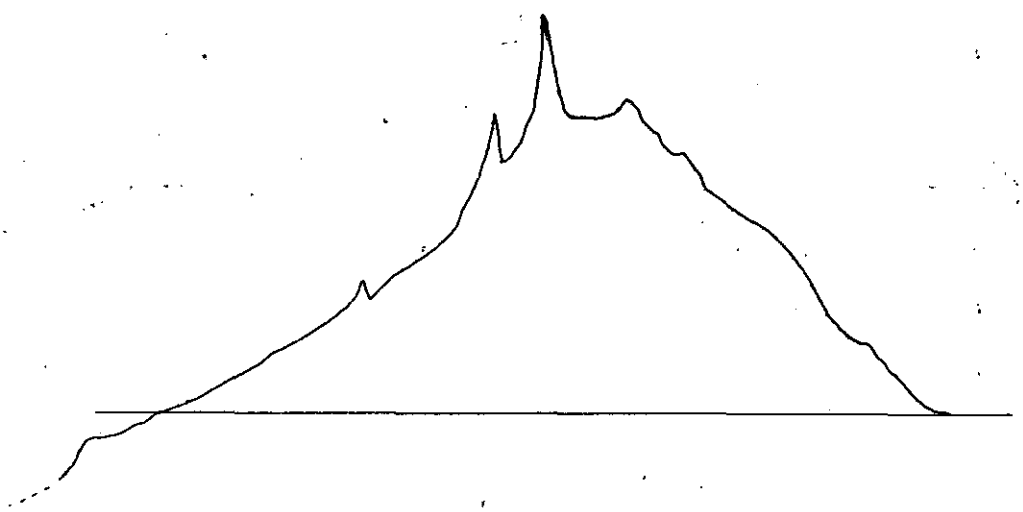

Comparison was made next, of peaks obtained under both 'wet' and 'dried' conditions.(see Table 4.4).

The differences observed were relatively small, suggesting only a small change in the number of surface sites available to pelargonic acid molecules, due to the presence of varying amounts of water. These results are inconclusive because, as demonstrated by the change from dried to wetted n-heptane, the

TABLE 4.4. ADSORPTION OF PELARGONIC ACID FROM $3g.l^{-1}$ SOLUTION IN n-HEPTANE ON RUTILE R1

PIGMENT PRETREATMENT	n-HEPTANE	HEAT OF DISPLACEMENT ($cals.g^{-1}$)	COMMENT
Dried	Dried	0.077	No Trough
Wetted	Dried	0.068	"
Wetted	Wetted	0.062	"
Dried	Dried	Change to wetted Heptane: 0.001	Extremely low heat evolution

difference between the wetted and dried pigment states is only marginal; both have extensively-hydroxylated surfaces, and negative troughs are observed with each type in aromatic solvent. The dried pigment still contains a number of adsorbed water molecules, since such a change ought to be accompanied by a large heat evolution as water becomes the adsorbed species.

Table 4.5. Effect of trace water on the heat of immersion of anatase in benzene[63].

Amount of water present ($\times 10^6$ moles.g^{-1})	Heat of immersion ergs.cm^{-2}
0.0	150
2.0	250
4.0	320
10.0	450
17.0	506
pure H_2O	520

Day and Parfitt[36] conclude from a study of the adsorption on pure rutile of aliphatic n-alcohols from solution in both n-heptane and p-xylene, that a rutile which after exposure to water vapour, is

outgassed at 25° for 30 minutes (surface S(3) which resembles most closely the likely condition of these surface-treated rutiles) is partially hydroxylated only. Physically adsorbed water molecules are strongly bound only by the hydroxyl groups and the non-hydroxylated portion of the surface, perhaps 40-50%, is at least partially exposed (though some weakly bound water is probably also present).

There is likely to be competition for adsorption on the non-hydroxylated portion, between solvent and solute. The former will engage in π electron-hydroxyl group interactions which are sterically flexible. In the presence of chemisorbed carboxyl groups, the weakly-held water associated with benzene will be induced to displacement.

The results quoted in section 4.3.2. of 2 K.cals. $mole^{-1}$ for the adsorption of stearic acid from benzene, appear at first sight to be extremely low if postulating a mechanism of ionic bonding. However, no allowance has been made for the removal of water thus, in aromatic solvent. Table 4.8. in section 4.4.3.1. shows heat of immersion data for rutile/water systems by various workers. A value of 405-425 ergs. cm^{-2}, equivalent to around 100 mcals.m^{-2} or + 6.6 K.cals. $mole^{-1}$ may be estimated from these data, for the dis-

placement of water. If this figure is added to that of 2 K.cals.mole^{-1}, a more realistic value of 8.6 K.cals. mole^{-1} is apparent: this is still a heat of exchange adsorption corrected only for desorption of water. Details are given later of a more vigorous correction procedure (section 4.4.3).

A correction of the same magnitude may be applied to the amine results. This is higher to start with, then the corresponding acid figure, possibly owing to the presence of species such as RNH_3^+ which would bond very strongly to the rutile surface.

4.4. Effect of Chain Length on Carboxylic Acid Adsorption

4.4.1. Results

Heats of exchange adsorption are quoted in Tables 4.6., 4.7., for pigments R1, 5a, 10b, of the adsorption from n-heptane of a series of carboxylic acids. For pigment 5a, results of adsorption from benzene are also quoted for the purposes of comparison. Figure 4.4. shows the heats of exchange adsorption plotted against acid chain length for adsorption on anatase 10b, for which the results are most extensive.

TABLE 4.6. ADSORPTION OF A SERIES OF ACIDS FROM 3g/l SOLUTION IN n-HEPTANE AND FROM BENZENE, ON DRIED RUTILE 5a.

ACID	HEAT OF EXCHANGE ADSORPTION m cals.m^{-2}	
	a) FROM n-HEPTANE	b) FROM BENZENE
Pelargonic $CH_3(CH_2)_7COOH$	16.5	7.2
Lauric $CH_3(CH_2)_{10}COOH$	15.3	8.2
Palmitic $CH_3(CH_2)_{14}COOH$	19.2	-
Stearic $CH_3(CH_2)_{16}COOH$	22.4	6.1
Oleic $CH_3(CH_2)_7CH = CH(CH_2)_7COOH$ (cis)	15.4	5.5
Elaidic " (trans isomer)	17.6	6.3
Benzoic C_6H_5COOH	18.4	7.3
Stearyl Hydrogen Phthalate, $CH_3(CH_2)_{16}COOC_6H_4COOH$	-	8.9

TABLE 4.7. ADSORPTION OF A RANGE OF ACIDS FROM $3g.l^{-1}$ SOLUTION IN n-HEPTANE ON a) DRIED RUTILE, R1, AND b) DRIED ANATASE 10b

ACID	HEAT OF EXCHANGE ADSORPTION m cals.m^{-2}	
	(a) RUTILE R1	(b) ANATASE 10b
Caprylic $CH_3(CH_2)_6COOH$	-	12.6
Pelargonic $CH_3(CH_2)_7COOH$	11.1	13.4
Capric $CH_3(CH_2)_8COOH$	-	15.6
Lauric $CH_3(CH_2)_{10}CCOH$	13.2	12.9
Myristic $CH_3(CH_2)_{12}COOH$	-	23.2
Palmitic $CH_3(CH_2)_{14}COOH$	52.1	60.2
Stearic $CH_3(CH_2)_{16}COOH$	48.8	62.2
Oleic $CH_3(CH_2)_7CH{:}CH(CH_2)_7COOH$ (cis)	11.1	12.0
Elaidic " (trans isomer)	13.3	11.2
Benzoic C_6H_5COOH	14.1	15.5

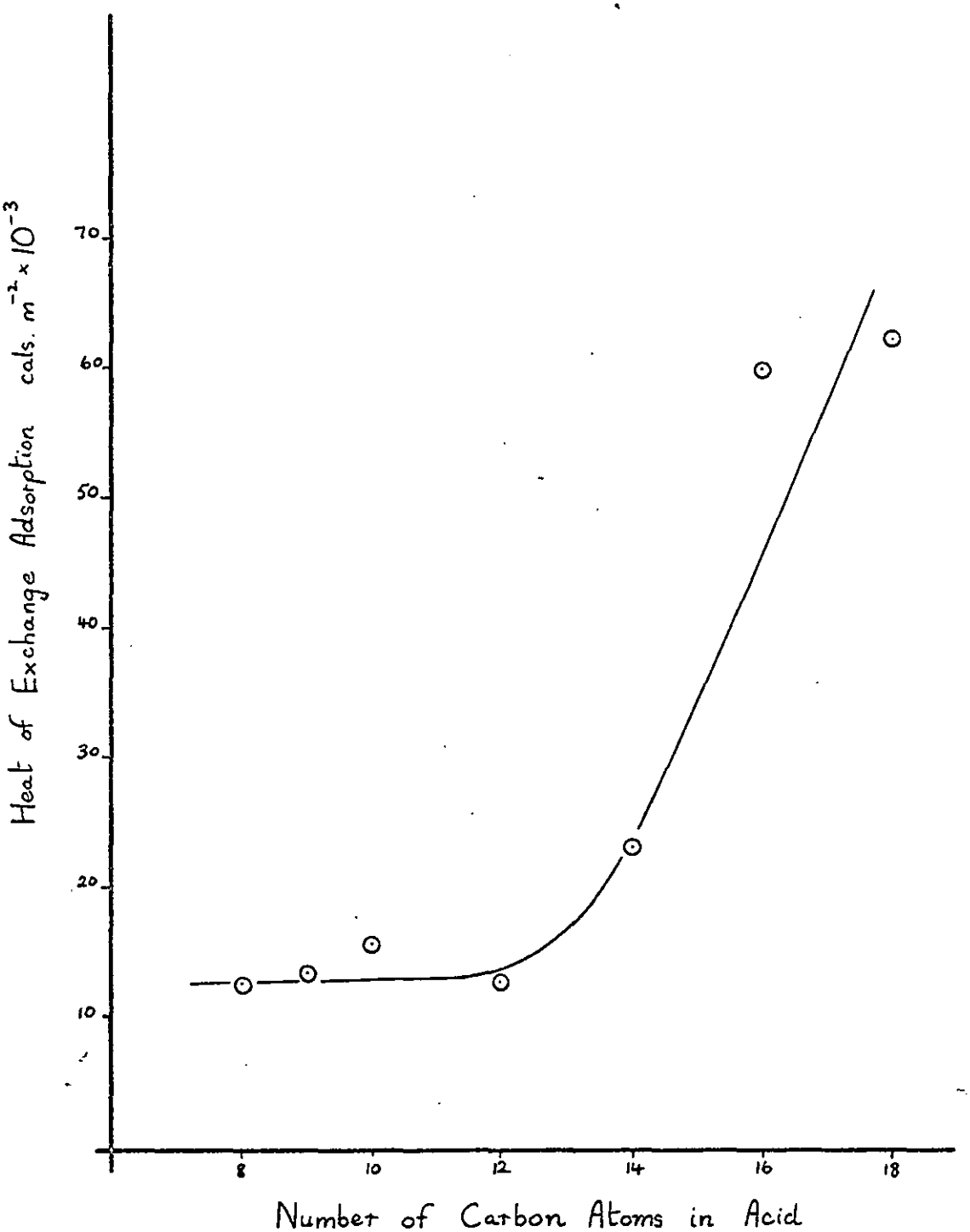

Fig. 4.4. The Variation of Heat of Exchange Adsorption with Chain Length of Acid, on Anatase

In several cases, only one peak was measured; only where any doubt arose, over the shape of the peak obtained for instance, were second and third peaks measured. No error limits have been evaluated: a maximum random error of not greater than ± 12% is assumed (see section 4.1.3.)

4.4.2. Discussion

The unusually large heats of exchange adsorption on the non-surface-treated pigments of stearic and palmitic acid are particularly noticeable. On the surface treated rutile 5a, they are not exceptional, however. This suggests a different adsorption mechanism, brought about by the zinc present in the latter but not the two former pigments. Rybicka and Kelman[44] have confirmed the carboxyl/oxide interaction to be a hydrogen-bonded system with pure oxide and an ionic-bonded system with the surface-treated or zinc-containing oxide.

Using the values quoted by Sherwood and Rybicka[9] for the specific adsorption of stearic acid from benzene, (7.8×10^{-6} moles.m^{-2} for 10b, 4.2×10^{-6} moles.m^{-2} for 5 a and 5.1×10^{-6} moles.m^{-2} for R1, The difference in solvent is not considered to

invalidate the use of this data, in this particular context), the heat of exchange adsorptions expressed as a function of the quantity of acid adsorbed are 8.0 K.cals.mole^{-1} on 10b, 5.35 K.cals.mole^{-1} on 5a and 9.6 K.cals.mole^{-1} on R1. However, these figures are not meaningful unless allowance is made for the heat of wetting by n-heptane and the heat of dissociation of stearic acid in n-heptane.

(It is interesting to note the resemblance of trend between these results and those of Groszek[47] who measured the heat of exchange adsorption of normal hydrocarbons from n-heptane solution on to cast iron powder in the flow microcalorimeter. Above carbon chain length of 16, the heat evolved starts to increase from around 8 K.cals.mole^{-1} to about 11 K.cals.mole^{-1} at chain length 20, and thereafter, linearly at least to chain length 32 (35 K.cals.mole^{-1}).

4.4.3. The Calculation of Heats of Adsorption from Heats of Exchange Adsorption

An examination of equation 1.33 is required in order that correction factors may be applied for each process relevant to the overall adsorption process in the calorimeter.

$\Delta H_A = \Delta H_{EA} - \Delta H_{w\ solvent} \pm$ effects due to:-

dimerisation
Intermolecular reaction
hydration
water displacement
dilution

(1.33.)

In the work with the carboxylic acid/n-heptane/anatase system, all materials were dried; although as suggested by the benzene results this would not remove all water, there was insufficient water content in the n-heptane to cause measurable hydration effects with the solute, and none from the pigment surface was displaced, as the peak observed was symmetrical and represented a wholly-exothermic process. Dilution effects were considered negligible at the level of concentration used.

There is doubt about the nature of the possible intermolecular reaction, that is, the inter-chain reaction between adjacent aligned molecules at the surface, particularly as far as the longer chain acids are concerned (see section 4.5.3.3.). Although such

an effect is ignored in the following few pages, since no heat values can be assigned to the effect, the possibility of its existence must not be forgotten. Strictly speaking, it is anyway legitimate to include it as an integral part of the adsorption process, so no separate allowance need be made.

Thus we see from equation 1.33., corrections allowing for dimerisation and wetting are necessary to be applied to the heat of exchange adsorption, to convert it to the heat of adsorption.

4.4.3.1. Heats of Wetting or Immersion

Values cited 'in the literature' for these quantities often refer to insufficiently - characterised systems. Of a considerable list of references checked only eight (7, 13, 17, 63, 64, 65, 66 and 67) have yielded data relevant to these systems, and none describes the identical system. An added variable is that of the outgassing temperature of the sample prior to the immersion process which has been found to be critical[67].

However, from Table 4.8., the average value for all types (except reference 17) of titanium dioxide immersed in either n-hexane, n-heptane, or n-octane

was taken and applied as correction factor in the present titanium dioxide/n-heptane series. That is 142 ± 8 ergs cm^{-2} which is equivalent to 34.0 ± 0.5 m cals.m^{-2}. This is naturally an approximate figure only:

1/ The immersion was recorded most frequently at temperatures other than 20°C.

2/ The outgassing temperatures varied widely; for an evacuated outgassed sample it is likely that Ti - O - Ti linkages are exposed, particularly at higher temperatures. Hydroxyl groups will probably remain if heated in contact with air, even to the region of 450°C [36], resulting in lower heats of immersion[17], and so for these samples, merely heated overnight in the oven, are still fully hydroxylated and it is likely that the value of 142 ergs cm^{-2} is considerably overestimated.

3/ Oxides studied are generally assumed to be non-pigmentary grades, that is, laboratory prepared and purified. Wade and Hackerman [67] have also shown variations in heats of immersion with particle size.

TABLE 4.8. HEATS OF IMMERSION

SOLID	SURFACE AREA $m^2.g^{-1}$	ACTIVATION TEMP. °C.	IMMERSED IN	AT TEMP °C	HEAT OF IMMERSION $ergs.cm^{-2}$	REFERENCE
Rutile	7.3	-	n-Hexane	25	135	64, 65
"	"	-	n-Heptane	"	144	"
"	"	-	n-Octane	"	140	"
"	"	-	n-Butanol	"	410	"
"	"	400	Water	"	550 ± 18	"
Rutile	-	-	"	"	410	"
Aerosil SiO_2	-	-	"	"	165	"
"	-	-	n-Heptane	"	118	"
Anatase	-	-	Benzene	"	150	7
"	-	-	Water	"	520	"
" ($water_{saturated}$)	-	-	"	"	120	"
Anatase	11.1	300	"	20	441 ± 14	66
Rutile	7.6	"	"	"	406 ± 2	"
Rutile (untreated)	6.4	250	n-Heptane	30	144 ± 7	13
"	"	"	n-Butanol	"	303 ± 9	"
Rutile (surface Treated, Al_2O_3/SiO_2)	11.2	"	n-Heptane	"	150 ± 6	"
	"	"	n-Butanol	"	380 ± 10	"
Anatase	10.5	100	Water	"	504	67
"	"	"	n-Hexane	"	137	"
Rutile	5.8	50	Water	-	409	63
"	"	100	"	-	498	"
∝ Alumina	2.7	160	"	-	693	"
"	"	"	n-Hexane	-	151	"
Alumina (amorphous)	104	"	Water	-	454	"
"	"	"	n-Hexane	-	85	"
Rutile	14.2	450	n-Heptane	25	36	17

It is worthy of note that the heptane and acid molecules do not exchange one for another owing to the difference in their molecular areas. Harkins [7] suggests an area of cross-section for the n-heptane molecule of 64 $\mathring{A}^2$. (determined by the Harkins and Jura relative method based on a two dimensional equation of state for condensed films [10]) Emmett and Brunauer [68] suggest 42.5 $\mathring{A}^2$ for this quantity, but their method assumes the molecule to be spherical. However, the generally accepted area occupied by a vertically-oriented straight-chain aliphatic acid is 20.5 - 21 $\mathring{A}^2$ so the removal of one n-heptane molecule, lying flat at the surface can be assumed to make room for three acid molecules. This does not affect heats of immersion corrections, however, provided the latter are quoted per unit area of surface.

The work by Sherwood and Rybicka [9] also makes it apparent that adsorbed stearic acid on titanium dioxide does not form a complete monolayer; presumably some solvent and/or water constitutes the remainder of the surface film.

4.4.3.2. Heats of Dissociation or De-dimerisation

It is known that acids exist in organic solvent

in a partially dimeric state. Monomer and dimer are in equilibrium, and whenever monomer is removed from the bulk solution, to the pigment surface, the equilibrium is disturbed and further dissociation takes place to restore balance. The heat of dissociation can be estimated as suggested by Davies and Sutherland[69], from knowledge of the temperature variation of the dissociation constant, K. For acetic acid in carbon tetrachloride, unfortunately the only example they quote, it is 9.3 ± 1 K.cals.mole^{-1}. That is, for each mole of dimer dissociated to give two moles of monomer, 9.3 K.cals. are evolved.

The corrected results, heat of adsorption figures are summarised in Table 4.9., together with the corresponding heats of exchange adsorption.

In obtaining these figures, several assumptions should be summarised:

1/ That stearic acid adsorbs in a vertical orientation. Evidence [18,29] for this is well-known and to this can be added that of Sherwood and Rybicka [9] who had to assume a vertical orientation; at the level of adsorption they have recorded, were the acid lying flat on the surface and occupying 114 $\AA^2$. molecule^{-1}, this would form an adsorbed layer nearly 6 molecules

TABLE 4.9. THE ADSORPTION OF STEARIC ACID ON TITANIUM DIOXIDE

	PIGMENT					
	RUTILE 5a		RUTILE R1		ANATASE 10b	
Surface Area, $m^2.g^{-1}$	14.7		7.2		9.3	
Amount adsorbed, moles.m^{-2} x 10^6	4.2		5.1		7.8	
% Surface Coverage	52		63		96	
	m cals.m^{-2}	K cals.$mole^{-1}$	m cals.m^{-2}	K cals.$mole^{-1}$	m cals.m^{-2}	K cals.$Mole^{-1}$
Heat of Exchange Adsorption, ΔH_{EA}	-22.4	-5.35	-48.8	-9.6	-62.2	-8.0
Heat of Immersion, ΔH_w solvent	-17.7		-21.4		-32.6	
Heat of Dimerisation, ΔH_{DIM}	+19.5		+23.7		+36.3	
Heat of Adsorption, ΔH_A	-24.2	-5.75	-51.1	-10.0	-64.9	-8.3

thick.

2/ Specific adsorption figures used here came from results obtained using benzene as solvent, and applied to a heptane system. Ottewill and Tiffany [18] used a rutile similar to R1, and heptane to obtain a maximum adsorption of 5.75×10^{-6} moles.m^{-2} (at 25°C) for stearic acid which is relatively close to the value of 5.1×10^{-6} moles.m^{-2} quoted in Table 4.9. It is likely that the adsorption figures from heptane and benzene dont differ widely for the other titanium dioxides.

3/ The value used of 9.3 K.cals.$mole^{-1}$ for the heat of dimerisation is extremely doubtful. although the dielectric constant of carbon tetrachloride is very close to that of n-heptane, it seems unlikely that the dissociation constant for long chain acids remains equal to that of acetic acid. However, no more relevant data has been found.

To overcome the limitations imposed in assumption 2, and in order to examine more closely the site-energy distribution of anatase 10b in particular, adsorption experiments were carried out using three

radio-actively labelled acids. The results were correlated with extensive heat curves measured by the calorimeter on the same system.

4.5. Adsorption on Anatase of Acids from Solution at Varying Concentrations

4.5.1. Results

Adsorption isotherms for lauric, stearic and oleic acids are shown in figures 4.5., 4.6., and 4.7. The corresponding heat curves are shown in figures 4.8., 4.9., and 4.10., respectively. The isotherm for adsorption of oleic acid was measured at 20°C by windowless counter of evaporated samples on planchets, the others by liquid scintillation counting at 25°C.

The saturated acids exhibit the frequently-observed Langmuir-shaped isotherm rising rapidly from zero concentration tending towards a plateau of maximum adsorption the extent of which will not be exceeded when the concentration is increased further. The maximum adsorption levels are $(6.7 \pm 0.6) \times 10^{-5}$ moles of lauric acid and about 7×10^{-5} moles of stearic acid per g of pigment. Similarity in these figures gives added support for the assumption that the acid molecules are vertically - or near - vertically-oriented at the surface; taking the area of cross

section of this orientation as 20.5 $\mathring{A}^2$, these adsorption figures represent about 90% coverage of the available surface.

Considerable scatter was observed with the points in the lauric acid adsorption isotherm, shown in figure 4.5., which was ascribed to the counting procedure when it was noticed that the counting level of the standard fluctuated from day to day. An improvement in the stearic acid isotherm, was achieved by: a) topping-up the level of silicone fluid in the castle.

b) the use of microscope lens tissues only, to wipe D.J. jars and ampoules, so avoiding accumulation of fibres in the castle.

c) avoiding possible non-removal of liquid from the sealed neck of the sealed standard.

d) closing the castle door more tightly at the locking screw.

These precautions, together with that of using the quenching curve to deduce initial count rates (see section 3.2.4.5.) were found to be quite effect-

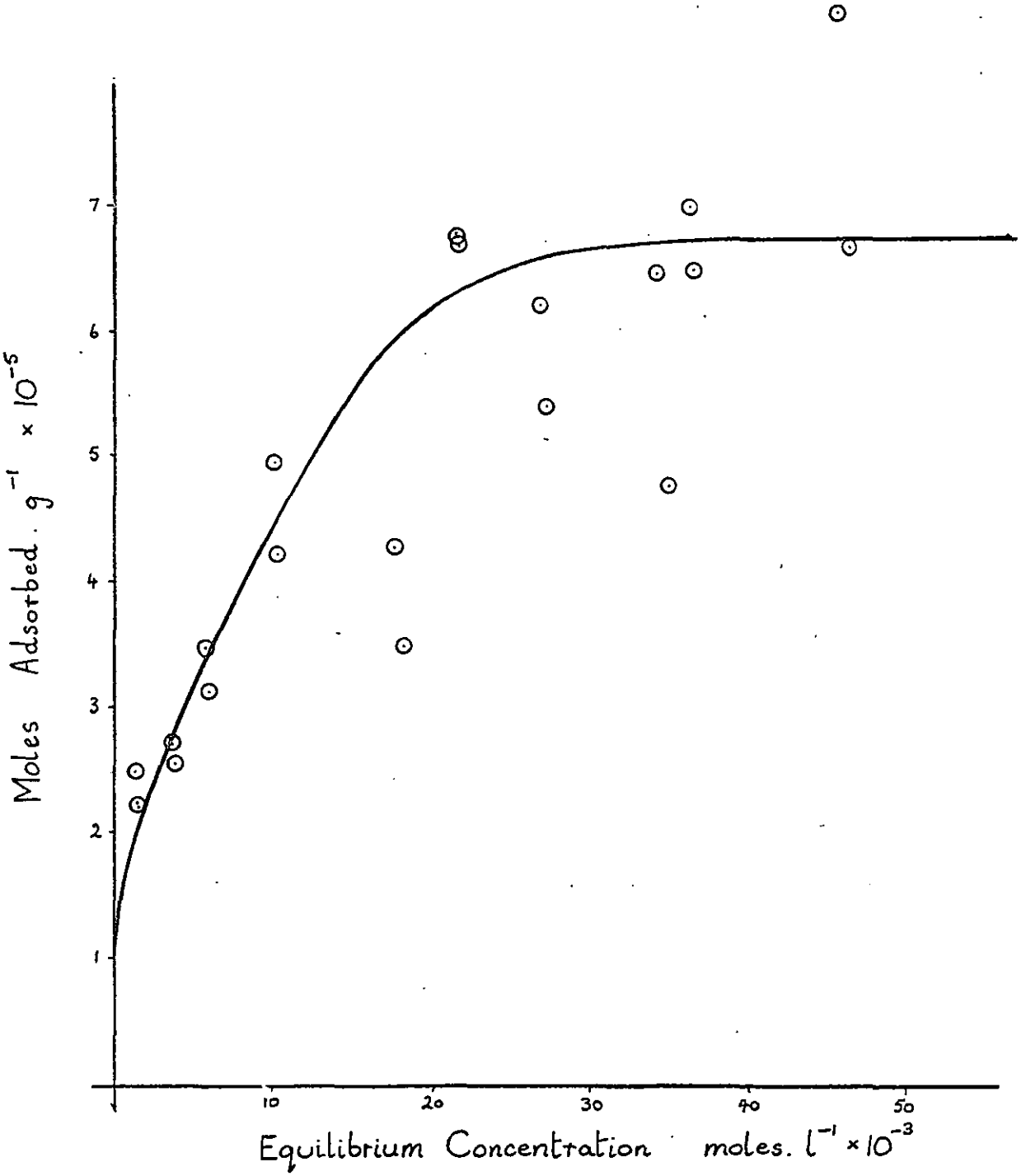

Fig. 4.5. The Adsorption Isotherm of Lauric Acid on Anatase

ive (see figure 4.6.) in reducing scatter on the subsequent isotherm.

Oleic acid was shown to give a stepped isotherm; (figure 4.7.) the first step is at 3.5×10^{-5} moles acid per g., but the upper limit cannot be estimated with any confidence as the adsorption is still rising rapidly above and beyond 40 mM solution. It is considerably higher than for lauric and stearic acid.

Each acid has a characteristic heat of exchange adsorption curve. For lauric acid, it is apparently constant beyond 35 mM solution concentration (figure 4.8) at 117 ± 13 m.cals.per g of pigment. For stearic acid it rises steadily (figure 4.9) to a probably maximum of between 500 and 600 m.cals per g while for oleic acid (determined at 20°C) there is some evidence of a 'step' similar in nature to that of the adsorption isotherm. This is at 70 m.cals per g, but does not start to increase at a corresponding solution concentration instead requiring rather more concentrated conditions about 30 mM solution. Random experimental errors were all in the region 11 - 12% (see section 3.3.6.1).

4.5.2. Differential Heats of Exchange Adsorption

If the heats of exchange adsorption measured are

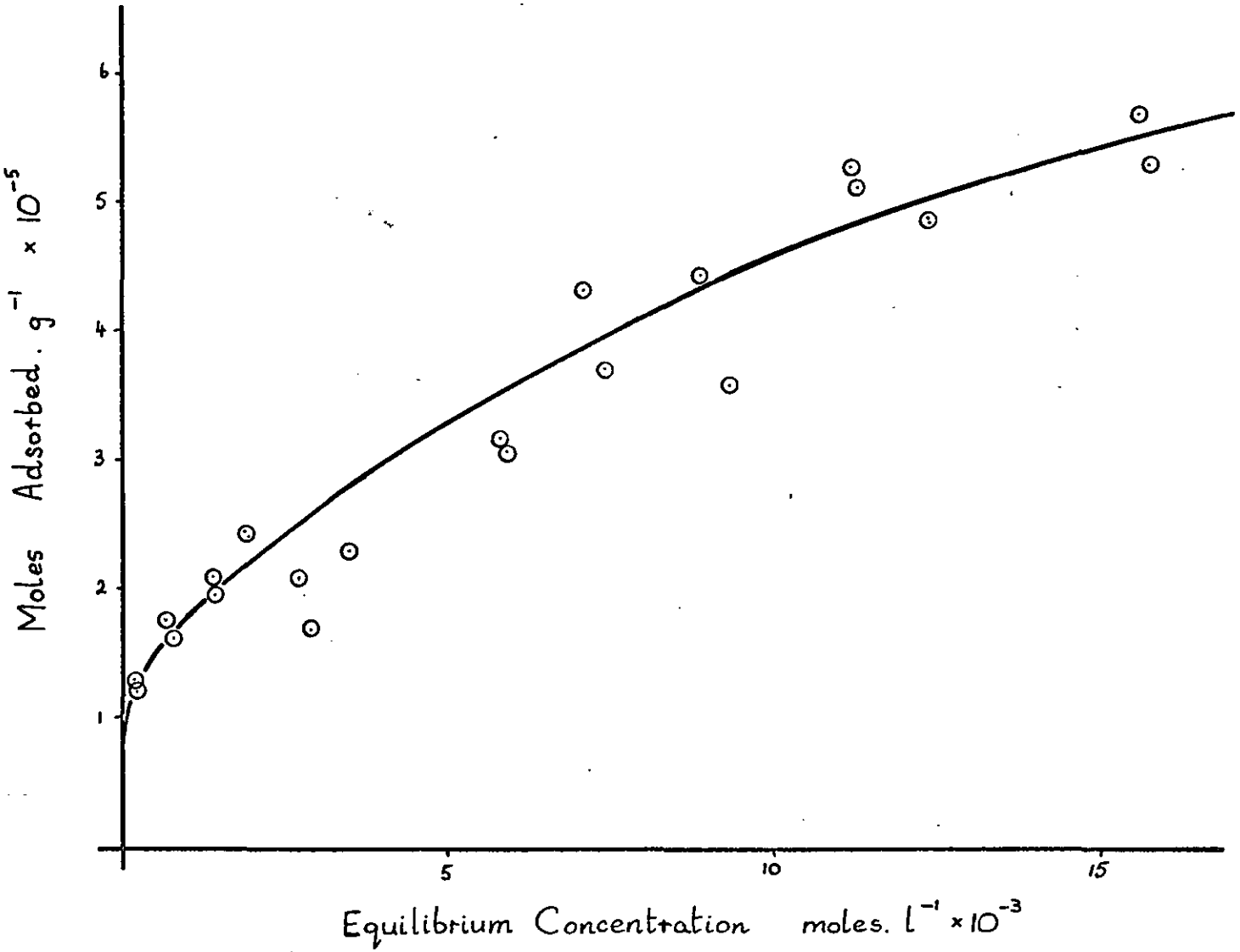

Fig. 4.6. The Adsorption Isotherm of Stearic Acid on Anatase

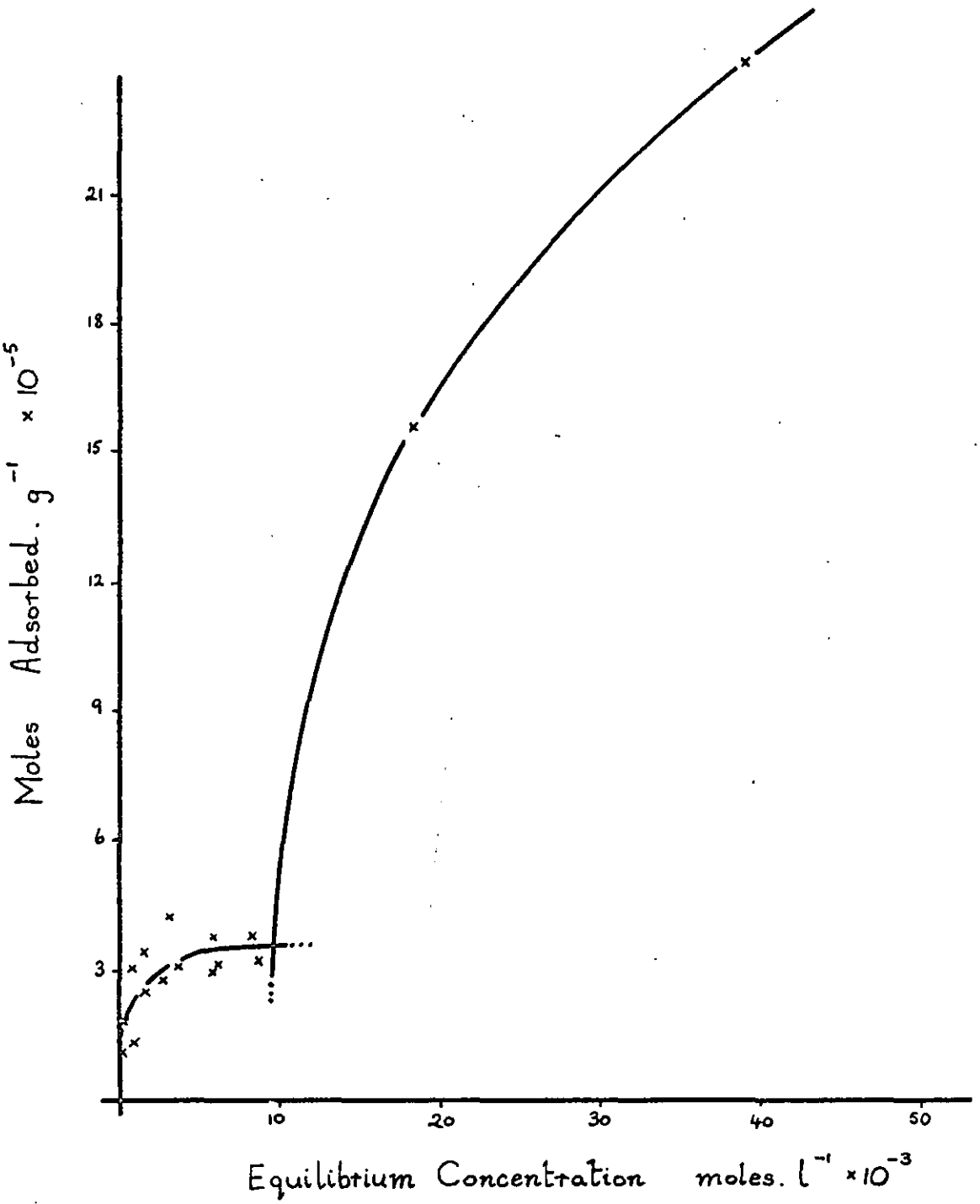

Fig. 4.7. The Adsorption Isotherm of Oleic Acid on Anatase

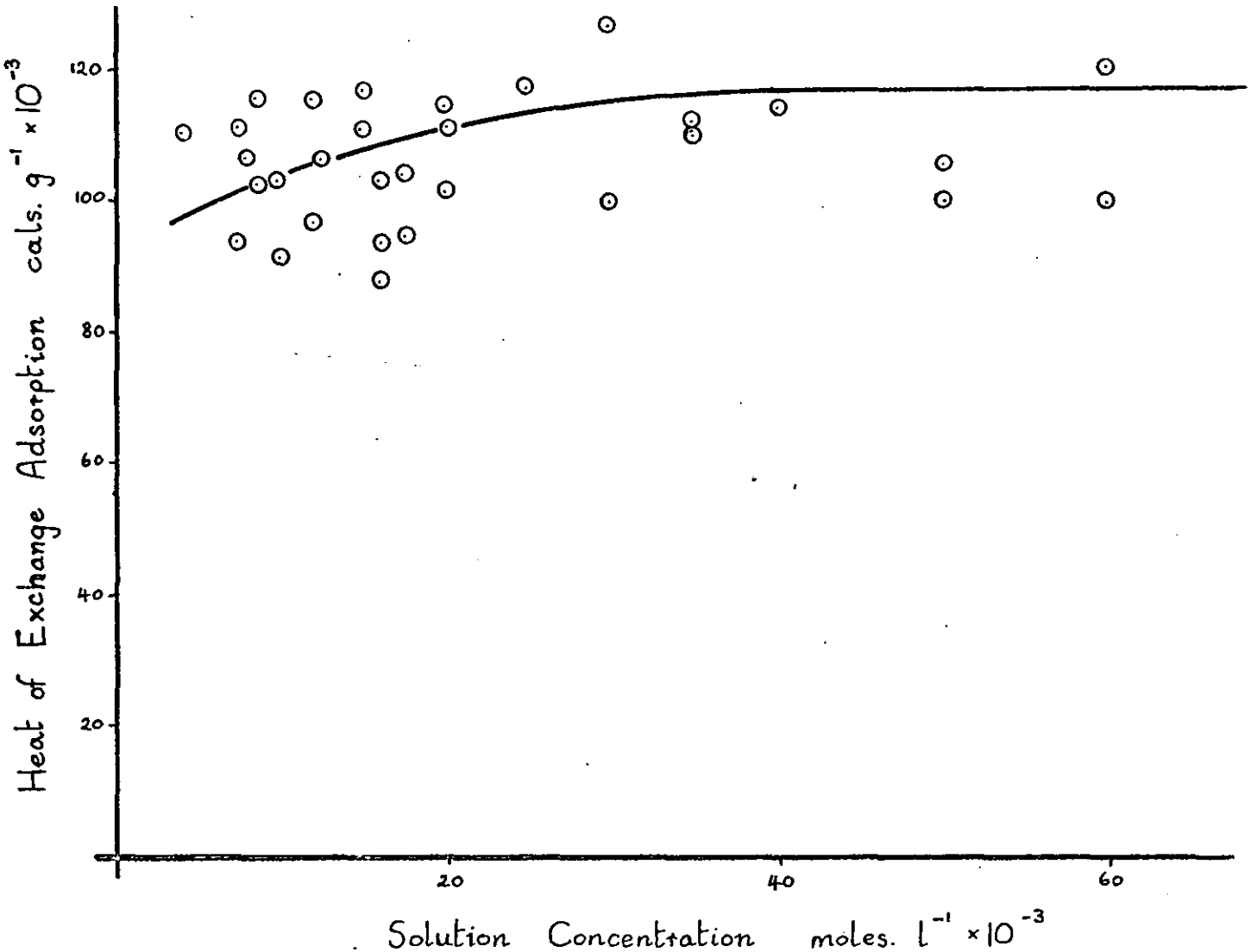

Fig. 4.8. The Heat of Exchange Adsorption of Lauric Acid on Anatase

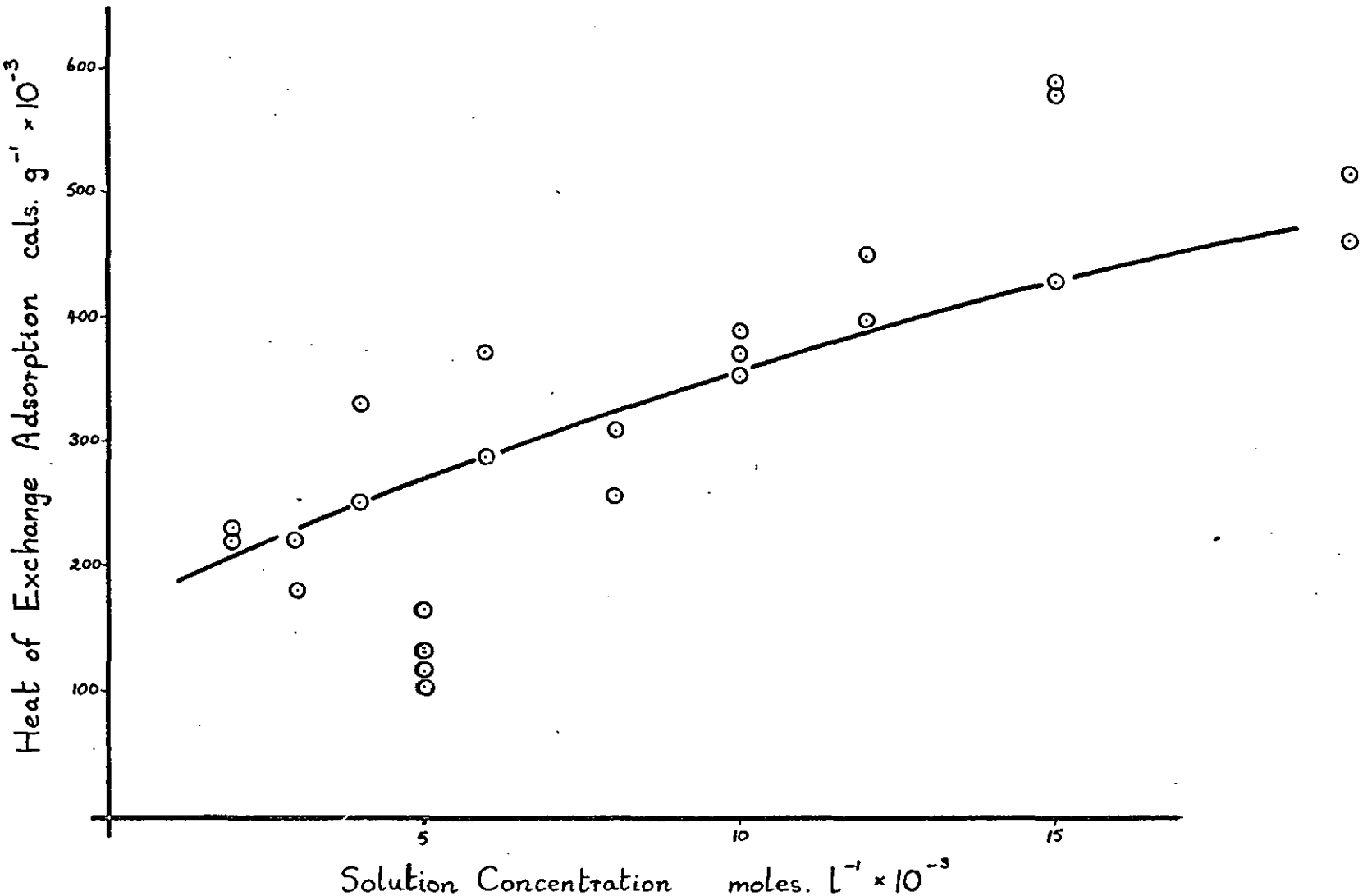

Fig. 4.9. The Heat of Exchange Adsorption of Stearic Acid on Anatase

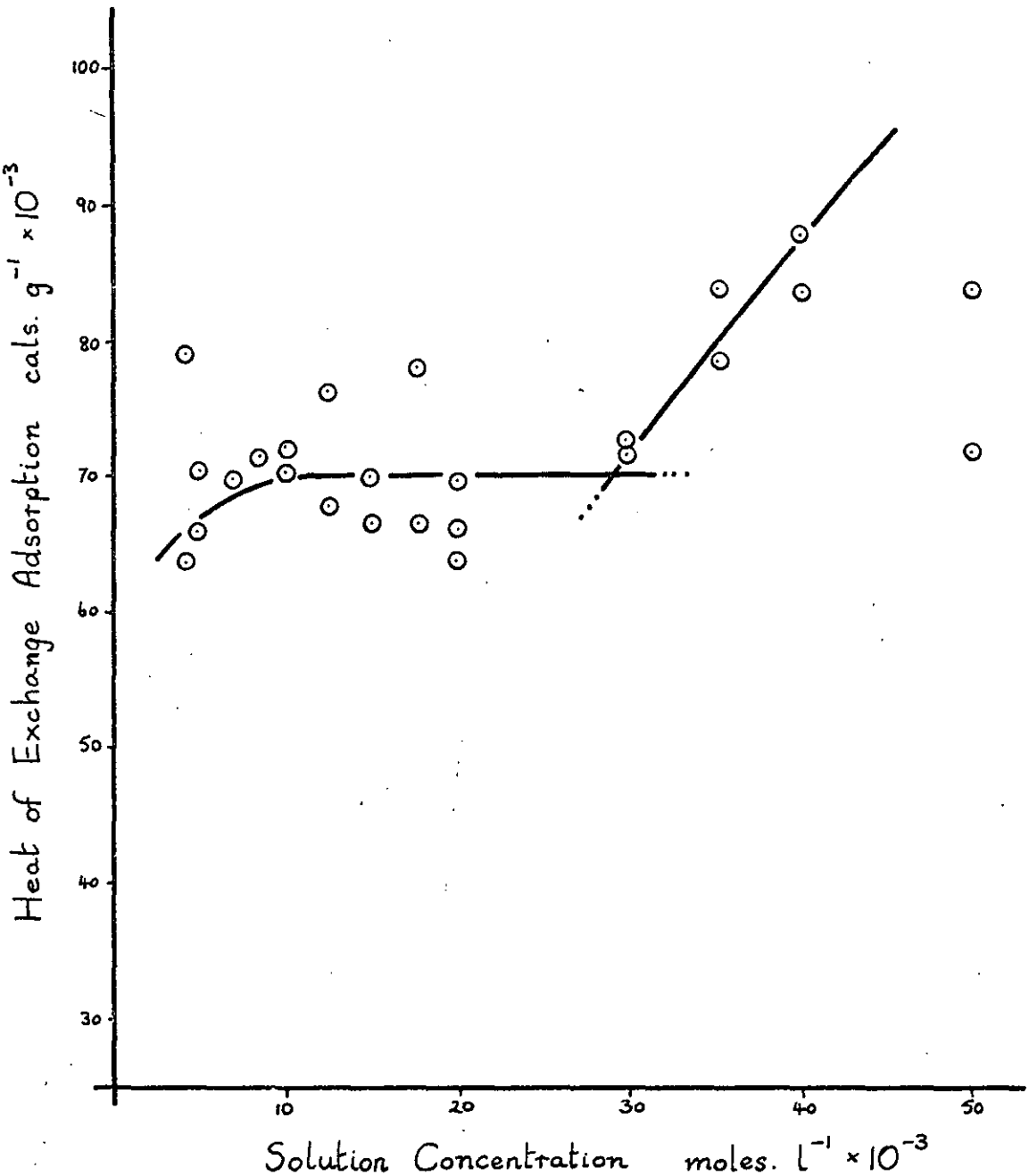

Fig. 4.10. The Heat of Exchange Adsorption of Oleic Acid on Anatase

now plotted against the number of moles of acid adsorbed, the gradient is equal to the differential heat of exchange adsorption. This quantity is more conveniently obtained by dividing a series of incremental heat changes over the whole range of concentration, by the corresponding incremental changes in the number of moles adsorbed, over the same range. It can in turn, be plotted against the number of moles adsorbed to give an indication of how the heat of exchange adsorption is varying as the pigment surface is gradually covered. The resulting curves are shown in figures 4.11., 4.12., and 4.13. The abscissa in two cases is scaled by two sets of units:

i) the number of moles acid adsorbed x 10^5

ii) % surface coverage, assuming a vertical orientation of the adsorbed acid molecules.

The % surface coverage was omitted from the oleic acid differential heat curve, owing to the discrepancy of the position of the steps in the two preceding graphs, and the uncertainty of the nature of orientation of the oleic acid molecules adsorbed.

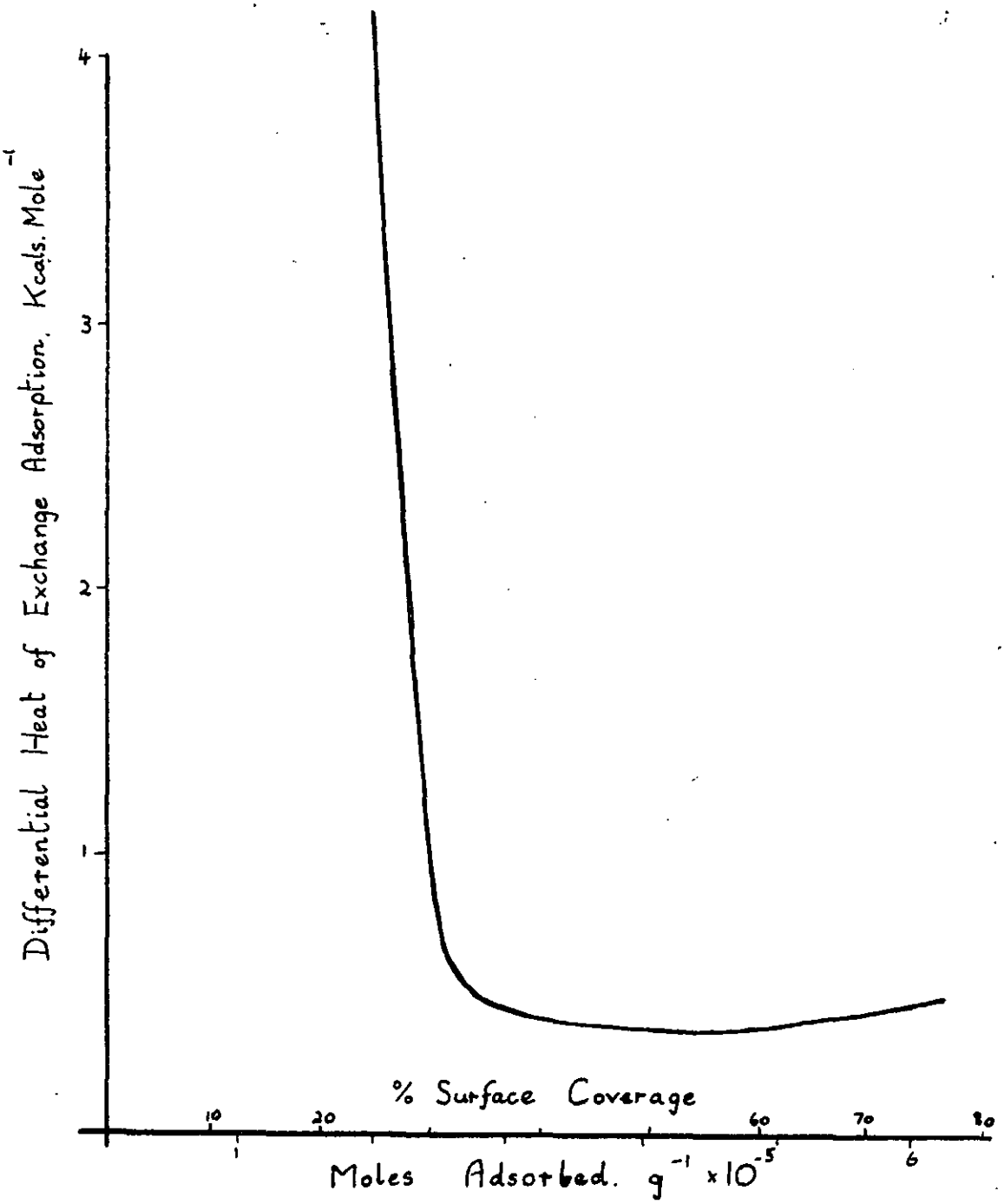

Fig. 4.11. The Differential Heat of Exchange Adsorption of Lauric Acid on Anatase.

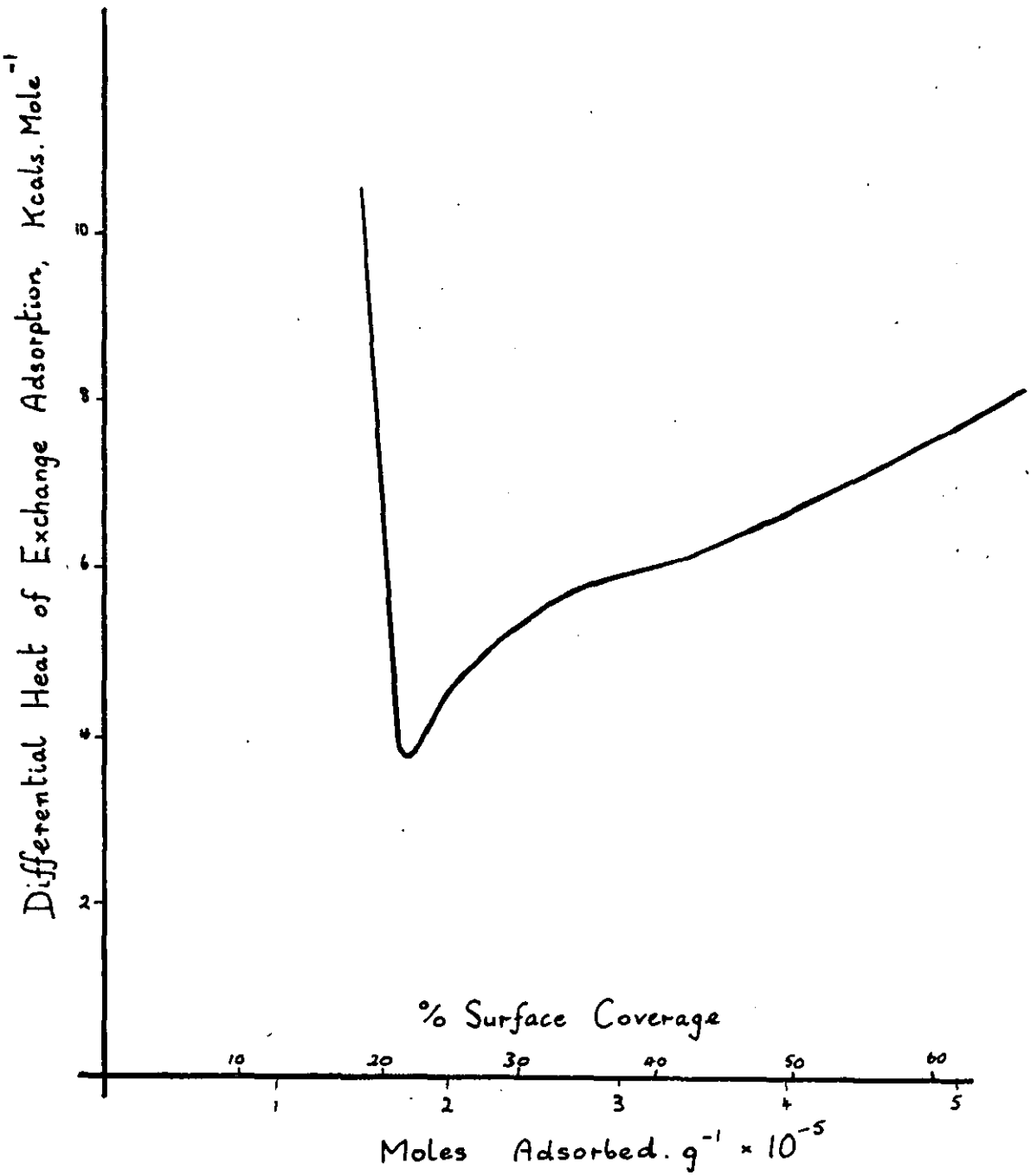

Fig. 4.12. The Differential Heat of Exchange Adsorption of Stearic Acid on Anatase.

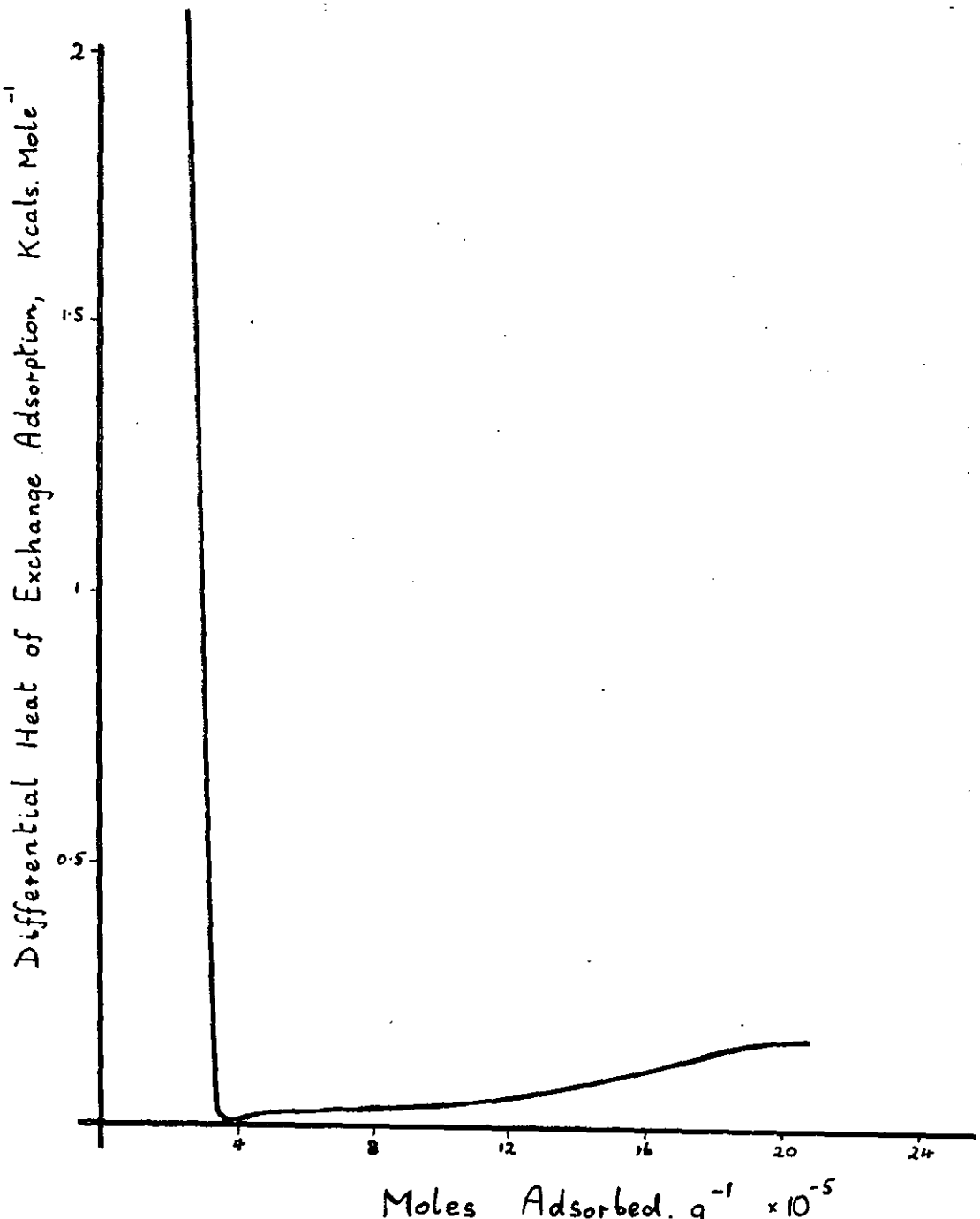

Fig. 4.13. The Differential Heat of Exchange Adsorption of Oleic Acid on Anatase.

4.5.3. Discussion

4.5.3.1. Adsorption Isotherms and Heat Curves

There is no record apparent in the literature of an adsorption isotherm of lauric acid on titanium dioxide. That of stearic acid exists; the adsorption from cyclohexane on titania is reported by Kipling and Wright[29], that from benzene on anatase 10b by Sherwood and Rybicka[9] and from n-heptane on rutile by Tiffany[17, 18]. It is interesting to note, however, that the shoulder effect is much more pronounced in the work of these authors. (i.e: there is a much steeper initial rise in the quantity of acid adsorbed followed by a more rapid levelling-off at plateau level). The latter three authors quote the plateau level as 7.4×10^{-5} moles.g^{-1} and 8.15×10^{-5} moles.g^{-1} for their respective systems.

Tiffany[17, 18] extended his study to include the oleic acid adsorption isotherm from n-heptane on rutile. His isotherm is stepped at 5×10^{-5} moles acid.g^{-1}, as opposed to 3×10^{-5} moles acid.g^{-1} as seen in figure 4.7. and this occurred in considerably more-dilute solution. The ultimate level of adsorp-

tion on rutile is probably little over half that on anatase on the evidence of these results. The heats of exchange adsorption quoted in Table 4.7. suggest an overall increase of adsorption on anatase of only about 8%, however. (This assumes the adsorption at 3 $g.l^{-1}$ ($\equiv$ 10.6m$\bar{M}$) solution concentration is taking place on effectively mono-energetic sites; figure 4.13. suggests that this is doubtful).

There is no record either, of heats of exchange adsorption measured over a range of concentration, which are relevant to this study. The value of - 10.0 $K.cals.mole^{-1}$ here given (Table 4.9.) for the heat of adsorption of stearic acid on rutile R1 is near the value of - 8.65 $K.cals.mole^{-1}$ given by Tiffany[17] for a similar rutile. These figures are of an order of magnitude consistent with postulation of a mechanism of hydrogen bonding in the adsorption process. Ionic bond formation on the other hand, should give rise to enthalpy changes of the order of 50 - 100 $K.cals.mole^{-1}$, but the heat of adsorption of stearic acid on rutile 5a, for which ionic bonding is operative[44] is lower, at - 5.75 $K.cals.mole^{-1}$ (Table 4.9.). No explanation of this result can be supplied except to say that there may be some desorption taking place, of surface moisture, from the

rutile 5a which will reduce the overall heat evolved. (Note particularly the low value of 6.1 m.cals.m^{-2} (Table 4.6.) for the heat evolved when rutile 5a adsorbs stearic acid from benzene).

4.5.3.2. Orientation of the Adsorbed Layer

It is generally accepted that straight chain acid and alcohol molecules will adopt a vertical or near-vertical orientation when adsorbed from a non-polar solvent. (Which does not compete for polar surface sites). In all subsequent discussion on the models of adsorption to be considered, the existence or otherwise of n-heptane molecules is ignored. It does not compete, and although the pigment is initially immersed in n-heptane and has a film completely or nearly-completely covering it, there is no evidence of any condition in which it is not easily displaced.

Although initially the saturated aliphatic molecules will adsorb in a horizontal orientation, as the quantity adsorbed increases so their orientation is postulated to pass through the stages of formation of a condensed film, viz: liquid expanded, intermediate, liquid condensed , to solid, which is a highly condensed film of vertically-oriented

molecules showing considerable forces of cohesion between one another.

Real transitions in re-orientation can only be detected with oleic acid. A similar model is adopted as before, illustrated by the liquid film on water in a Langmuir Trough[70]. Three distinct orientations can be defined:

1/ the molecules lie flat on the surface

2/ the carboxyl head group and the unsaturation centre provide "anchorage" and the hydrocarbon tail extends into the bulk solution.

3/ the carboxyl head group provides the only point of attachment, and the chain, slightly bent, extends into the bulk solution. This is compressible as with the saturated acids.

At the 'step' point on the isotherm and heat curve the point of attachment at the double bond is squeezed out from the surface: its heat of adsorption is lost but the heat of adsorption of the carboxyl head group of incoming molecules oriented as in (3) is gained. As always, increases in the quantity of

acid withdrawn from the solution to the surface are accompanied by a dissociation of dimers to maintain the monomer $\rightleftharpoons$ dimer equilibrium there.

Several other theories have been put forward to account for stepped isotherms. These include that of Langmuir[21] who suggested they may arise from surface or crystal irregularities and even different crystal faces. Dintenfass[39, 40] has been a protagonist of this theory, although he did not observe a stepped oleic acid adsorption isotherm[39]. They can safely be disregarded here as there has been no evidence of stepping with the isotherm or heat curve of either saturated acids, yet the same surface is being examined by a basically-similar adsorbate.

The presence of moisture has also been used to account for stepped isotherms on polar solids;[71] hydrogen bonding is permitted of the first adsorbed layer, but subsequent adsorption depends on intermolecular cohesive forces and the transition from one mechanism to the other is indicated by a step. Again, no evidence to support this was obtained, even though a pigment which was equilibrated first with an atmosphere of 60% relative humidity was used.

4.5.3.3. Active Sites

There has been an awareness of the existence of active sites on titanium dioxide since the first days of precision calorimetry. These are believed to comprise crystal edges and corners at which the presence of oxygen atoms, whether or not hydroxylated, would lead to enhanced adsorption bonding with a polar adsorbate, i.e: it is an area of high electron density. On each crystal face there is a regularly-packed array of oxygen atoms taking the profile of a ridge and furrow condition. (each row is flanked by another at a slightly lower level). One would never expect 100% surface coverage by one particular acid; some sites will be partially blocked by existing adsorbed species and not all the surface as measured by nitrogen adsorption will be available to the larger acid molecules. This means in fact that the effective surface area of the vertically oriented acid is not 20.5 $\mathring{A}^2$ but 26.4 $\mathring{A}^2$ [17]. The original figure has been used in computing surface coverages to avoid confusion. Although packing may not be effectively close in a surface film composed solely of acid, since the adsorption sites are not separated precisely by the diameter of the acid, a portion of the film will contain the smaller n-heptane molecules. Probably the effective area occupied per acid molecule is some

value between the two suggested.

Examination of figures 4.11. and 4.12. shows there to be a considerable amount more heat evolved for the coverage of the first portion of the surface than for subsequent coverage. This corresponds to the occupation of active sites as the concentration of acid in the system is increased. According to lauric acid adsorption, they account for 30% of the anatase surface, and to stearic acid, 22%. This discrepancy between these two figures can be explained by the fact that at low coverage in dilute solution the adsorbed molecules are not rigidly vertically-oriented but may more resemble seaweed attached to a rock. This is an intermediate state, the chains may be up to 20° from the vertical, and the longer stearic acid chain will thus present greater obstruction than lauric acid of the surface sites. One may conclude that near to 25% of the anatase surface comprises active sites.

Uncertainty arises from the oleic acid differential heat curve, figure 4.13., for two reasons. One is that the acid cross-sectional area will tend to change over the whole concentration range as the orientation varies. The other is that there is a discrepancy between the positions of the

step in the adsorption isotherm, figure 4.7., and the heat curve, figure 4.10. The concentration at which the second increase in either the number of moles adsorbed or the heat of exchange adsorption takes place must be in error, as they should coincide. In order to construct the differential heat curve, figure 4.13., the adsorption isotherm was assumed to be incorrect (the secondary rise was taken to commence not at 10 mM solution, but at 28 mM solution, which contradicts the evidence of only two experimental points) so as to obtain the slight increase in the differential heat starting above 3.5×10^{-5} moles.g^{-1} instead of in the region of 2×10^{-4} moles.g^{-1} adsorbed. This figure for the number of moles of acid adsorbed corresponds closely with that of 3.2×10^{-5} moles.g^{-1} required for a complete monolayer of acid oriented in two-point attachments (area occupied, 48 $\mathring{A}^2$. $mol.^{-1}$) The values above, derived from figure 4.13., are approximate only, as that figure, together with 4.11., 4.12. is derived from graphs containing such scattered results and as such is highly subjective. The chief interpretational problem remaining is to establish the cause of varying values of the differential heat of exchange adsorption over the various surface coverages. About 4 K.cals.$mole^{-1}$ is a reasonable

level of enthalpy change for H-bonding on the active sites by lauric acid. This acid also indicates the remaining surface to be roughly homogeneous, as a constant heat of about 0.5 K cal.mole^{-1} is evolved as the surface layer is completed. Any inhomogeneity is so slight as to be undetectable from figure 4.8. It is believed that over this portion of the curve, the majority of the layer is comprised of loosely-held, non-bonded acid molecules and the heat evolved is derived from intermolecular reactions taking place within the layer.

However, the differential heat curve for stearic acid shows an overall increase in heat changes involved. Bonding at active sites is highly exothermic, yet there is no proof of ionic bonding occurring. The region of coverage from 20% to 60% also shows there to be some strongly exothermic reaction to be taking place. The heat values of between 4 and 8 K.cals.mole^{-1} are considered too large to arise solely from some type of interchain reaction: this had been suggested as a possible mechanism partly because a longer chain acid would form a closer-packed, lower-entropy solid film than the shorter acid, and because of existing evidence that adsorbed layers of stearic acid conferred much

greater stability than did lauric acid on a non-aqueous dispersion of titanium dioxide.

Infra red absorption spectra were obtained and examined for anatase 10b coated with the acids. Each sample was divided in two for examination: one was used as obtained (unwashed) and the other washed with n-heptane to remove loosely-held material. Portions of the spectra are shown in figures 4.14 and 4.15. The important features are the absorption bands at 1712-1714cm^{-1} frequency for lauric acid and 1719-1710, 1696cm^{-1} frequency for stearic acid. These represent the presence of a variety of associated acid groups, monomers and dimers in particular. The fact that the peak size is considerably reduced by washing in each case, suggests that there is a significant quantity of such material easily washed off. The association of this material takes place at the pigment surface, between already - adsorbed monomers and gives rise to a moderate evolution of heat.

The C=O absorption band is of low intensity in each case, stretching from ~1700-1540cm^{-1}. The low intensity signifies decreased polarity of adsorbate or a decreased quantity present. However, CH_2 - CH_3 stretching frequency bands were observed at full strength in the region 2970-2850cm^{-1}, so there must be plenty of acid present. The bands at 1470-1475cm^{-1} corresponding

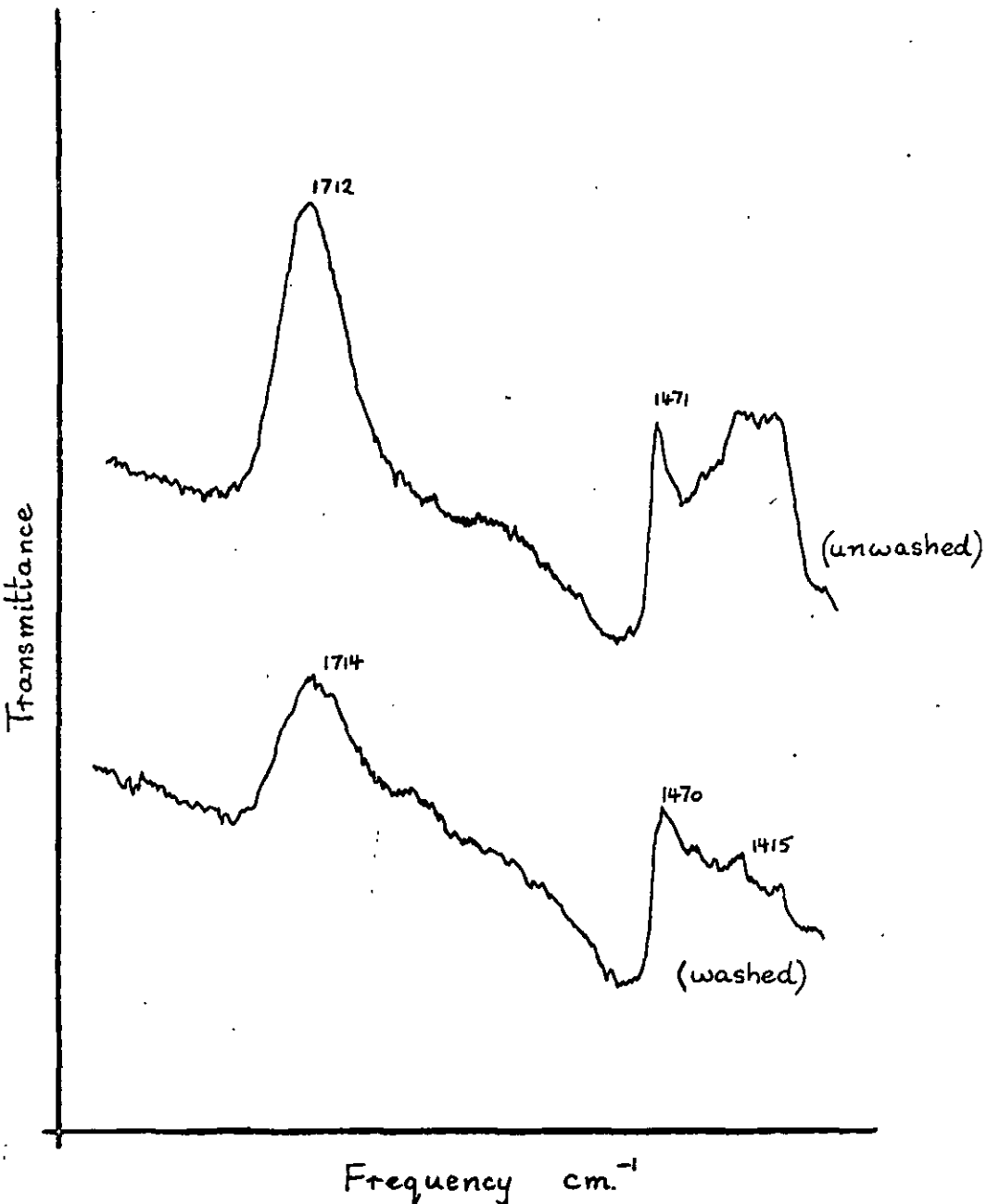

Fig. 4.14. Infra Red Absorption Spectra of Anatase Treated with 60mM Lauric Acid Solution

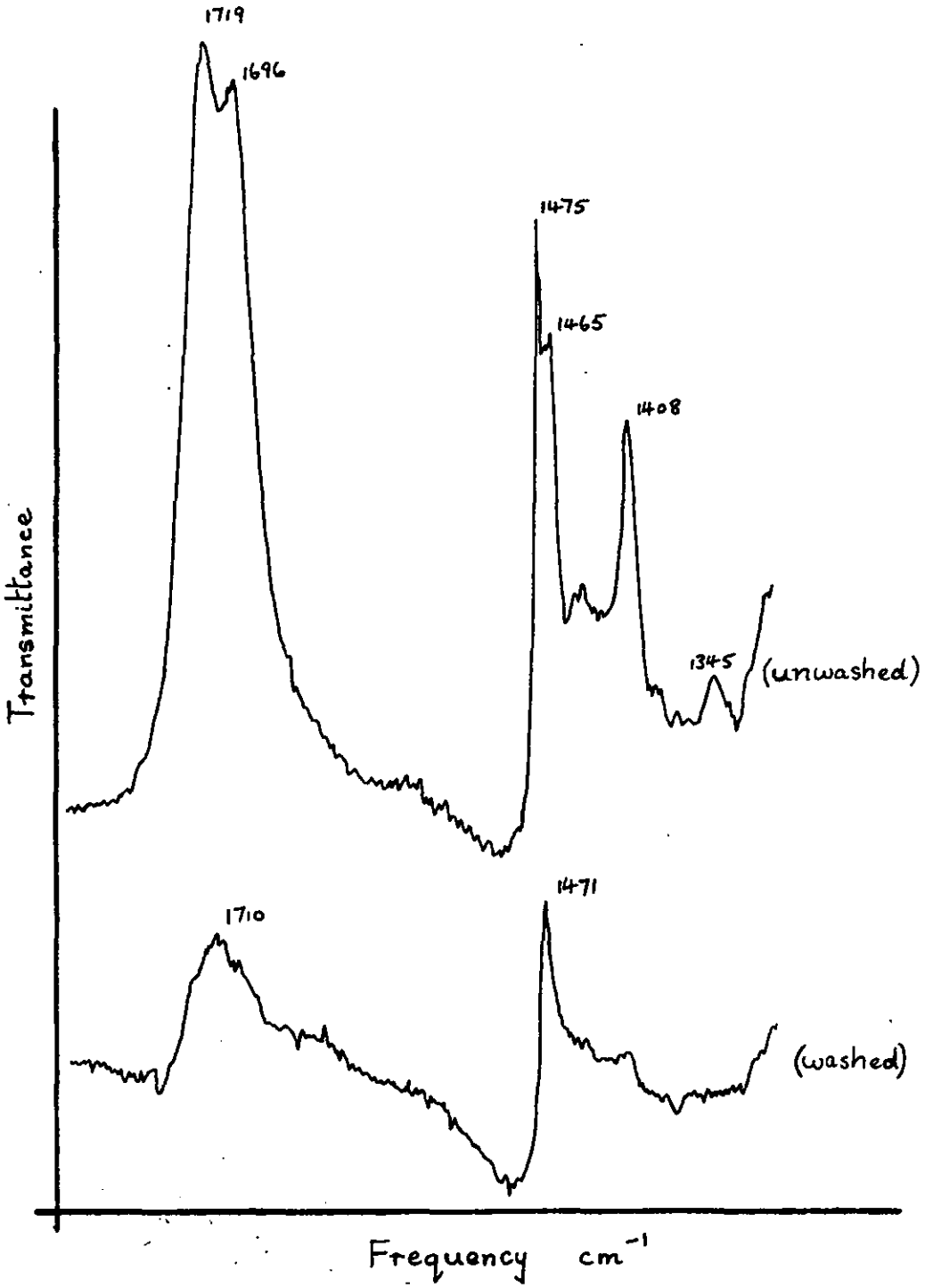

Fig. 4.15. Infra Red Absorption Spectra of Anatase Treated with 30mM Stearic Acid Solution

probably to the CH_2 - CH_3 bending frequency, are also strong.

An alternative explanation may lie in the possibility that some stearic acid molecules may somehow be adsorbed in a reverse orientation (that is, with carboxyl groups pointing away from the surface) either in the first layer, or forming a second layer. This would result from an increased intermolecular attraction of adjacent C_{18} acid chains, according to Koelmans and Overbeek[3]. There is no evidence in the adsorption isotherm to refute the possibility of a second adsorbed layer.

Further evidence to support this suggestion is derived from the fact that stearic acid (but no shorter-chain acid) shows a remarkable tendency to retraction on a glass slide withdrawn from a solution. It is highly oleophobic, that is, will tend to repel any incoming molecules which will be generally hydroxyl - first oriented.

However, it seems unlikely that this should commence at a level of adsorption corresponding to only 22% of a monolayer coverage, so the former explanation, the formation of dimers, is more appealing.

The close packing of oleic acid at the surface approaching 100% coverage by two point attached molecules is believed to result in dislodging the double bond, and a

vertically - oriented but slightly bent molecule remains, attached only at the carboxyl group. If the area occupied by such a molecule vertically - oriented is taken as 20.5$\AA^2$, the monolayer value will be 7.5×10^{-5} moles.g^{-1}; the adsorption isotherm, figure 4.7, clearly shows multi - layer adsorption to be taking place, an observation supported by Sherwood and Rybicka[9] and Tiffany[17]. The infra red absorption spectrum has not been included in this study but evidence is supplied in the former of these two papers from infra red data which shows both methylene groups and the unsaturation centre are involved in a surface interaction. The multilayer is probably formed by a mechanism involving a reaction between the centres of unsaturation of the first layer and the carboxyl head groups of the next layer.

REFERENCES

1. Verwey,E.J.W. and Overbeek,J.Th.G. - "The Theory of the Stability of Lyophobic Colloids" Elsevier 1948.

2. Derjaguin,B. and Landau,L. - (a) Trans. Faraday Soc.(1940),36,203
(b) Acta. Physico Chim.(U.S.S.R. 194 14,633

3. Koelmans,H. and Overbeek,J.Th.G. - Disc. Faraday Soc. (1954),18,52

4. McGown,D.N.L. and Parfitt,G.D. - Kolloid Z.(1967),219,No.1,48

5. Crowl,V.T. and Malati,M.A. - Disc. Faraday Soc.(1966),42,301

6. Heimenz,P.C. and Vold,R.D. - J.Coll. Sci.(1965),20,635

7. Harkins,W.D. "The Physical Chemistry of Surface Films" - Reinhold Publishing Corp., New York, (1952)

8. Zettlemoyer,A.C., Young,G.J., Chessick,J.J., and Healey,F.H., J.Phys.Chem.(1953),57,649

9. Sherwood,A.F., and Rybicka,S.M. - J. Oil and Colour Chemists' Assoc. (1966),49,No.8,648

10. Harkins,W.D. and Jura,G. - J.Am.Chem.Soc.(1944),66,1366

11. Healey,F.H., Chessick,J.J., Zettlemoyer,A.C. and Young,G.J. J.Phys.Chem.(1954),58,887

12. Chessick,J.J., Zettlemoyer,A.C., Healey,F.H. and Young,G.J. Can.J.Chem.(1955),33,251

13. Romo,L.A. - J.Coll.Sci.(1961),16,139

14. Everett,D.H. - Trans. Faraday Soc.,(1950),46,453,957

15. Hill,T.L. - (a) J. Chem. Phys.,(1949),17,520
(b) " " " (1950),18,246

16. Adamson,A.W. - "Physical Chemistry of Surfaces" Interscience Publishers Inc. New York(1960),50

17. Tiffany,J.M. - Ph.D. Thesis, Cambridge (1966)

18. Ottewill,R.H. and Tiffany,J.M. - J. Oil and Colour Chemist's Assoc. (1967),50,No.9,844

19. Freundlich,H. - Z.Physik. Chem.(Leipzig),(1907),57,385

20. Freundlich,H. - "Colloid and Capillary Chemistry" Methuen, London, (1926)

21. Langmuir,I. - J. Am. Chem. Soc.(1916),38,2221,(Part 1)
" (1917),39,1848,(Part 2)
" (1918),40,1361,(Part 3)

22. Ostwald,W. and de Izaguirre,R. - Kolloid Z.(1922),30,279

23. Kipling,J.J. - "Adsorption from Solutions of Non-Electrolytes" Academic Press, London and New York (1965)

24. Schay,G., Nagy,L.G. and Szekrenyesy,T. - Periodica Polytech. (Budapest),(1960),4,95

25. Schay,G. and Nagy,L.G. - J. Chim. Phys. (Paris),(1961),149

26. Everett,D.H. - Trans. Faraday Soc. (1964),60,1803

27. Everett,D.H. - Trans. Faraday Soc. (1965),61,2478

28. Parfitt,G.D. - Private Communication, 1968

29. Kipling,J.J. and Wright,E.M.H. - J. Chem. Soc.,(1964),3535

30. Young,G.J., Chessick,J.J., and Healey,F.H. - J.Phys.Chem. (1956),60,394

31. Wells,A.F. - "Structural Inorganic Chemistry" Clarendon Press, Oxford (1962)

32. Ermolaeva,T.A. - Zhur.Vsesoius.Khim.Obsh. in Mendeleyeva (U.S.S.R.), (1967),12,No. 4,437

33. Boehm,H.P. - Advances in Catalysis (1965),16,250

34. Yates,D.J.C. - J.Phys.Chem. 1961,65,746

35. Griot,O. - Trans. Faraday Soc. (1966),62,2904 - No.370(1968)

36. Day,R.E. and Parfitt,G.D. - Trans Faraday Soc.(1967),63,708

37. Sherwood,A.F. and Rybicka,S.M. - Paint Research Station (Teddington) Research Memo No.370 (1968)

38. Smith,I.T. - Nature (1964),201,67

39. Dintenfass,L. - Kolloid Z. (1957),155,No.2,121

40. Dintenfass,L. - J. Oil and Colour Chemists' Assoc. (1958),41,125

41. Kajanne,P. - Acta.Chem.Finn.(Helsinki),(1958), 31B,182

42. Petit,J., Jacovic,M., Helmi,J.P. and Bosshard,G. - C.R.Acad.Sci.(Paris),(1963)257,25,3878

43. Sherwood,A.F. - Paint Research Station (Teddington) Research Memo No.347(1966)

44. Rybicka,S.M. and Kelman,B.A. - Paint Research Station (Teddington) Research Memo No.349(1966)

45. Doorgeest,T. - J. Oil and Colour Chemists' Assoc. (1967),50,No12,1079

46. Groszek,A.J. - Am.Soc.Lubricating Engineers Trans. (New York),(1962),5,105

47. Groszek,A.J. - Nature (1962),196,531

48. Groszek,A.J. - A.S.L.E.Trans.(1966),9,67

49. Groszek,A.J. - Nature (1964),204,680

50. Groszek,A.J. and Wood,H.W. - Chem. and Ind.(1964),2057

51. Groszek,A.J. and Wood,H.W. - J.Phot.Sci.,(1965),13,133

52. Wood,H.W. - J.Phot.Sci.,(1966),14,72

53. Tidswell,M.W. - Private Communication (1968)

54. Brunauer,S., Emmett,P.H. and Teller,E.J. - J.Am.Chem.Soc. (1938),60,309

55. British Standard in draft form (Second proof: 68/13813)

56. Perrin,D.D., Armarego,W.L.F. and Perrin,D.R. - "Purification of Laboratory Chemicals", Pergammon Press London (1966)

57. Fischer,K. - Angew Chem.(Berlin,etc.),(1935),48,394

58. Whalley,C. - Paint Research Station, Tech. Paper 176 (1951)

59. Smith,D.M., Bryant,W.M.D. and Mitchell,J.(Jnr.) - J. Am. Chem. Soc.(1939),61,2407

60. Handbook of Chemistry and Physics (48th edition),(1967-8) The Chemical Rubber Co.

61. Groszek,A.J. - Chem. and Ind.,(1966),42,1754

62. Sherwood,A.F., Crowl,V.T., Milne,J.A., Rybicka,S.M. and White,M.C. - Paint Research Station, Research Memo in print.

63. Zettlemoyer,A.C. - Ind. Eng. Chem.(1965),57,No.2,27

64. Zettlemoyer,A.C., Chessick,J.J., and Hollobaugh,C.H. - J. Phys. Chem. (1958),62,489

65. Chessick,J.J. and Zettlemoyer,A.C. - Advances in Catalysis, (1959), XI, 263

66. Guderjahn,C.A., Paynter,D.A., Borghausen,P.E. and Good,R.J. J.Phys.Chem.(1959),63,2066

67. Wade,W.H., and Hackerman,N. - J.Phys.Chem.(1961),65,1682

68. Emmett,P.H., and Brunauer,S.J. - J.Am.Chem.Soc.(1937),59,1553

69. Davies,M.M. and Sutherland,G.B.B.M - J.Chem.Phys.(1938),6,767

70. Shaw,D.J. - "Introduction to Colloid and Surface Chemistry" Butterworths, London (1966)

71. Long,J.S., Schwarz,M., Chang,Y.S., Schuler,R.E. and Sturgeon,R. Offic. Dig. Federation Soc. Paint Tech.(1963),35,11